University of Alberta

A Role for the Nuclear Transport Machinery in Regulating the Dynamic Localization of the Spindle Assembly Checkpoint Protein Mad1p.

by

Robert John Scott 

A thesis submitted to the Faculty of Graduate Studies and Research
in partial fulfillment of the requirements for the degree of

Doctor of Philosophy

Department of Cell Biology

Edmonton, Alberta
Spring, 2008

Your file Votre référence
ISBN: 978-0-494-45596-8
Our file Notre référence
ISBN: 978-0-494-45596-8

Abstract

Nuclear pore complexes (NPCs) are the sole sites of macromolecular exchange across the nuclear envelope (NE) of eukaryotic cells. The NPC is composed of around 30 *bona fide* nucleoporins (nups). In addition to the nups, NPCs are host to numerous NPC-associated proteins that are docked on both its cytoplasmic and nucleoplasmic aspects. Here, we have investigated the NPC association of two of these: the spindle assembly checkpoint (SAC) proteins Mad1p and Mad2p. Mad1p is a predominantly coiled-coil protein with a Kap60p/Kap95p-dependent nuclear localization signal (NLS) that is required for efficient targeting to NPCs. At NPCs, Mad1p interacts with a presumed complex of Nup60p/Mlp1p/Mlp2p and interacts directly *in vitro* with Nup60p. In addition to its interactions with the Nup60p/Mlp1p/Mlp2p complex, Mad1p also interacts directly with Nup53p, a nucleoporin that is an important determinant of mitotic duration. From its anchorage at NPCs during interphase, Mad1p is recruited to kinetochores during mitosis in an energy-dependent fashion. Additionally, Mad1p dynamically associates with kinetochores and NPCs with a $t_{1/2}$ of ~30 s. Interestingly, Mad1p also contains an Xpo1p-dependent nuclear export signal (NES). This NES is required for the targeting and turnover of Mad1p at SAC-activated kinetochores. Correspondingly, functional Xpo1p is also required for Mad1p kinetochore targeting, and inhibition of its function results in an inability of Mad1p to associate with kinetochores. Interestingly, Xpo1p is found in the nucleus but is also found in association with spindle pole bodies (SPBs). During SAC arrest, Xpo1p itself is redistributed from SPBs to kinetochores. Consistent with the possibility that the two form a complex, the association of Mad1p and Xpo1p

with kinetochores is interdependent and mutating either protein results in mislocalization of the other.

Dedication

To my wife Kathy,

for her steadfast support, encouragement and understanding throughout these years.

Acknowledgements

It has been my privilege to be a part of Rick Wozniak's research group. I have worked alongside people who have taught me, supported me and inspired me, all the while forming lifelong friendships. At the head of this list is Rick, himself. My fondest memories of Rick are of our conversations about science as a discipline, an entity and as a method. His understanding and appreciation for science, its application and consequence are something I continue to strive towards. Rick, thank-you for this education, your support of my work and your fellowship.

Any good fortune I have had scientifically are a result of the stage where I learned and performed science. The cast assembled in Rick's lab over the years have gone on to do amazing things and will no doubt continue to do so. The cast, in order of appearance: Patrick Lusk, Lisa Hawryluk-Gara, Andrea Anderson, Dave Van de Vosse, Jana Mitchell, Tadashi Makio, Chris Ptak, Neil Adames, Luc Cairo and Chris Neufeldt. Pat, thanks for the lessons as a scientist then and now as a friend. Andrea, your mettle, confidence and sense of humour make you a valued companion. Lisa, nothing more or less than thank-you. You have held my hand and led the way and for this I owe you a debt of gratitude. Dave, thanks for always bringing the broader picture to my desk. You all are what a University experience is about. It has been fun.

I would like to thank my family, especially my wife, Kathy, for her support in this degree. My parents, Janet and Jack Scott, provided me with a youth devoid of concern in which I was free to pursue my curiosity and for this I am eternally appreciative.

Thank-you to the Alberta Heritage Foundation for Medical Research for their financial support throughout my degree.

Table of Content

List of Tables

List of Figures

List of Symbols, Abbreviations and Nomenclature

5-FOA	5'-fluoroorotic acid
αF	α-factor
APC	anaphase promoting complex
ATP	adenosine triphosphate
Ben	benomyl
bp	base pair
BP	broad pass
°C	degrees Celsius
cNLS	'classical' NLS
Da	Dalton
DNA	deoxyribonucleic acid
ECL	enhanced chemoluminescence
EM	electron microscopy
ER	endoplasmic reticulum
FD	Faraday
Fig.	Figure
FG	phenylalanine, glycine
g	gram
g	gravitational force
Gal	galactose
G1	gap one phase
G2	gap two phase
GAP	GTPase activating protein
GDP	guanosine diphosphate
GEF	guanosyl exchange factor
GFP	green fluorescent protein
GFP+	enhanced green fluorescent protein
Glc	glucose
GST	glutathione-S-transferase
GT	glutathione
GTP	guanosine triphosphate
GTPase	guanosine triphophatase
h	hour
HA	Hemagluttinin
hnRNP	heterogenous nuclear RNP
HU	hydroxyurea
HRP	horseradish peroxidase
IgG	immunoglobulin G
INM	inner nuclear membrane
IPTG	isopropyl-β-D-thiogalactoside
Kap	karyopherin
LP	long pass
min	minutes

μ.....micro
m.....milli
M.....Mitotic phase/moles per litre/Mega ($1x10^6$)
n.....nano
mRNA.....messenger RNA
NE.....nuclear envelope
NEBD.....nuclear envelope breakdown
NES.....nuclear export signal
NLS.....nuclear localization signal
Noc.....nocodazole
NPC.....nuclear pore complex
Nup.....nucleoporin
OD.....optical density
ONM.....outer nuclear membrane
ORF.....open reading frame
pA.....protein A
PAGE.....polyacrylamide gel electrophoresis
PCR.....polymerase chain reaction
pH.....$-\log[H^+]$
PM.....pore membrane
pom.....pore membrane protein
RFP.....red fluorescent protein
RNA.....ribonucleic acid
RNAi.....RNA interference
RNP.....ribonucleoporin
sec.....second
S.....Synthesis Phase
SDS.....sodium dodecyl sulphate
SM.....synthetic media
snRNP.....small nuclear RNP
SPB.....spindle pole body
SUMO.....small ubiquitin-related modifier
TCA.....trichloracetic acid
tRNA.....transfer RNA
ts.....temperature sensitive
U.....unit
V.....volt
YPD.....yeast extract peptone and dextrose
YP-Gal.....yeast extract peptone and galactose
YP-Raf.....yeast extract peptone and raffinose

Epigraph

The truth knocks on the door and you say, "Go away, I'm looking for the truth," and so it goes away. Puzzling.

Excerpt from Zen and the Art of Motorcycle Maintenance *by Robert M. Pirsig*

Chapter I: *Introduction*

1.1 Preface

Eukaryotic cells are typified by a complex arrangement of internal membranes and cytoskeletal components that together compartmentalize and separate cellular processes. Among these membrane systems is the common and defining feature of all eukaryotes: the nuclear envelope (NE). Within the confines of the NE is the cell's DNA and all associated DNA metabolism including chromosome segregation. As with all membrane systems, the physical separation created by the NE between the nucleoplasm and cytoplasm requires a transport system to facilitate movement of cargos across the NE. This transport machine is called the nuclear pore complex (NPC). NPCs, in concert with soluble transport carriers, mediate all bidirectional flux across the NE and consequently regulate access to the nuclear contents. In addition to well studied roles in nuclear transport, NPCs are also ideally situated to influence the activities of other cellular processes, including mitotic events and chromosome segregation.

A subset of NPC constituents and NPC-associated proteins are localized to distal regions of the nucleoplasmic face of the NPC. Here, these components provide a docking site for, among others, a complex of spindle assembly checkpoint (SAC) proteins. During SAC arrest, these proteins shuttle from NPCs onto unattached kinetochores and from here signal to prevent premature cell cycle progression. Understanding how the NPC and nuclear transport machinery influence the mobility and activity of these SAC proteins is a critical step in developing a more comprehensive picture of both NPC and the SAC.

1.2 The Nuclear Envelope

The NE is composed of two concentric lipid bilayers: the inner nuclear membrane (INM) and the outer nuclear membrane (ONM). The INM and ONM are fused at distinct regions in the envelope called the pore membrane domain (POM) (Mattaj et al., 2004). Each of these membrane domains can be distinguished according to their protein complement. The ONM is continuous with the rough endoplasmic reticulum (RER) and as such is studded with ribosomes but also hosts ONM-specific protein complexes (Kvam and Goldfarb, 2004). The INM is defined by a unique protein array, most notably the nuclear lamina in animal cells. The lamina was originally suggested to support the NE and has also been proposed to be involved in other nuclear processes including NE assembly (Goldman et al., 2002). Lower eukaryotes like the Baker's yeast *Saccharomyces cerevisiae* lack an apparent nuclear lamina but do contain unique INM constituents (Murthi and Hopper, 2005; King et al., 2006).

Connecting the ONM with the INM is the POM. Here, occupying the transcisternal pores formed by the POM are NPCs, the macromolecular assemblies responsible for soluble bidirectional exchange across the NE. Importantly, NPCs also are thought to influence INM content by regulating INM protein movement across the POM (King et al., 2006 and reviewed in Lusk et al., 2007).

1.3 Nuclear Pore Complexes

Callan and Tomlin first identified pores embedded within the animal NE by EM (Callan and Tomlin, 1950). Several years later, the name *pore complex* was proposed for the cylindrical formations penetrating the NE of animal cells (Watson, 1959). Negative

staining later revealed that pore complexes display octagonal rather than circular symmetry about an axis perpendicular to the NE (Gall, 1967; Figure 1-1). Over the past ~40 years, a vastly clearer structural and functional understanding of pore complexes (NPCs) has emerged. NPCs have been studied in both yeast and animal cells, and proteomic analyses of NPCs have yielded size estimates of the yeast NPC in the ~ 50 MDa vicinity, while the vertebrate NPC is thought to be ~ 60 MDa, although the measured mass may be a considerably larger 125 MDa (Reichelt et al., 1990; Fabre and Hurt, 1997; Rout et al., 2000; Cronshaw et al., 2002; Alber et al., 2007b). The difference in measured and estimated NPC sizes may reflect additional mass contributed by NPC-associated proteins lost during NPC purification procedures. Despite the similarity in overall molecular mass between yeast and vertebrate NPCs, NPC dimensions vary considerably with yeast and vertebrate NPCs having diameters of ~960 Å and 1200-1450 Å respectively (Yang et al., 1998; Akey and Radermacher, 1993). These size discrepancies are another reflection of the mass differences observed between yeast and vertebrate NPCs. Detailed descriptions of the NPC have been largely derived from EM studies of both yeast and vertebrate cell types (Reichelt et al., 1990; Akey and Radermacher, 1993; Yang et al., 1998; Kiseleva et al., 2004). More recently, a comprehensive study of the yeast NPC made use of several experimental approaches including ultracentrifugation, affinity purification, quantitative immunoblotting, overlay assays, EM, immuno-EM and cell fractionation experiments, along with computational approaches. Data gathered from these analyses were collected and computationally integrated with known NPC physical constraints to generate a high-resolution

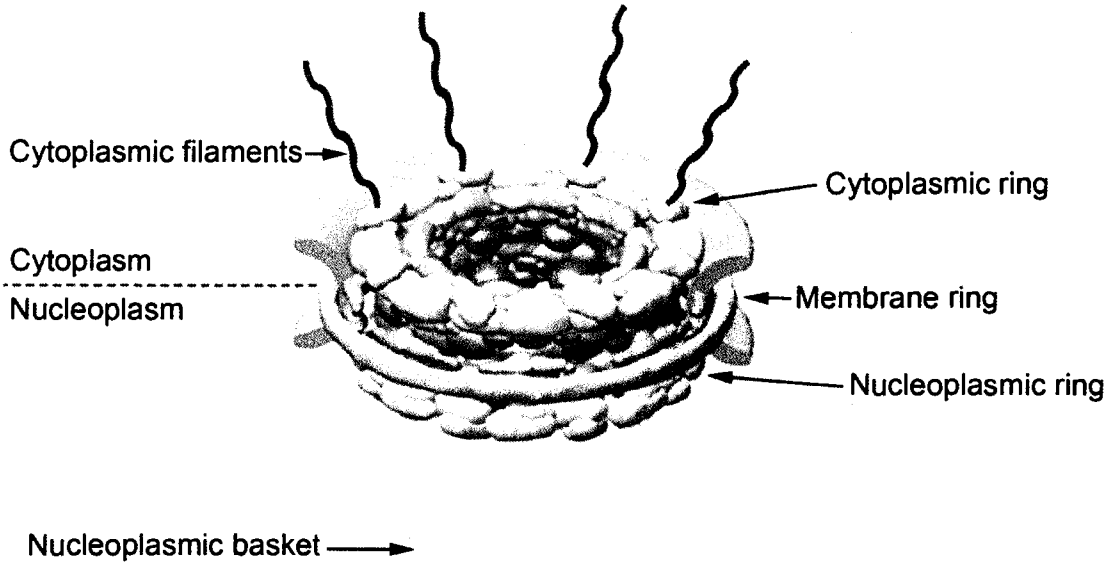

Figure 1-1. A model of the NPC.

A representation of the NPC embedded in the NE, (grey). The core of the NPC is composed of a membrane ring and nucleoplasmic and cytoplasmic rings. Emanating from the core into the nucleoplasm and cytoplasm, respectively, are the nucleoplasmic basket and the cytoplasmic rings. Here, nups are represented according to their predicted localization volumes and are coloured according to their localization in one of five distinct substructures. Nups of the outer ring are represented in yellow, inner rings in purple, membrane ring in brown, linker nups in blue and pink and structural portions of the FG nups in green. Adapted from Alber et al., 2007b.

reconstruction of the NPC (Alber et al., 2007a; 2007b; reviewed in Aitchison and Wozniak, 2007). While discrete subcomplexes of the NPC have been defined and analyzed in numerous studies (Grandi et al., 1993; Belgareh et al., 1998; Marelli et al., 1998; Belgareh et al., 2001; Lutzmann et al., 2002; Hawryluk-Gara et al., 2005; Madrid et al., 2006), this work has coalesced these subcomplexes with one another and has provided a clarified view of the structural organization of the yeast NPC core.

Encircling the central transporter are nucleoplasmic and cytoplasmic outer rings, inner rings on both sides of the equator of the NPC and a membrane ring that surrounds the NPC in the luminal space between the INM and ONM (Beck et al., 2004; Alber et al., 2007b) (Figure 1-1). Bridging the NPC rings are linker nucleoporins. The rings and the linker nucleoporins are layered on top of one another like doughnuts. The stacks align such that the NPC forms 16 columns that form eight spokes that give the NPC its characteristic eight-fold symmetry. Overall, these components constitute the core complex of the NPC (Alber et al., 2007b).

Emanating from the core complex of the NPC are the cytoplasmic filaments and the nucleoplasmic basket. As their name implies, the cytoplasmic filaments extent into the cytoplasm and provide docking sites for the initial steps in nuclear import (Rout et al., 2000; Beck et al., 2004). The nuclear basket extends into the nucleoplasm but unlike the cytoplasmic filaments, terminates in a ring at its distal tip (Fig. 1-1). Here, the nuclear basket interacts with the underlying chromatin and also the nuclear lamina of higher eukaryotes (Hawryluk-Gara et al., 2005; Feuerbach et al., 2002; Ishii et al., 2002; Dilworth et al., 2005). The interactions of the NPC with chromatin have been suggested to imply alternative functions for the NPC as a gene gating structure that interacts with

transcriptionally active regions of the genome (Blobel, 1985; Ishii et al., 2002; Casolari et al., 2004; Cabal et al., 2006; Luthra et al., 2007).

1.4 Nucleoporins

With size estimates of the NPC in the 50-60 MDa range, it can be predicted that the NPC would be composed of hundreds of proteins. For comparison, the eukaryotic ribosome, which is ~4.2 MDa, contains more than 80 proteins (Fatica and Tollervey, 2002). Yet despite the massive size of NPCs, each is composed of a limited set of proteins termed nucleoporins (nups), of which there are only ~30 in both yeast and vertebrates (Rout et al., 2000; Cronshaw et al., 2002). The small number of proteins is thought to yield the higher order NPC through modular assemblies that are repeated throughout the NPC (Schwartz, 2005). An example of this modularity is provided by the eight-fold symmetry of the NPC where each spoke is thought to be identical. Further modularity within the NPC is revealed by computational analysis of the nups that predict that these proteins are predominantly composed of three fold types: α-solenoid, β-propeller and coiled-coil motifs, in addition to large stretches of predominantly unfolded protein, although exceptions have been described (Devos et al., 2004; 2006; Schrader et al., 2008).

The NPC is anchored to the POM with three transmembrane nups that collectively are referred to as poms. The remainder of the NPC is composed of nups that fall into one of two categories (Table 1-1). The first are the FG-(phenylalanine-glycine) nups. These nups are characterized by clustered FG repeats of varying number positioned throughout the protein. The final group of nups is the non-FG nups. These nups are devoid of FG

repeats and are thought to provide a structural framework for the NPC (Suntharalingam and Wente, 2003).

Table 1-1. Nucleoporins of yeast and vertebrate cell types*

Vertebrate	*S. cerevisiae*	Nup type
Nup358	—	FG
Nup214	Nup159p	FG
gp210	—	Pom
Nup205	Nup192p	Non-FG
Nup188	Nup188p	Non-FG
Nup160	Nup120p	Non-FG
Nup155	Nup170p/Nup157p	Non-FG
Nup153	Nup1/2, Nup60p	FG
Nup133	Nup133p	Non-FG
POM121	Pom152p	Pom
—	Nup100p	FG
—	Nup116p	FG
Nup107	Nup84p	Non-FG
Nup98	Nup145-Np	FG
Nup96	Nup145-Cp	Non-FG
Nup93	Nic96p	Non-FG
Nup88	Nup82p	Non-FG
Nup85/75	—	Non-FG
p62/Nup62	Nsp1p	FG
Nup58	Nup49p	FG
Nup54	Nup57p	FG
Nup53	Nup53p/Nup59p	FG
Nup50	—	FG
Nup45	—	Non-FG
Nup43	—	Non-FG
Nup37	—	Non-FG
Sec13	Sec13p	Non-FG
Seh1	Seh1p	Non-FG
RAE1	—	Non-FG
Gle1	Gle1p	Non-FG
Gle2	Gle2p (Rae1p)	Non-FG
hCG1	Nup42p	FG
Ndc1	Ndc1p	Pom
—	Pom34p	Pom
—	Nup85p	Non-FG
—	Cdc31p	Non-FG

* Modified from Hetzer et al., 2005.

1.4.1 Poms

There are three known poms in yeast and vertebrate cell types. The poms are thought to be required to anchor the NPC to the NE and certain poms are required for NPC assembly. The yeast poms are Pom34p, Pom152p, and Ndc1p, a shared component of the NPC and the yeast spindle pole body (SPB) (Wozniak et al., 1994; Chial et al., 1998; Rout et al., 2000; Miao et al., 2006). Vertebrate poms include gp210, Pom121, and Ndc1 (Gerace et al., 1982; Wozniak et al., 1989; Hallberg et al., 1993; Mansfeld et al., 2006). Ndc1 is conserved across species as are Pom121 and Pom152 (Wozniak et al., 1994; Mans et al., 2004). Supporting this, *in vitro* data suggest that Pom121 and Pom152 are functional homologues (J. Mitchell and R. Wozniak, personal communication). In yeast, both Pom34p and Pom152p are non-essential, while Ndc1p is required for viability. Interestingly, these three poms are proposed to assemble into a complex (Alber et al., 2007b) and form the membrane ring that surrounds the NPC in the NE lumen. Deletion of *POM34* or *POM152* has little or no effect on nup localization to the NPC or on nuclear transport; however, depletion of Ndc1p from cells results in a dramatic mislocalization of nups and inhibition of nuclear import that is exacerbated in a *pom152Δ* mutant (Madrid et al., 2006). These data support roles for Ndc1p and Pom152p in NPC assembly and function. Consistent with this, overexpression of Nup53p results in proliferation of the inner nuclear membrane and formation of lamellae (Marelli et al., 2001). These membranes have pore-like perforations but lack complete NPCs. Notably, Nup53p along with Ndc1p and Pom152p were found in association with these membranes and together are thought to represent an intermediate in NPC assembly.

In higher eukaryotes, where the NE breaks down and must reassemble before and after each mitosis, there is further evidence for poms in NPC assembly. In *in vitro* NE assembly assays using *Xenopus* egg extracts, depletion of Pom121 from membrane vesicles does not alter vesicle binding to chromatin but blocks subsequent vesicle fusion steps required to form a closed NE (Antonin et al., 2005). Interestingly, depletion of a soluble complex of nups, the Nup107-160 complex, abrogates this block in fusion, suggesting that a checkpoint monitors NPC reassembly and coordinates it with NE fusion (Antonin et al., 2005; Walther et al., 2003). More recently, a study using both *Xenopus* and HeLa cell model assays has implicated Ndc1 in NPC and NE assembly (Mansfeld et al., 2006). Collectively, data from yeast, *Xenopus* and humans suggest that Pom152p and Ndc1p of yeast and Pom121 and Ndc1 of metazoans are required for normal NE and NPC assembly, further supporting the notion that Pom152p and Pom121 are functional homologues.

1.4.2 FG Nucleoporins

Within the NPC, the FG-nups are thought to provide the docking sites for nuclear transport events. In yeast, 11 of the ~30 nups contain classical FG-repeat motifs that have clustered arrays of the FG dipeptide of varying length separated by spacer sequences (Strawn et al., 2004). Consistent with a role for FG-nups in nuclear transport, numerous studies have detected direct physical interactions between the FG-nups and the soluble nuclear transport factors (termed karyopherins or kaps) (Rexach and Blobel, 1995; Radu et al., 1995; Kraemer et al., 1995; Aitchison et al., 1996; Liu and Stewart, 2005). Specifically, kaps interact directly with the FG domains of FG-nups. Structurally,

the FG-containing regions of FG-nups are thought to adopt an unfolded configuration and are referred to as natively unfolded (Denning et al., 2002; 2003). This supports the hypothesis wherein the FG nups form a meshwork lining the NPC through which nuclear transport occurs (Rout et al., 2000; Ribbeck and Görlich, 2001).

All models of nuclear transport invoke the kap-binding properties of the FG-nups (see Section 1.5). Consistent with a meshwork of FG-nups lining the NPC, FG-nups can be categorized according to their localization in one of three regions. FG-nups can be found on either the nucleoplasmic or cytoplasmic side of the NPC while others are found symmetrically positioned on both sides of the NPC (Rout et al., 2000; Strawn et al., 2004). A surprising observation in yeast demonstrated that over half the total FG mass could be deleted from the NPC without compromising cell viability or producing gross alterations in nuclear transport efficiency (Strawn et al., 2004; Zeitler and Weis; 2004). Simultaneous deletion of all asymmetrically distributed FG domains did not affect cell survival or nuclear transport but deletion of symmetrically distributed FG domains did perturb specific transport pathways (Strawn et al., 2004). Moreover, inverting the asymmetry of the NPC yielded no apparent defects in import or export pathways (Zeitler and Weis; 2004).

How the FG-nups behave as kap-binding sites in the context of the NPC to mediate nuclear transport has recently become hotly contested and understanding their behaviour is pivotal for gaining a clear understanding of nuclear transport. In one model, the FG-nups have been proposed to arrange as a hydrogel through reversible hydrophobic interactions that can be broken by kaps as they sieve through this matrix (Frey et al., 2006; Frey and Görlich, 2007). Another group has suggested that the FG-nups form

extended polymer brushes that collapse during kap docking (Lim et al., 2006; 2007a; 2007b). These studies and their implications for models of nuclear transport are discussed in greater detail in Section 1.5.

1.4.3 Non-FG-nucleoporins

The non-FG nups are nups that do not contain the FG dipeptide repeat. The non-FG nups are thought to form the core scaffold of the NPC and bridge the poms with the FG-nups (Suntharalingam and Wente, 2003; Alber et al., 2007b). Two of the most well studied NPC subcomplexes are the yeast Nup84 complex and its vertebrate homologue, the Nup107-160 complex. Each makes up almost 1/3 of the total nucleoporin complement. *In vitro* reconstitution of the yeast Nup84 complex has revealed a Y-shaped heptamer (Sinossoglou, 1996; Belgareh et al., 2001; Vasu et al., 2001; Lutzmann et al., 2002; Harel et al., 2003, Walther et al., 2003). Co-crystallization of Nup84 complex members Sec13p –Nup145Cp has led to the suggestion that these nups form a hetero-octamer *in vivo* and that the remainder of the Nup84 complex is anchored around this structure (Hsia et al., 2007). In yeast, mutation of specific members of the Nup84 complex results in a clustering of NPCs and an mRNA export defect (Sinossoglou et al., 1996; Aitchison et al., 1995a). The Nup107-160 complex in vertebrates is also required for mRNA export and furthermore, depletion of the complex by RNAi from HeLa cells or by immunodepletion from nuclear assembly reactions yields nuclei with continuous NE but devoid of NPCs suggesting an essential role for the Nup107-160 subcomplex in NPC assembly (Walther et al., 2003; Harel et al., 2003).

In yeast, a dramatic example of the role that non-FG nups play in overall NPC architecture comes from Nup170p. *NUP170* genetically interacts with the major pore membrane protein Pom152p, consistent with a role for the non-FG nups in linking the core NPC scaffold to the poms. In both *nup170 Δ* cells and *pom152Δ* cells depleted of Nup170p, NPC formation appears to be impaired resulting in apparent NPC assembly intermediates accumulating in the NE (Aitchison et al., 1995b; T. Makio and R. Wozniak, personal communication). In addition, Nup170p is required for the normal localization of the FG nups Nup1p and Nup2p to the NPC (Kenna et al., 1996). This is consistent with a role for Nup170p in defining the central transporter dimensions of the NPC via its interactions with FG-nups lining this channel. This is supported by observation from the Goldfarb group which has shown that in cells lacking Nup170p, the diameter of the NPC diffusion channel is increased resulting in lower net rates of nuclear transport (Shulga et al., 1996; 2000).

1.4.4 NPC-associated proteins

Proteomic analyses of both the yeast and vertebrate NPCs yielded ~30 *bona fide* nups (Rout et al., 2000; Cronshaw et al., 2002). However, several proteins have been identified that localize to NPCs but were not identified in these analyses or do not meet the criteria outlined for yeast nups (Rout et al., 2000; Cronshaw et al., 2002). Included in this list of NPC-associated proteins is the nuclear transport accessory factor, RanGAP (GTPase activating protein) (Matunis et al., 1996). RanGAP is localized predominantly to the cytoplasm but SUMO-modified RanGAP is localized to the cytoplasmic fibers of the NPC through its interaction with Nup358 (RanBP2). Additionally, SUMO-modified

RanGAP localizes to the mitotic spindle and to kinetochores and is essential for microtubule-kinetochore interactions (Joseph et al., 2002; 2004). Interestingly, the SUMO conjugating enzyme Ubc9 is itself localized to NPCs of vertebrate cells and the SUMO deconjugating enzyme SENP (Ulp1p in yeast) is localized to NPCs. In vertebrates, SENP is associated with NPCs through an interaction with Nup153 while in yeast, Ulp1p associates with NPCs via the kaps Kap121p and Kap60p/Kap95p and an interaction with the Mlps (Saitoh et al., 1997; Zhang et al., 2002; Panse et al., 2003; Zhao et al., 2004; Makhnevych et al., 2007). The localization of both the SUMO conjugating and deconjugating enzymes to the NPC suggests that the NPC and nuclear transport factors play a key role in regulating protein sumoylation and indeed Kap121p is required for targeting Ulp1p to septin rings during mitosis (Makhnevych et al., 2007).

Another example of an NPC-associated non-nucleoporin comes from the DEAD-box RNA helicase, Dbp5p (Hodge et al., 1999; Schmitt et al., 1999). Dbp5p is essential for mRNA export and localizes to the cytoplasmic fibers of NPCs in association with Nup159p (Weirich et al., 2004). Dbp5p also requires the nup Gle1p and production of inositol hexakisphosphate for RNA-dependent ATPase activity for mRNA export (Alcázar-Roman et al., 2006; Weirich et al., 2006). Interestingly, Ipk1p, an enzyme required for inositol hexakisphosphate production, is also localized at NPCs, thereby facilitating spatial control of inositol hexakisphosphate production for mRNP remodelling during RNA export (York et al., 1999; Alcázar-Roman et al., 2006; Weirich et al., 2006). Dbp5p is thought to remodel RNPs in order to prevent their return to the nucleus by removing RNA binding proteins as they are exported through the pore and encounter the cytoplasmic face of the NPC (Tran et al., 2007; Stewart et al., 2007).

Extending from the nucleoplasmic face of the yeast NPC are two large predominantly coiled-coil myosin-like proteins (Mlp) proteins, Mlp1p and Mlp2p (Kolling et al., 1993; Strambio-de-Castillia et al., 1999). Mlp1p and Mlp2p are highly homologous, and a related protein, Tpr of vertebrate cells, is also localized to the nucleoplasmic face of the NPC (Byrd et al., 1994; Cordes et al., 1997). The Mlp proteins have been suggested to form filaments that extend into the nucleoplasm to provide a conduit for substrates entering or exiting the nucleoplasm (Strambio-de-Castillia et al., 1999). Like the nups Ndc1p and Cdc31p, Mlp2p is a shared component of NPCs and SPBs and is required for efficient SPB assembly (Niepel et al., 2005). The Mlps have a disputed role in telomere anchoring at the nuclear periphery and are also required for establishing transcriptional silencing (Galy et al., 2000; Feuerbach et al., 2002; Andrulis et al., 2002; Hediger et al., 2002a; 2002b).

Another notable group of NPC-associated proteins are the SAC proteins Mad1p and Mad2p. Although they perform their primary cellular function within the nucleoplasm specifically on mitotic kinetochores, during interphase, Mad1p and Mad2p are localized to the nucleoplasmic face of the NPC (Campbell et al., 2001; Iouk et al., 2002; Ikui et al., 2002; Musacchio and Hardwick, 2002; Musacchio and Salmon, 2007). Mad1p and Mad2p are anchored at NPCs through interaction with a presumed Nup60p/Mlp1p/Mlp2p complex. These proteins will be discussed in detail in Section 1.8 and in Chapters III and IV.

1.4.5 NPC and nucleoporin conservation

Despite the remarkable conservation of the overall NPC structure from species to species, nups themselves are not well conserved. Only a handful of nups can complement defects of mutants in their correlate homologues across species (Suntharalingam et al., 2003). An interesting example of homology within a species is seen in the yeast *Saccharomyces cerevisiae* where an ancient genomic duplication resulted in two copies of certain yeast nups (*e.g. NUP53* and *NUP59*) (Scannell et al., 2007). This duplication is proposed to have yielded an eight-spoked NPC in which each spoke contains two columns with each column harbouring a distinct nup complement (Alber et al., 2007b). Higher eukaryotes are missing this apparent level of complexity leading to the prediction that they host more uniform NPCs.

Despite the lack in nup sequence homology across species, there is a remarkable degree of structural homology and conservation of nup-nup interactions. As discussed in Section 1.4.3, the proteins and interactions of the Nup84/Nup107-160 complex are conserved across species (Belgareh et al., 2001; Lutzmann et al., 2002; Suntharalingam and Wente, 2003; Devos et al., 2006). Another well studied NPC subcomplex conserved through evolution is the Nup53-containing complex. In yeast, the complex consists of Nup53p, Nup59p, Nup170p, and Nic96p, while in vertebrates the complex is composed of homologues of these proteins referred to as Nup53, Nup155 and Nup93 (Marelli et al., 2001; Hawryluk-Gara et al., 2005; 2008). During yeast mitosis, the Nup53-containing complex is rearranged, exposing a Kap121p binding site on Nup53p (Lusk et al., 2002). This provides a docking site for Kap121p at mitotic NPCs, inhibiting mitotic transport by this kap (Makhnevych et al., 2003). Notably, an interaction between vertebrate Nup53

and Kapβ3 has not been identified. This may reflect the open mitosis of vertebrates contrasting the closed mitosis of yeast, a time when the Kap121p-Nup53p interaction is most readily detected (Makhnevych et al., 2003).

1.5 Nucleocytoplasmic transport

The NE encapsulates all nuclear processes. NPCs provide conduits to deliver transport substrates across the NE both passively for small molecules and by a facilitated mechanism for larger molecules. A vast array of molecules including proteins, snRNPs, mRNAs, tRNAs and ribosomal subunits must be actively transported bidirectionally across the NE. Within specific macromolecules are nuclear localization or nuclear export sequences that specify their end location. In concert with NPCs, another class of molecules, nuclear transport receptors, recognize these signal sequences and are required for the facilitated aspect of macromolecular transport across the NE.

1.5.1 Karyopherins

Transport receptors are an essential component of the nuclear transport machinery. These receptors recognize cargos that harbour signal sequences, interact with the NPC and deliver cargo to its destination. Kaps are the largest family of transport receptors and, in yeast, there are 15 kaps that mediate bidirectional transport across the NE while vertebrates contain at least 22 (Wozniak and Aitchison, 1998; Görlich and Kutay, 1999; Strom and Weis; 2001; Macara, 2001; Fried and Kutay; 2003). Import kaps are referred to as importins while export kaps are often referred to as exportins. Members of the kap family share limited homology with the first identified kap, kap β1. In

addition to kap β's, the α-kaps, of which there is one in yeast and at least six in vertebrates, function as adaptor molecules and bridge the interaction between kapβ1 (Kap95p) and classical nuclear localization signal (cNLS)-containing cargo molecules (Goldfarb et al., 2004). While the kap α–β heterodimer was the first kap import pathway identified, most β-kaps recognize their cargo directly.

The β-kaps have molecular masses between ~90-140 kDa and are characterized by an N-terminal RanGTP binding motif and indeed, several β-kaps were identified based on their ability to bind RanGTP (Schlenstedt et al., 1997; Görlich et al., 1997). Beyond their N-termini however, β-kaps share minimal sequence homology with one another but are predicted to have similar tertiary structures (Fukuhara et al., 2004). Crystal structures have been solved for the importins Kap-β1 and Kap-β2 and for the exportins Xpo1 (Crm1) and Cse1 and, despite their lack of sequence identity, all appear to contain conserved HEAT repeats. Together, the HEAT repeats of kaps assemble to produce a common superhelical twist and despite their divergent roles in nuclear transport, both importins and exportins share the same overall architecture (Cingolani et al., 1999; Chook and Blobel; 1999; Fukuhara et al., 2004; Matsuura and Stewart, 2004; Petosa et al., 2004)). The number of HEAT repeats generally varies from ~18-20 and each HEAT repeat is ~ 40 residues long and form two antiparallel α-helices separated by a turn (Conti et al., 2006). Kap-β1 (Kap95 in yeast) has been crystallized in complex with RanGTP, cargo or with nups (Lee et al., 2003; 2005; Liu and Stewart 2005). Although a structure for unbound Kap-β1 has not has been solved, small angle x-ray scattering studies have suggested that cargo or RanGTP binding induces distinct

conformational changes and that different kaps respond differently to these cues (Fukuhara et al., 2004). Furthermore, these studies imply that β-kaps are inherently flexible and suggest that flexibility is an important element in allowing kaps to interact with cargo, Ran and the NPC during nuclear transport cycles. A dramatic example of kap flexibility is provided by the exportin Xpo1 that, during nuclear export, forms a cooperative trimeric complex with Ran and an export cargo (Fornerod et al., 1997). Structural evidence suggests a model in which a conformational change in the Ran binding domain of Xpo1 is responsible for the cooperativity of Ran-GTP and export substrate binding. In this model, RanGTP binds to the N-terminus of Xpo1 resulting in a conformational change that exposes the cargo-binding site of Xpo1 (Fornerod et al., 1997; Matsuura and Stewart, 2004). This model relies on kap flexibility to allow for simultaneous Ran and cargo binding.

1.5.2 Nuclear Signal Sequences

NPCs, along with kaps, provide the machinery for active transport across the NE with transport rates estimated at ~100 MDa/sec and 10^3 translocation events/sec per NPC (Ribbeck and Görlich, 2001). All molecules that are actively translocated across the NE contain signals that interact with transport factors and this initial interaction defines the first step in nuclear transport. Two classes of localization sequences exist and are classified as nuclear localization or nuclear export sequences (NLSs or NESs, respectively) according to the final destination of the cargo protein to which they belong. cNLSs are characteristically short, lysine-rich sequences that are recognized by kap α of the Kapα/β complex (Kap60p/Kap95p in yeast). Other β kaps recognize their signal

sequences directly but few substrates have been identified for most β kaps, likely a reflection of the diverse substrate binding abilities of these proteins (Cingolani et al., 1999; 2002; Lee et al., 2003). In the case of nuclear export, the exportin Xpo1 has the broadest array of identified substrates. Xpo1 (Crm1) was first identified in *Schizosaccharomyces pombe* as a gene required for normal chromosome structure (Adachi and Yanagida, 1989). Subsequently, Xpo1p was defined as the first nuclear exportin (Stade et al., 1997). The majority of Xpo1p substrates contain a short leucine-rich NES that was first identified in the Rev protein of HIV and the protein kinase A inhibitor (Wen et al., 1995; Fischer et al., 1995). NES binding to Xpo1, and to exportins in general, is greatly enhanced in the presence of RanGTP (Fornerod et al., 1997); however, the affinity of NES cargo for Xpo1 is low and artificial high-affinity NES-Xpo1 complexes are blocked in nuclear export due to retention on the cytoplasmic filaments (Engelsma et al., 2004; Kutay and Güttinger, 2005). These results are consistent with the suggestion that low-affinity Xpo1-NES interactions are crucial for the completion of productive nuclear export cycles. Recent evidence has indicated that, in addition to roles in nuclear transport, Xpo1 is involved in other cellular processes including chromosome segregation and centrosome duplication (Arnaoutov et al., 2005; Wang et al., 2005). Interestingly, Xpo1 targets to kinetochores during M-phase in HeLa cells, and it is thought that here Xpo1 exerts its function in chromosome segregation cooperatively along with Nup358 (RanBP2), Ran-GAP1 and the small G-protein, Ran (Arnaoutov et al., 2005).

Most mRNAs are exported from the nucleus through interactions between the transcription/export (TREX) complex and the export heterodimer, Mex67(TAP)/

Mtr2(p15). This export pathway relies on TREX NES recognition by TAP/p15. Interestingly, recent work has also shown that mRNA themselves can be directly recognized by TAP/p15 and that specific mRNA sequences are sufficient for export (Palazzo et al., 2007). Additionally, mature tRNAs interact directly with exportin-t (Los1p in yeast) in the absence of protein adaptors (Arts et al., 1998; Kuersten et al., 2002). These findings suggest that kaps have a broader substrate repertoire than previously suspected as a result of multiple interaction modalities.

Signal sequences have also been described that serve both to mediate nuclear import of specific factors and additionally target them to their appropriate subnuclear destination (Hatanaka, 1990; Pemberton et al., 1999). The nucleus is organized into discrete compartments that perform specific tasks. This is exemplified by the nucleolus, where rRNA subunits are synthesized and are processed to form mature ribosomal subunits (reviewed in Fromont-Racine et al., 2003). Indeed, certain resident nucleolar proteins, including HTLV-I and HIV-I, contain nucleolar-targeting sequences that serve in delivering proteins to the nucleolus (Hatanaka, 1990). Another example of nuclear organization is provided by chromatin's distinct transcriptional states, the transcriptionally active euchromatin and inactive heterochromatin (Grunstein et al., 1995). TATA-binding protein (TBP) contains a Kap114p-specific NLS that is also required for targeting to double stranded DNA. Interestingly, double stranded TATA-containing DNA assists in releasing TBP from Kap114p in a Ran-GTP-dependent fashion (Pemberton et al., 1999). These discrete domains within the nucleus create a requirement for targeting elements to ensure the adequate protein complement arrives at its

destination. These examples suggest that targeting sequences are important for defining and maintaining subnuclear organization and function.

1.5.3 Ran

The small GTPase Ran is the key regulator of β kap-substrate interactions. While the NPC and kaps provide the mechanics for nuclear transport, Ran is required to provide spatial cues to both import and export complexes. Ran itself is a member of the Ras superfamily of GTPases and is the only known member of this family to be localized predominantly inside the nucleus (Drivas et al., 1990; Moore and Blobel, 1994). Ran exists in two forms determined by the guanine nucleotide that is bound (Fig. 1-2). RanGTP is predominant within the nucleus while RanGDP is found in the cytoplasm. This results in a steep gradient of RanGTP/RanGDP across the NE. Several proteins maintain this gradient, the first of which is the nuclear transport factor exclusive for Ran, Ntf2 (Ribbeck et al., 1998; Smith et al., 1998). This results in the observed accumulation of Ran within the nucleus. In the nucleus, RanGTP is maintained by chromatin-bound RanGEF (Prp20p in yeast) that assists in loading Ran with free GTP (Ohtsubo et al., 1989; Bischoff and Ponstingl, 1991). In the cytoplasm, RanGAP (Rna1p in yeast) enhances the intrinsic GTPase activity of Ran resulting in RanGTP to RanGDP conversion (Bischoff and Ponstingl, 1995). Intriguingly, the Ran gradient, and consequently the direction of transport through the NPC, can be reversed by artificially increasing cytoplasmic levels of RanGTP (Nachury and Weis, 1999). This lends strong

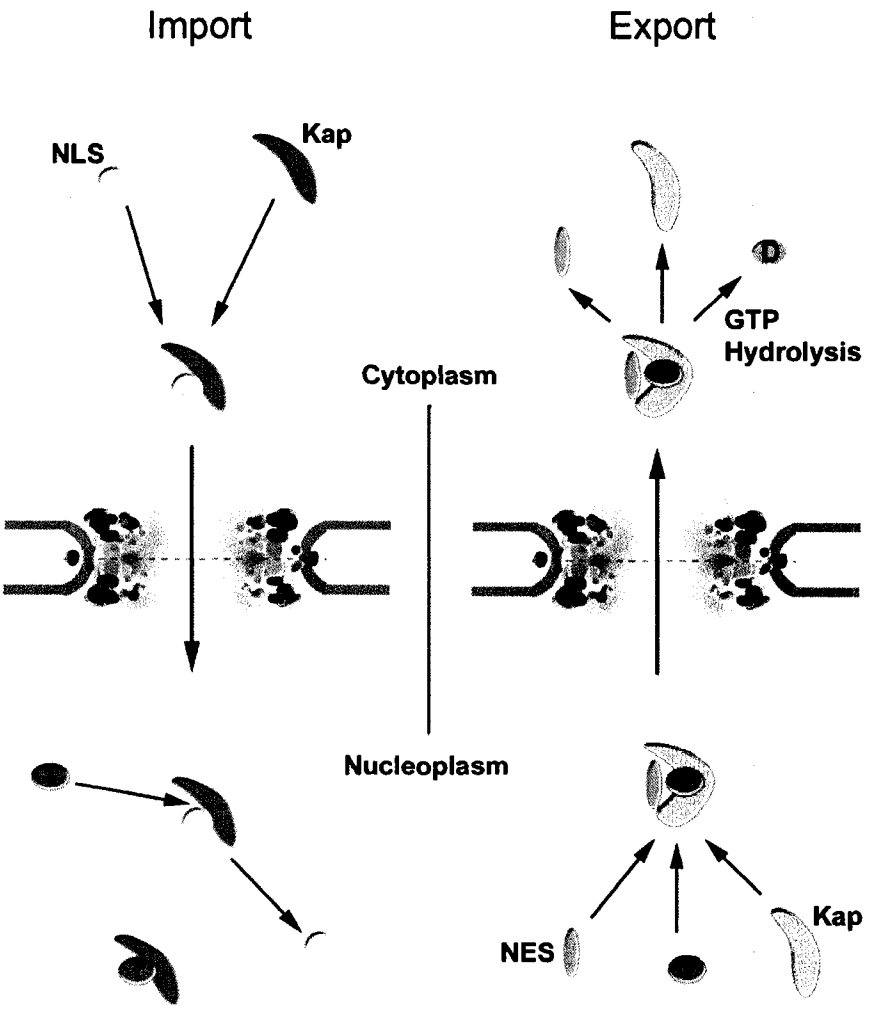

Figure 1-2. The kap-mediated nuclear transport cycle.

Importins (blue) recognize NLS-containing cargos (yellow) in the cytoplasm. The complex then transits through the NPC and in the nucleoplasm encounters high concentrations of GTP-bound Ran (T) resulting in cargo release. Exportins (pink) cooperatively bind RanGTP and NES-containing cargo (green) and are transported through the NPC. In the cytoplasm, the complex encounters RanGAP, enhancing Ran-mediated GTP hydrolysis resulting in RanGDP production (D) and cargo release. Modified from Alber et al., 2007b.

support to the idea that Ran and its nucleotide bound state provide spatial cues for nuclear transport.

While RanGAP is predominantly cytoplasmic, evidence in both yeast and vertebrates suggests that it enters the nucleus and can associate with mitotic kinetochores (Feng et al., 1999; Joseph et al., 2002; Arnaoutov et al., 2005; Nishijima et al., 2006). Consistent with RanGAP shuttling between the nucleus and cytoplasm, *Saccharomyces cerevisiae* RanGAP contains both an NLS and an NES and its export is dependent on the export kap Xpo1p (Feng et al., 1999). This suggests that, within the RanGTP-rich nuclear environment, microdomains of RanGDP exist and may be important for regulating specific processes.

Ran modulates nuclear transport by regulating the formation and dissociation of transport complexes (Görlich and Kutay, 1999; Weis, 2003; Terry et al., 2007). In the cytoplasm, import complexes form between an importin and an import cargo and are stable in the presence of RanGDP. This complex traverses the NPC, and in the nucleoplasm, encounters RanGTP. RanGTP binds to the N-terminus of the importin resulting in a conformational change that changes the affinity of the importin for its cargo (Fig. 1-2, left). This results in cargo release in the nuclear compartment. In contrast, exportin-cargo nuclear export complexes are formed in the nucleoplasm in the presence of and cooperatively with RanGTP (Fornerod et al., 1997). These trimeric complexes transit through the NPC and at the cytoplasmic face of the NPC encounter RanGAP, in vertebrates tethered to the cytoplasmic fibrils via Nup358, stimulating RanGTP hydrolysis to RanGDP (Matunis et al., 1996; Fornerod et al., 1997). This results in the release of cargo in the cytoplasm, completing nuclear export (Fig. 1-2, right).

1.5.3.1 Other roles for Ran

In addition to its well characterized role in nuclear transport, Ran also functions in mitotic spindle assembly and post-mitotic nuclear assembly (Dasso, 2002). In spindle assembly, decreased levels of RanGTP yield low spindle density, and conversely, higher RanGTP levels cause ectopic microtubule proliferation (Zhang et al., 1999; Wilde et al., 2001; Carazo-Salas et al., 2001). Because RanGEF is chromatin-associated, a simple model emerged wherein high RanGTP levels are maintained in proximity to chromosomes. This model is corroborated by fluorescent resonance energy transfer data showing that RanGTP is maintained in the vicinity of *Xenopus* chromosomes during mitosis (Kalab et al., 2002). This was further clarified by several studies that together demonstrated that RanGTP stimulates the release of spindle assemble factors from kapβ1 and kapα surrounding mitotic chromosomes (Gruss et al., 2001; Nachury et al., 2001; Wiese et al., 2001). During metazoan mitosis, the NE is dissolved and the membrane constituents are redistributed throughout the ER. Experiments using *Xenopus* egg extracts suggest a role for Ran early in NE reassembly. NE vesicle fusion on chromatin is severely impaired by depletion of Ran, RanGEF or following addition of a non-hydrolyzable GTP analogue (Hetzer et al., 2000). In addition to its role in post-mitotic NE reformation, RanGTP is also required for *de novo* NPC insertion on both the cytoplasmic and nucleoplasmic sides of the pre-existing NE in both animal cells and yeast (Ryan et al., 2003; D'Angelo et al., 2006).

1.6 Nuclear transport models

NPCs, kaps, and accessory proteins that mediate nuclear transport have been extensively catalogued, revealing a strikingly clear snapshot of the machinery. Despite this insight, the mechanism of translocation through the NPC remains relatively poorly understood. Several models have been proposed, aimed at understanding how the biophysical barrier of the NPC selectively allows nuclear transport while excluding non-cargo molecules. Two models are presented that attempt to explain the NPC as either a physical or an energetic barrier and a final model discusses translocation steps through the NPC.

1.6.1 The Selective Phase

In the selective phase model proposed by Ribbeck and Görlich, the NPC acts as a physical permeability barrier formed by a meshwork of interactions between the FG regions of FG nups (see Section 1.4.2) (Ribbeck and Görlich, 2001). The NPC is thought to be lined by these FG nups, and this model predicts that they would form a gel-like meshwork through intermolecular hydrophobic interactions between FG repeats. This meshwork would only allow the passage of transport receptors due to their inherent affinity for FG nups and their ability to disrupt interactions between nups and partition into the FG-nup meshwork. Support for this model comes from studies showing that nuclear transport is non-directional and energy-independent (Kose et al., 1997; Nakielny and Dreyfuss, 1998; Ribbeck et al., 1998; 1999; Schwoebel et al., 1998; 2002; Englmeier et al., 1999; Nachury and Weis, 1999). Similarly, the permeability barrier of the NPC can be disrupted with aliphatic alcohols that dissolve hydrophobic interactions (Shulga and

Goldfarb, 2003; Ribbeck and Görlich, 2002). Recently, purification and concentration of the FG-domain of Nsp1p was used to form a hydrogel that is dependent on its FG repeats (Frey et al., 2006; Frey and Görlich, 2007). Interestingly, this hydrogel allows the entry of transport receptors while excluding similarly sized inert molecules (Frey and Görlich, 2007). This model, while proposing a palatable mechanism through which the NPC creates a 'selective phase', does not explain how cargo directionality is specified once partitioned into this gel matrix (Bickel and Bruinsma, 2002).

1.6.2 The Virtual Gate

The Virtual Gate model, proposed by Rout and colleagues, suggests that the NPC functions as an energetic barrier that repels non-FG-binding molecules (Rout et al., 2000; 2003; Terry et al., 2007). This model suggests that the NPC is coated on its cytoplasmic and nucleoplasmic faces and lined with flexible FG nups that form an entropic barrier. As in the selective phase model, only molecules with affinity for the FG nups can gain entry to the NPC. In this way, kaps serve an enzymatic role by decreasing the entropic barrier of the NPC. This model is supported by studies showing that the FG nups are natively unfolded and by atomic force imaging demonstrating that the natively unfolded, extended polymer state of FG nups can be collapsed by kap binding (Denning et al., 2002; 2003; Lim et al., 2006; 2007). Once kap-cargo has accessed the NPC, this model suggests that movement through the NPC is mediated by Brownian motion (Rout et al., 2000; 2003).

1.6.3 The Affinity Gradient

In the Virtual Gate model, cargo enters and diffuses through the central channel of the NPC by Brownian motion. How this model can accommodate the massive flow rates NPCs allow is unclear (Ribbeck et al., 2001). The Affinity Gradient model suggests that differences in kap affinity for FG nups allows nuclear transport to proceed down a gradient of nups with increasing affinity for a given kap (Ben-Efraim and Gerace, 2001). Experimental evidence has shown that a kapα–β cargo complex does indeed have increasing affinity for FG nups from cytoplasmically biased nups to nucleoplasmic nups (Pyhtila and Rexach, 2003). The Affinity Gradient model thus proposes that kaps are guided through the NPC by a series of increasingly stronger affinity interactions.

1.7 NPC functions during mitosis

As a clearer picture of the NPC and nuclear transport constituents has emerged, so too has evidence linking the NPC to non-transport related processes. Included in this are several studies linking the NPC with mitotic processes. Physically, the relationship between the NPC and mitosis can be viewed both in terms of NPC proteins that target to or influence mitotic structures or processes and mitotic proteins that associate with NPCs during interphase. In the following section, NPC dynamics during mitosis, nucleoporin localization during mitosis and interphase localization of key mitotic regulators will be discussed.

1.7.1 The NPC and chromosome segregation

Several observations suggest a role for specific nups in chromosome segregation that appear to be independent of their functions in nuclear transport. Notably, yeast strains containing mutations in *NUP170*, an evolutionarily conserved nup, exhibit a chromosome loss phenotype. Moreover, in *NUP170* mutants, transcription of a reporter through an assembled kinetochore was detected, suggesting a defect in kinetochore integrity (Kerscher et al., 2001). These defects were specific for *NUP170* mutants, as mutants in *NUP157*, a paralogue of *NUP170*, did not show similar defects in chromosome segregation and kinetochore integrity. These were the first results directly implicating specific nups in mitotic processes.

1.7.2 The NPC during mitosis

In higher eukaryotes, NE breakdown (NEBD) begins near the entry into mitosis. These nuclear changes including NEBD, chromosome condensation and segregation are among the most cytologically distinguishable events in biology. At this time, NPCs are reversibly disassembled individually and as subcomplexes and are predominantly redistributed throughout the cytosol and ER (Burke and Elenberg, 2002; Hetzer et al., 2005; Terry et al., 2007). Pre-existing subcomplexes are presumably maintained throughout mitosis for reincorporation into newly forming NPCs from telophase onward.

While the majority of nups are redistributed throughout the cytoplasm during mitosis, several exceptions have been noted. A fraction of the evolutionarily conserved Nup107-160 complex (Nup84 complex in yeast) has been found in association with mitotic kinetochores (Belgareh et al., 2001; Enninga et al., 2003; Salina et al., 2003;

Loïodice et al., 2004). Interestingly, the Nup107-160 complex interacts with CENP-F, a kinetochore protein that itself transiently localizes to NPCs immediately preceding NE breakdown (Zuccolo et al., 2007). Nup358 (RanBP2) along with SUMOylated RanGAP1 also relocalize in part to kinetochores and mitotic spindles during mitosis (Joseph et al., 2002). siRNA depletion studies of the Nup170-160 complex have revealed that it lies upstream of the RanGAP1-Nup358 complex at kinetochores (Zuccolo et al., 2007) and, furthermore, that its depletion results in mitotic delay, impaired chromosome congression and reduced kinetochore tension. Additionally, depletion of Nup358 results in the mislocalization of RanGAP1, Mad1, Mad2 and the kinetochore proteins, CENP-E and CENP-F (Joseph et al., 2004). This results in a reduction in stable microtubule-kinetochore attachments suggesting that Nup358 is required for generating competent microtubule-binding kinetochores (Salina et al., 2003; Joseph et al., 2004). A model based on these findings suggests that nucleoporin recruitment to kinetochores constitutes a signal that reports on the status of the NE (Hetzer et al., 2005). Not until the NE has dissolved, releasing nups, can a fully functional kinetochore be assembled for efficient kinetochore-microtubule attachments.

1.7.3 Mitotic proteins at the NPC

During mitosis, the NPC contributes several nups to kinetochores. Reciprocally, several mitotic proteins have been identified at NPCs during interphase. Among these is the kinetochore protein CENP-F (Liao et al., 1995; Fletcher et al., 2003). CENP-F is found in the nucleoplasm throughout G1, S and early G2 phase but transiently localizes to NPCs immediately prior to the G2/M transition marked by NE breakdown. The

functional significance of this interaction is unclear, although CENP-F does partially assist in recruiting the Nup107-160 complex to mitotic kinetochores (Zuccolo et al., 2007).

Mad1 and Mad2, in contrast to all other spindle assembly checkpoint proteins (discussed in Section 1.8), have also been identified in association with NPCs (Campbell et al., 2001; Iouk et al., 2002; Ikui et al., 2002). In vertebrates, Mad1 and Mad2 are associated with NPCs until prometaphase, at which time they are redistributed onto kinetochores. Both proteins are maintained on kinetochores until the metaphase-anaphase transition, suggesting that kinetochore microtubule occupancy is required for their release (Campbell et al., 2001; Shah et al., 2004; Howell et al., 2004). In yeast, Mad1p and Mad2p are maintained at NPCs throughout the cell cycle and are only recruited to kinetochores following microtubule disruption by depolymerising drugs like nocodazole (Iouk et al., 2002). The association of Mad1p and Mad2p with NPCs is partially dependent on Nup53p, and deletion of *MAD1* results in the mislocalization of Mad2p, indicating that the complex is associated with NPCs via Mad1p (Iouk et al., 2002). Interestingly, Mad2p, but not Mad1p, localization at yeast NPCs is dependent on nuclear Ran levels (Quimby et al., 2005).

In addition to its role in the spindle assembly checkpoint, Mad1p also plays a role in NPC function. Yeast cells lacking Mad1p display import defects specific for the kap Kap121p (Iouk et al., 2002). This finding suggests that Mad1p may influence NPC permeability or modulate specific import pathways.

1.8 The Spindle Assembly Checkpoint

While Mad1p and Mad2p are docked at interphase NPCs, their primary role in the cell appears to be in the spindle assembly checkpoint (SAC). During each eukaryotic division, every cell must faithfully segregate its genetic material equally between two new daughter cells. The safety mechanism that monitors this process is the SAC (Fig. 1-3). The SAC was identified in two independent screens designed to establish genes required for wild type yeast to arrest on media containing microtubule depolymerising drugs (Li and Murray, 1991; Hoyt et al., 1991). Identified in this screen were *MAD1*, *MAD2*, *MAD3* (BubR1 in humans) and *BUB1* and *BUB3*. The essential SAC kinase Mps1p was identified in later studies (Hardwick et al., 1996). These genes are conserved throughout evolution and, in all cases studied, are involved in a checkpoint that is active during prometaphase to prevent premature chromosome segregation and the formation of aneuploid cells (Musacchio and Hardwick, 2002; Taylor et al., 2004) (Fig. 1-3). The SAC is discussed below with a particular emphasis on the yeast aspect of this checkpoint.

1.8.1 The origin of the SAC

Following initial studies identifying SAC genes, a hypothesis emerged suggesting that the SAC mediated its effects on cell cycle progression from kinetochores (Li and Murray; 1991; Hoyt et al., 1991; McIntosh, 1991; Gorbsky, 1995). Observations linking the SAC to kinetochores include the findings that mutations in specific kinetochore proteins resulted in SAC-dependent cell cycle arrest (Goh and Kilmartin, 1993; Wang and Burke, 1995; Pangilinan and Spencer, 1996). Furthermore, photoablation of a single

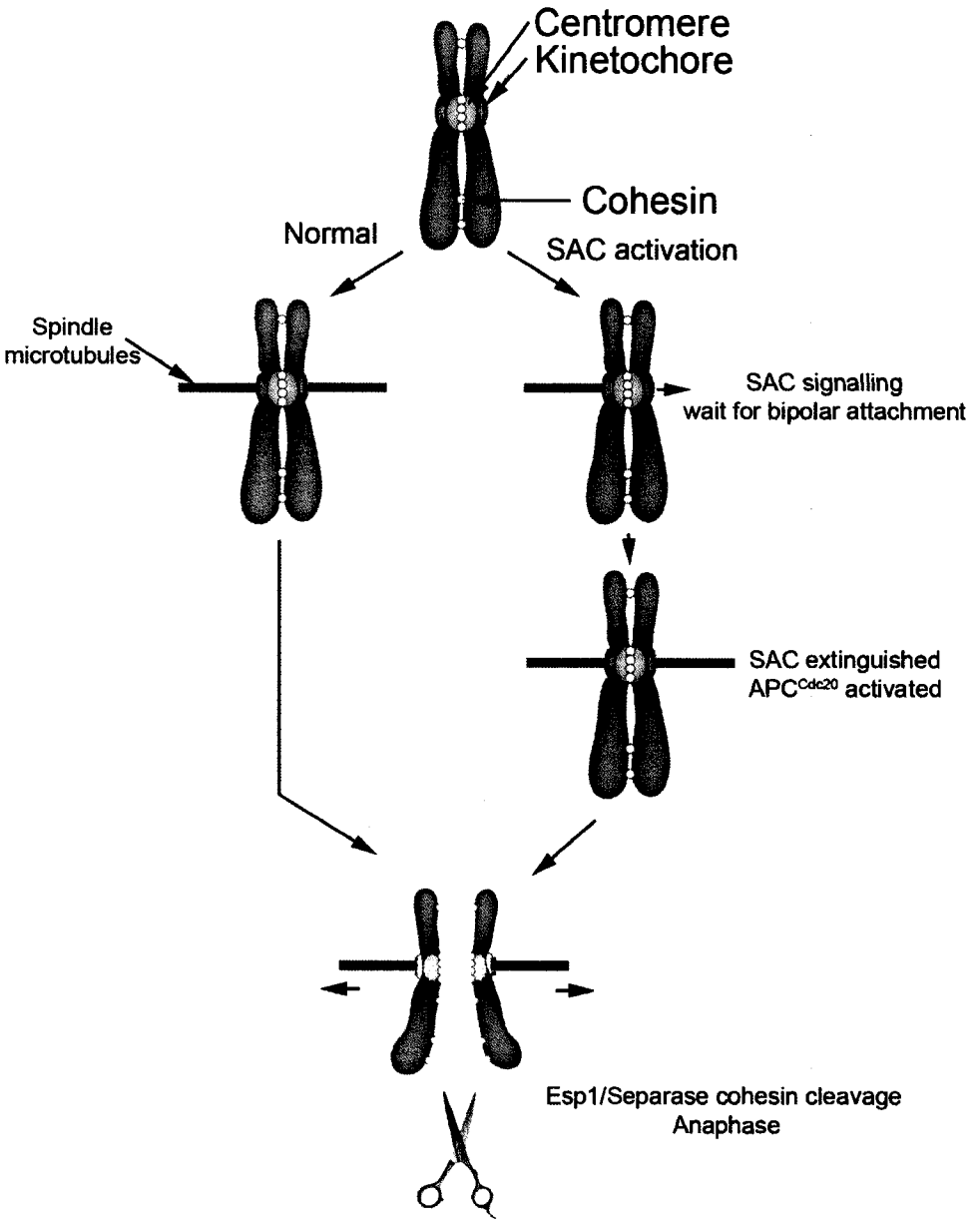

Figure 1-3. The spindle assembly checkpoint.

Unattached kinetochores generate a wait signal until bipolar attachment is achieved. Mad1 and Mad2 are enriched on unattached kinetochores (red) but are depleted as bipolar attachments are achieved (white). After depletion of Mad1 and Mad2 from kinetochores, Cdc20-mediated APC inhibition is alleviated resulting in Esp1/Separase activation, cohesin cleavage and chromosome segregation visualized in anaphase. Modified from Musacchio and Salmon, 2007.

microtubule-kinetochore attachment was sufficient to induce metaphase arrest (Rieder et al., 1994; 1995). This hypothesis was further strengthened when human homologues of SAC proteins were found at unattached kinetochores during mitotic prophase and were dispersed following bipolar attachment of all kinetochores (Chen et al., 1996; 1998; Li and Benezra, 1996; Taylor and McKeon, 1997; Taylor et al., 1998) (Fig. 1-3).

1.8.2 Kinetochore structure and the SAC

A unique feature of eukaryotic chromosomes is the presence of specific chromatin domains called centromeres. Centromeres are defined by the presence of a unique histone H3 variant, Cse4p (CENP-A in humans), and here kinetochores are assembled (Krude, 2002). Kinetochores are multiprotein complexes that form the attachment sites between spindle microtubules and chromosomes (Fig. 1-3). Kinetochores, together with spindle microtubules, are responsible for generating the tension required for chromosome segregation, and provide a platform from which the SAC can signal. EM studies of kinetochores in higher eukaryotes have revealed a trilaminar structure with an electron dense domain tightly apposed to the centromeric DNA, a less dense central plate and a diffusely arranged outer plate that provides kinetochores with microtubule-binding activity (Roos, 1973; McAinsh et al., 2003; De Wulf et al., 2003; Wei et al., 2005). Reflecting their layered architecture, kinetochores are assembled hierarchically, with the CBF3 complex first loading onto centromeric DNA followed by the Ndc80 complex which provides a docking site for microtubule-binding proteins of the outer kinetochore (He et al., 2001; Enquist-Newman et al., 2001; Jones et al., 2001; Janke et al., 2001; 2002; reviewed in McAinsh et al., 2003). It is at the interface between microtubules and

kinetochores that SAC proteins monitor this attachment (Fig. 1-3). The kinetochores of higher eukaryotes bind 30 or more microtubules each, while those of *S. cerevisiae* bind a single microtubule (McDonald et al., 1992; Winey et al., 1995). Despite this apparent reduction in complexity, yeast kinetochores contain at least 60 proteins arranged into multiprotein subcomplexes that are thought to assemble with the same overall trilaminar structure (McAinsh et al., 2003; Tanaka et al., 2005).

1.8.3 SAC proteins at kinetochores

A common characteristic of SAC proteins is their eventual recruitment to kinetochores. In yeast, Bub1p and Bub3p are recruited to kinetochores every cell cycle, while Mad1p and Mad2p are only recruited in the presence of spindle damage or by SAC-activating kinetochore mutations. Mad1p and Mad2p recruitment to kinetochores is dependent on the presence of Bub1p and Bub3p at kinetochores (Iouk et al., 2002; Kerscher et al., 2003; Gillett et al., 2004). In vertebrates, Mad1 and Mad2 are recruited to kinetochores during every cell cycle (Campbell et al., 2001; Shah et al., 2004; Howell et al., 2004). This likely reflects differences in spindle morphogenesis across species, and the stability of the kinetochore-microtubule interaction in yeast which, unlike in vertebrates, rarely, if ever, is broken throughout the cell cycle (Winey and O'Toole, 2001; Tanaka et al., 2002; Gillett et al., 2004). Higher eukaryotes host additional SAC proteins, including ROD, ZW10, ZWILCH (RZZ complex) and $p31^{comet}$ that are thought to be required for Mad1 and Mad2 kinetochore recruitment, monitor tension and play important SAC regulatory roles (Karess and Glover, 1989; Starr et al., 1997; Chan et al., 2000; Scaerou et al., 2001; Williams et al., 2003; Habu et al., 2002; Xia et al., 2004;

Mapelli et al., 2006; Famulski and Chan; 2007). Notably, ROD and ZW10 are enriched at kinetochores lacking tension. This accumulation depends on the activity of Aurora B kinase activity (Famulski and Chan, 2007). These findings lend further support to the idea that ROD and ZW10 function in the branch of the SAC that is thought to detect tension across sister kinetochores.

1.8.4 The anaphase promoting complex and SAC target Cdc20p

The SAC prevents premature chromosome segregation through its inhibition of the anaphase promoting complex/cyclosome (APC/C). The APC is a ubiquitin ligase responsible for ubiquitination of key cell cycle regulators, including cyclin B and securin (Clb2p and Pds1p in yeast, respectively) (King et al., 1995; Ciosk et al., 1998). Following APC-mediated ubiquitination of Clb2p and Pds1p, these proteins are targeted for destruction by the 26S proteasome. Pds1p is an inhibitor of Esp1p/separase, a protease required for cleavage of the cohesin complex that maintains sister chromatid cohesion until the metaphase-anaphase transition (Ciosk et al., 1998; Peters, 2006). Pds1p degradation releases Esp1p, allowing sister chromatid segregation. Similarly, Clb2p degradation inactivates the master mitotic kinase Cdk1/Cdc28p, signalling for mitotic exit (Murray et al., 1989; Rudner et al., 2000; Peters, 2006). As such, the APC represents a key regulator of cell cycle progression. In order to halt premature chromosome segregation, the SAC must signal to and inhibit the APC. To do this, the SAC targets and negatively regulates the APC activator, Cdc20p (Hwang et al., 1998; Kim et al., 1998). A likely SAC effector is the mitotic checkpoint complex (MCC), an evolutionarily conserved complex that contains the SAC proteins Mad2p, Mad3p, Bub3p

and the APC activator, Cdc20p (Hardwick et al., 2000; Sudakin et al., 2001; Tang et al., 2001; Fraschini et al., 2001; Fang et al., 2002; King et al., 2007). Kinetochores are thought to sensitize the APC in order to prolong the interaction with the MCC (Sudakin et al., 2001; Chan et al., 2005). In addition to the SAC proteins in the MCC, Bub1p, Mps1p, Ipl1p/aurora-B and Mad1p are also required to amplify the SAC signal, assist MCC formation and sense the lack of tension across kinetochores (Hardwick et al., 1996; Biggins and Murray; 2001; Musacchio and Salmon; 2007; Famulski and Chan; 2007).

1.8.5 Mad1p and Mad2p in the SAC

In all organisms studied, Mad1p and Mad2p form a complex throughout the cell cycle (Chen et al., 1999; Chung and Chen, 2002). During SAC activation, Mad1p and Mad2p are recruited to kinetochores from the NPC (Campbell et al., 2001; Iouk et al., 2002). Their association with both NPCs and kinetochores is dependent on Mad1p, indicating that Mad1p is required for anchoring the complex to NPCs and for its interaction with kinetochores (Iouk et al., 2002; Chung and Chen; 2002; Gillett et al., 2004). Stoichiometrically, Mad2p is in excess of Mad1p, and all Mad1p appears to be bound by Mad2p, leaving a large unbound pool of Mad2p (Chen et al., 1999; Chung and Chen, 2002). While both Mad1p and Mad2p are recruited to kinetochores during mitosis, several studies from vertebrate model systems indicate that their behaviour on kinetochores is strikingly different. In vertebrates, Mad1 is stably associated with kinetochores. In contrast, Mad2 consists of two kinetochore pools, a stably associated pool and a dynamic pool with rapid turnover rates (Howell et al., 2000; 2004; Shah et al., 2004). During SAC activation, Mad2p is continuously recruited to kinetochores and is

released in a form competent for Cdc20p binding and inhibition as part of the MCC (Howell et al., 2004; Shah et al., 2004).

These findings, along with the unique observation that Mad1-bound Mad2 and free Mad2 have unique structures, have been used to develop two models for SAC activation (Sironi et al., 2002; Luo et al., 2002). The first is the Mad2 exchange model in which kinetochore-bound Mad1 recruits unbound Mad2 [open Mad2 (O-Mad2)] and converts it to closed Mad2 (C-Mad2), competent to bind Cdc20p (Luo et al., 2004). In this model, Mad1p acts as a catalyst in stimulating the conversion of O-Mad2 to C-Mad2. This model is weakened by structural evidence indicating that Mad1 and Cdc20 bind the same pocket of Mad2, implying that Mad1 and Cdc20 compete for Mad2 binding (De Antoni et al., 2005a). Similarly, the exchange model is not consistent with Mad1 and Mad2 forming a tight complex throughout the cell cycle or with the existence of a kinetochore-bound and unbound pool of Mad2 (Chen et al., 1998; Iouk et al., 2002; Chung and Chen, 2002). To accommodate these results, the Mad2 template model incorporates the finding that O-Mad2 and C-Mad2 can bind one another as a conformational dimer (Luo et al., 2004; De Antoni et al., 2005a; 2005b). In this model, Mad1 and C-Mad2 form a stable kinetochore-associated complex. This complex recruits free O-Mad2 and mediates its conversion to C-Mad2 for Cdc20p inhibition. This implies that Mad1-bound C-Mad2 is non-exchanging, while O-Mad2 dynamically associates with kinetochores during its conversion to C-Mad2 (Fig. 1-4). This model has been corroborated experimentally in both HeLa cells and in baker's yeast

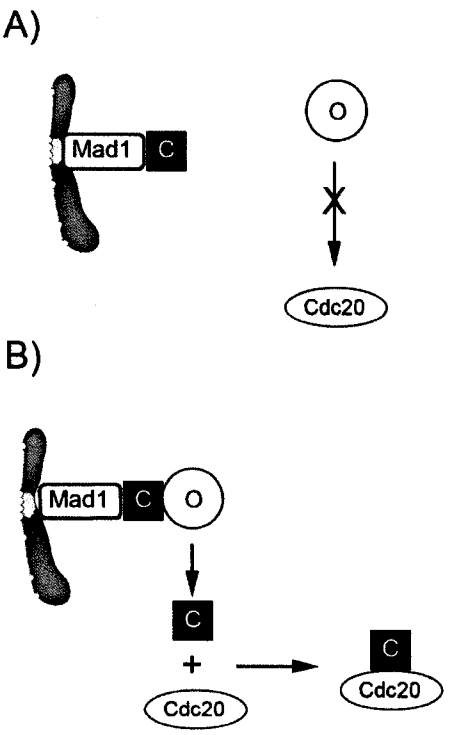

Figure 1-4. The Mad2 template model.

This model proposes a mechanism through which Cdc20-bound Mad2 is created. Two distinct pools of Mad2 exist within the cell: Open (O) and Closed (C). O-Mad2 is not capable of interacting with Cdc20 (A). The Mad2 template model of SAC activation incorporates the findings that C-Mad2 is stably bound to Mad1, and during SAC arrest is targeted to kinetochores. At kinetochores, the Mad1/C-Mad2 template complex recruits free O-Mad2 and aids its conversion to C-Mad2, competent for Cdc20 binding and inhibition of the APC.

using Mad2 mutants incapable of converting from O- to C- or C- to O-, resulting in SAC inactivation (De Antoni et al., 2005a; 2005b; Nezi et al., 2006).

1.9 Thesis Focus

In yeast, Mad1p and Mad2p are NPC-associated throughout the cell cycle. This thesis investigates the functional significance of the association of Mad1p with NPCs and its movement during mitosis from NPCs onto kinetochores. Through deletion and mutational analysis, a presumptive NPC subcomplex-containing Nup60p/Mlp1p/Mlp2p is defined that is required for Mad1p NPC association. We also show that Mad1p is targeted to kinetochores specifically in mitosis. During mitosis, Mad1p dynamically exchanges between kinetochores and NPCs. We show that the exportin Xpo1p is targeted to kinetochores during mitosis and that it is required for the targeting and turnover of Mad1p to kinetochores.

Chapter II: *Experimental Procedures*

2.1 Yeast strains and media

All strains were grown at 30°C in YPD (1% yeast extract, 2% bactopeptone and 2% glucose) unless otherwise noted. Strains propagating plasmids with prototrophic yeast markers were grown in the appropriate synthetic media (SM) containing 2% glucose (Sherman et al., 1983). For both plasmid and integrative transformation, yeast were grown to mid/late log phase (OD_{600} of ~ 0.6-1.4). Cells were harvested by centrifugation (Eppendorf 5810R, 4000 RPM for 1 min) and washed with ddH_20 followed by a 1 M sorbitol wash for osmotic stability. Cells were then concentrated ~ 1000-fold in sorbitol, and 0.1-0.25 μg of plasmid DNA was added to the cell suspension (Becker and Guarente, 1991; Thompson et al., 1998). Suspensions were mixed gently and incubated on ice for 15 min. These suspensions were transferred to a 0.2 cm BioRad electroporation cuvette and electroporated at 1.5 kV, 25 μFD, 200 ohms with a BioRad Gene Pulser. Immediately, 0.2-1.0 mL of cold sorbitol was added to the cuvette and the suspension was plated on the appropriate selective media. To produce Y3020, a *KANR* gene cassette was PCR-amplified using chromosomal DNA isolated from *mad1Δ* as a template (Giaever et al., 2002). The 5' sense oligonucleotide annealed at -402 (where A of the *MAD1* ATG start codon is +1) to -382, and the 5' antisense oligonucleotide annealed at +2619 to 2639. The resulting PCR product was transformed as above into BY4741 yeast and the deletion of *MAD1* in the resulting transformants was confirmed by both PCR and western blot analysis with anti-Mad1p antibodies. For a list of all yeast strains used in this thesis, see Table 2-1. To produce the strains Y3149, Y3150 and Y3153, AvrII-cut pRS305 MAD1, pRS305mad1-L569A and pRS305mad1-

L575A, respectively, were transformed into Y3145 and selected on SM lacking uracil. *URA+* colonies were selected and confirmed by PCR and western blotting.

Endogenous genomic integrations of the *GFP*$^+$, *RFP* and *pA* ORFs were done in haploid yeast strains (BY4741, BY4742 or YPH499). For these integrations, oligonucleotides designed to anneal to sequences within the plasmids pGFP$^+$/HIS5, pGFP$^+$/Nat^R, pRFP/HIS, pRFP/ Nat^R or pDW01 to amplify *GFP*$^+$, *RFP* and *pA*, respectively, with appropriate selectable markers. These oligonucleotide primers were designed with 60 bp 5' overhangs that annealed to regions 120-60 bp upstream and 60-120 bp downstream of the endogenous stop codon within the gene of interest.

Correct integration of each GFP, RFP or pA fusion was confirmed by western blotting using antibodies directed against Mad1p, Xpo1p, Nup60p, Nup53p (Marelli et al., 1998) or GFP. The correct integration and synthesis of Mtw1-RFP and Spc42-RFP was confirmed microscopically.

Table 2-1. Yeast Strains

Name	Genotype	Reference
BY4741	*MATa his3Δ1 leu2Δ0 met15Δ0 ura3Δ0*	Brachmann et al. 1998
Y3028	*MATa his3Δ1 leu2Δ0 met15Δ0 ura3Δ0 MAD1-GFP::HIS5 (BY4741)*	This study
Y3029	*MATa his3Δ1 leu2Δ0 met15Δ0 ura3Δ0 MAD1-1-325-GFP::HIS5 (BY4741)*	This study
Y3030	*MATa his3Δ1 leu2Δ0 met15Δ0 ura3Δ0 MAD1-1-250-GFP::HIS5(BY4741)*	This study
Y3020	*MATa his3Δ1 leu2Δ0 met15Δ0 ura3Δ0 mad1::KanMX (BY4741)*	This Study
Y3021	*MATa his3Δ1 leu2Δ0 met15Δ0 ura3Δ0 mad1::HIS5 (BY4741)*	This Study

Name	Genotype	Reference
mad1Δ	*MATα his3Δ1 leu2Δ0 lys2Δ0 ura3Δ0 mad1::KanMX (BY4742)*	Giaever et al., 2002
YMB1911	*MATa ura3-52 lys2-801 his3-200 leu2-3,112 trp1-1 mad1::kanMX (DF5)*	This Study
Y3031	*MATa his3Δ1 leu2Δ0 met15Δ0 ura3Δ0 mad1::KanMX MTW1RFP::HIS5 (BY4741)*	This Study
DF5a	*MATa ura3-52 lys2-801 his3-200 leu2-3,112 trp1-1*	
kap121-34	*MATa ura3-52 lys2-801 his3-200 leu2-3,112 trp1-1 kap121::HIS3::LEU2 pkap121-34::TRP1 (DF5)*	Leslie et al., 2002
kap95-14	*MATa ura3-52 lys2-801 his3-200 leu2-3,112 trp1-1 kap95::HIS3 pkap95-14::TRP1 (DF5)*	Leslie et al., 2002
Y3032	*MATa ura3-52 lys2-801 his3-200 leu2-3,112 trp1-1 kap95::HIS3 pkap95-14::TRP1 mad1::KanMX (DF5)*	This study
CPL32	*MATa his3Δ1 leu2Δ0 met15Δ0 ura3Δ0 nup53::kanMX (BY4741)*	This study
nup59Δ	*MATα his3Δ1 leu2Δ0 lys2Δ0 ura3Δ0 nup59::KanMX (BY4742)*	Giaever et al., 2002
nup170Δ	*MATα his3Δ1 leu2Δ0 lys2Δ0 ura3Δ0 nup170::KanMX (BY4742)*	Giaever et al., 2002
nup157Δ	*MATα his3Δ1 leu2Δ0 lys2Δ0 ura3Δ0 nup157::KanMX (BY4742)*	Giaever et al., 2002
Y3034	*MATα his3Δ1 leu2Δ0 lys2Δ0 ura3Δ0 nup60::KanMX (BY4742)*	This study
nup2Δ	*MATα his3Δ1 leu2Δ0 lys2Δ0 ura3Δ0 nup2::KanMX (BY4742)*	Giaever et al., 2002
pom34Δ	*MATα his3Δ1 leu2Δ0 lys2Δ0 ura3Δ0 pom34::KanMX (BY4742)*	Giaever et al., 2002
gle1Δ	*MATα his3Δ1 leu2Δ0 lys2Δ0 ura3Δ0 gle1::KanMX (BY4742)*	Giaever et al., 2002
nup42Δ	*MATα his3Δ1 leu2Δ0 lys2Δ0 ura3Δ0 nup42::KanMX (BY4742)*	Giaever et al., 2002
gle2Δ	*MATα his3Δ1 leu2Δ0 lys2Δ0 ura3Δ0 gel2::KanMX (BY4742)*	Giaever et al., 2002
nup120Δ	*MATα his3Δ1 leu2Δ0 lys2Δ0 ura3Δ0 nup120::KanMX (BY4742)*	Giaever et al., 2002
nup100Δ	*MATα his3Δ1 leu2Δ0 lys2Δ0 ura3Δ0 nup100::KanMX (BY4742)*	Giaever et al., 2002
nup188Δ	*MATα his3Δ1 leu2Δ0 lys2Δ0 ura3Δ0 nup188::KanMX (BY4742)*	Giaever et al., 2002

Name	Genotype	Reference
nup116Δ	*MATα his3Δ1 leu2Δ0 lys2Δ0 ura3Δ0 nup116::KanMX (BY4742)*	Giaever et al., 2002
pom152Δ	*MATα his3Δ1 leu2Δ0 lys2Δ0 ura3Δ0 pom152::KanMX (BY4742)*	Giaever et al., 2002
mlp1Δ	*MATα his3Δ1 leu2Δ0 lys2Δ0 ura3Δ0 mlp1::KanMX (BY4742)*	Giaever et al., 2002
mlp2Δ	*MATα his3Δ1 leu2Δ0 lys2Δ0 ura3Δ0 mlp2::KanMX (BY4742)*	Giaever et al., 2002
mlp1Δ mlp2Δ	*MATα his3Δ1 leu2Δ0 lys2Δ0 ura3Δ0 mlp1::KanMX mlp2::natR (BY4742)*	This study
Y3036	*MATα his3Δ1 leu2Δ0 lys2Δ0 ura3Δ0 nup2::KanMX MAD1-GFP::HIS5 (BY4742)*	This study
Y3037	*MATα his3Δ1 leu2Δ0 lys2Δ0 ura3Δ0 pom34::KanMX MAD1-GFP::HIS5 (BY4742)*	This study
Y3040	*MATa his3Δ1 leu2Δ0 met15Δ0 ura3Δ0 nup60::KanMX MAD1-GFP::HIS5 (BY4741)*	This study
Y3068	*MATa his3Δ1 leu2Δ0 met15Δ0 ura3Δ0 nup59::KanMX (BY4741)*	This study
Y3058	*MATa his3Δ1 leu2Δ0 met15Δ0 ura3Δ0 nup60::KanMX (BY4741)*	This study
Y3057	*MATa his3Δ1 leu2Δ0 met15Δ0 ura3Δ0 nup60::KanMX MAD1-GFP::HIS5 MTW1-RFP::NatR (BY4741)*	This study
Y3061	*MATα his3Δ1 leu2Δ0 lys2Δ0 ura3Δ0 mlp1::KanMX mlp2::natR MAD1-GFP::HIS5 (BY4742)*	This study
Y3062	*MATa his3Δ1 leu2Δ0 met15Δ0 ura3Δ0 nup60::KanMX MAD1-GFP::HIS5 MLP2-RFP::NatR (BY4741)*	This study
Y3064	*MATα his3Δ1 leu2Δ0 lys2Δ0 ura3Δ0 mlp1::KanMX mlp2::natR MTW1-RFP::HIS5 (BY4742)*	This study
Y3065	*MATα his3Δ1 leu2Δ0 lys2Δ0 ura3Δ0 mlp1::KanMX MAD1-GFP::HIS5 (BY4742)*	This study
Y3066	*MATα his3Δ1 leu2Δ0 lys2Δ0 ura3Δ0 mlp2::KanMX MAD1-GFP::HIS5 (BY4742)*	This study
Y3067	*MATα his3Δ1 leu2Δ0 lys2Δ0 ura3Δ0 nup53::KanMX MAD1-GFP::HIS5 (BY4742)*	This study
CPL61	*MATa ura3-52 lys2-801 ade2-101 his3-200 trp1-63 leu2-1 GAL1-NmycMPS1 (YPH499)*	This study

Name	Genotype	Reference
CPL62	*MATa ura3-52 lys2-801 ade2-101 his3-200 trp1-63 leu2-1 GAL1-NmycMPS1 nup53Δ::kanMX (YPH499)*	This study
CPL63	*MATa ura3-52 lys2-801 ade2-101 his3-200 trp1-63 leu2-1 GAL1-NmycMPS1 nup59Δ::kanMX (YPH499)*	This study
CPL64	*MATa ura3-52 lys2-801 ade2-101 his3-200 trp1-63 leu2-1 GAL1-NmycMPS1 mad1Δ::kanMX (YPH499)*	This study
YVG5	*MATa leu2-3,112 his3-11,15 trp1Δ ade2-1 ura3-1 MLP1:: pA-HIS5*	Galy et al., 2004
YVG7	*MATa leu2-3,112 his3-11,15 trp1Δ ade2-1 ura3-1 MLP2:: pA-HIS5*	Galy et al., 2004
Y3161	*MATa his3Δ1 leu2Δ0 met15Δ0 ura3Δ0 nup60::LEU2 kap95::kanR Mad1-GFP+::hphR Mtw1-RFP::natR pkap95-14*	This study
Y3116	*MATa his3Δ1 leu2Δ0 met15Δ0 ura3Δ0 nup60::LEU2 msn5::kanR Mad1-GFP+::hphR Mtw1-RFP::natR*	This study
Y3156	*MATa his3Δ1 leu2Δ0 met15Δ0 ura3Δ0 nup60::LEU2 kap95::kanR Mad1-GFP+::hphR Mtw1-RFP::natR pkap95-14*	This study
Y3091	*mata ade2-101 his3D200 tyr1 prp20-7 ura3-52 Mad1-GFP::natR nup60::kanR Mtw1-RFP::HIS5*	This study
Y3151	*MATa his3Δ1 leu2Δ0 met15Δ0 ura3Δ0 nup60::LEU2 Mad1-GFP+::natR::URA3 Mtw1-RFP::HIS5*	This study
Y3152	*MATa his3Δ1 leu2Δ0 met15Δ0 ura3Δ0 nup60::LEU2 mad1-L575A-GFP+::natR::URA3 Mtw1-RFP::HIS5*	This study
Y3154	*MATa his3Δ1 leu2Δ0 met15Δ0 ura3Δ0 nup60::LEU2 mad1-L569A-GFP+::natR::URA3 Mtw1-RFP::HIS5*	This study
Y3101	*MATa his3Δ1 leu2Δ0 met15Δ0 ura3Δ0 Xpo1::HIS3 Spc42-RFP::natR*	This study
Y3109	*MATa his3Δ1 leu2Δ0 met15Δ0 ura3Δ0 Xpo1::HIS3 Mtw1-RFP::HIS5*	This study

Name	Genotype	Reference
Y3095	*MATa ura3-52 lys2-801 ade2-101 trp1-delta63 his3-delta200 leu2-delta1 nup60::kanR Mad1-GFP::natR Mtw1-RFP::HIS5 gsp1-G21V::URA3*	This study
Mad1-pA	*MATa ura3-52 lys2-801 his3-200 leu2-3,112 trp1-1 Mad1-pA::HIS5*	This study

2.2 Plasmids

The following plasmids were provided by others and used for work in this thesis: pPho4-NLS (pPho4$_{140\text{-}166}$-GFP$_3$; EBO836) and pACPho4-GFP (gifts from the laboratory of Dr. Erin O'Shea, University of California, San Francisco, San Francisco, CA) (Kaffman et al., 1998); pKW440 (*XPO1*), pKW457 (*xpo1-1*), pKW711 (*xpo1-T539C*) and pNLS-GFP-NES (gifts of Dr. Karsten Weis, University of California, Berkeley, Berkeley, CA).

The inserts in the following plasmids were all made using PCR with the Expand High Fidelity PCR system (Roche). pMad1-NLS-GFP$_3$ was constructed by digesting pPho4$_{140\text{-}166}$—GFP$_3$ (Kaffman et al., 1998) with BglII and EcoRI, releasing the nucleotides encoding Pho4$_{140\text{-}166}$. A PCR product encoding Mad1 residues 499-533 (bi-partite NLS plus 6 flanking residues N and C-terminally) was introduced into this backbone with BglII and EcoRI linkers [note: ΔNLS constructs were deleted from the first residue of the predicted bipartite NLS (K506) to the last (K527)]. Plasmid-borne *GFP* fused to *MAD1* truncations were made by digesting the CEN/*URA3* plasmid pACPHO4-GFP (Kaffman et al., 1998) with BglII and EcoRI to remove *PHO4* and inserting individual *MAD1* cDNAs with BamHI and EcoRI linkers. These included the following plasmids (note: nucleotides of *MAD1* are shown in parentheses where 1 is the

A of the ATG start codon): pMad1-GFP, p*250-325-GFP* (750-975), p*318-749-GFP* (954-2247) and p*475-749-GFP* (1425-2247). Plasmids expressing the *MAD1* ORF fragments lacking the NLS were similarly constructed from two separate DNA fragments and inserted into pRS316 or pACPHO4-GFP to produce the plasmids p*mad1-ΔNLS-GFP*, p318-749-ΔNLS-GFP and p475-749-ΔNLS-GFP. *MAD1* gene fragments were inserted into the pYEX-BX plasmid (2μ/*URA3*) (BD Biosciences Clontech, San Jose, CA) to produce pMad1, p*mad1-ΔNLS,* p1-325, p318-749 and p475-749. The *MAD1* cDNAs were inserted into pGEX-6P-1 (Amersham Biosciences, Baie D'Urfé, Quebec, Canada) to produce pGEX-Mad1 (1-2250), pGEX-1-325 (1-975), pGEX-318-749 (954-2250), and pGEX-475-749 (1425-2250). The plasmids pGFP$^+$/HIS5 and pRFP/HIS5 were constructed by removing *GFP* from pGFP/HIS5 (Dilworth et al., 2001) and replacing it with the *GFP*$^+$ ORF (Scholz et al., 2000) (a gift from Dr. Michael Niederweis, Erlangen, Germany) or the *RFP* ORF (a gift of Dr. Ray Truant, McMaster University, Canada). The plasmid pRFP/Nat^R was a gift from Dr. Richard Rachubinski, University of Alberta. The plasmids p*NUP53* and p*NUP53ΔKBD* are based on pRS315 that includes the *NUP53* promoter region with a BamHI site immediately 5' and in-frame with the ATG start codon and the *NUF2* terminator with a BamHI site at its 5' end. Briefly, the wild type *NUP53* ORF was amplified by PCR and inserted using BamHI linkers. *NUP53ΔKBD* was PCR-amplified with BamHI linkers from pΔ405–430-GFP (Lusk et al., 2002).

pSV40-NLS/Mad1-NES-GFP$_3$ was constructed by digesting pPho4$_{140\text{-}166}$-GFP (Kaffman et al., 1998), with BglII and EcoRI liberating the nucleotides encoding Pho4$_{140\text{-}166}$. A PCR product encoding the SV40 NLS (PKKKRKV) and Mad1 residues 563-576

separated by an NheI site was introduced into this backbone with BglII and EcoRI linkers. The sequences of the oligonucleotides used in making this construct were 5': GCAGCAGATCT***CCTAAGAAGAAGCGTAAGGTA***GCTAGCCAGCTACTACAAGA AAAA and 3': GCAGCGAATTCGAAGGGGCCGTCACGTAA, where the bold italicized residues indicate the SV40 NLS coding sequence. Point mutations of the NES (L569A and L575A) were introduced using the Stratagene QuikChange II XL site directed mutagenesis kit. The oligonucleotide pair used to introduce the L569A mutation were 5': GAGTAAAGCACAAACTACAATTCAGCTACTACAAGAAAAAGCAGA AAAGTTAACTAAACTAAAG and 3': CTTTAGTTTAGTTAACTTTTCTGCTTT TTCTTGTAGTAGCTGAATTGTAGTTTGTGCTTTACTC and for the L575A mutation were 5': CAATTCAGCTACTACAAGAAAAATTAGAAAAGTTAACTAAAGCAA AGGAGAAAAAAATACGTATA and 3': TATACGTATTTTTTTCTCCTTTGCTTTA GTTAACTTTTCTAATTTTTCTTGTAGTAGCTGAATTG. Plasmids for integrating *MAD1*, *mad1-L569A* and *mad1-L575A* were produced by digesting a fragment of *MAD1* from pRS316 Mad1 (Scott et al., 2005) with HindIII and SacII. This fragment was ligated into the HindIII and SacII sites of cut pRS306. The resulting plasmids pRS306-Mad1, pRS306-mad1-L569A and pRS306-mad1-L575A were subsequently cut with AvrII to direct their integration to the endogenous *MAD1* locus. Plasmids encoding *XPO1* (pKW440), *xpo1-1* (pKW457), *xpo1-T539C* (pKW711) and the NLS-GFP-NES construct were a generous gift of Dr. Karsten. The *GSP1* and *gsp1-G21V* integrating plasmid were made by amplifying *GSP1* from wild type genomic DNA and *gsp1-G21V* from the plasmid pRS424 Gsp1 G21V with BamHI linkers (a gift from Dr. Pamela Silver, Harvard University) and ligating the fragments into pRS306 GAL1/CYC1

(pTM1012) (a gift from Dr. Tadashi Makio, University of Alberta). These plasmids were subsequently cut with StuI to direct their integration to the *URA3* locus. A GST-Xpo1 construct used for antibody production was produced as follows. *XPO1* was PCR-amplified from wild type yeast genomic DNA with BamHI linkers. This fragment was ligated into pGEX 6P1 yielding pGEX 6P1 Xpo1.

2.3 Antibodies

Antibodies against Nup170p, Mad1p, Mad2p, Gsp1p, Xpo1p and GFP were all raised in rabbits. Plasmids expressing GST fusions of each of the above proteins (see Section 2.2) (except for GST-Nup170-M, Central fragment, Dr. C. P. Lusk, University of Alberta, unpublished construct) were transformed into BL21 Codon *Escherichia coli* and induced as follows: 50 ml cultures of pGEX-6P1-Mad1, pGEX-6P1-Mad2 and pGEX-6P1-Xpo1 were grown to an OD_{600} of 1.0 at 37°C in 2 x YT media (1.6% tryptone, 1.0% yeast extract and 0.5% NaCl) and then shifted to 23°C. Expression of the fusions was induced by the addition of 0.5 mM IPTG for 3 h. 50 ml cultures of pGEX-Gsp1 and pGEX-6P1-GFP were grown to an OD_{600} of 0.75 at 37°C and induced with 0.1 mM IPTG for 1 h at 23°C. 100 ml cultures of pGEX4T1-Nup170-M (aa 538-1106) were grown at 23°C to an OD_{600} of 1.0 and induced for 6 h with 1.0 mM IPTG. In all cases, cells were pelleted by centrifugation at 2250 x *g* (Eppendorf 5810R, 4000 RPM for 10 min) and resuspended in 15 mL of Lysis Buffer A (See Table 2-2) supplemented with 0.3 M NaCl and placed on ice. Lysozyme (0.67 mg/ml) was added to the resuspended culture and cells were incubated on ice for an additional 15-30 min. The lysates were then vigorously sonicated (Branson 250 Sonifier at output level 6 with 90% duty cycle for 3-6

sets, 30 sec each set) until the lysates became fluid. Lysates were then transferred to JA17 centrifuge tubes and were

Table 2-2. Buffers

Buffer	Composition
Lysis Buffer A	50 mM Tris-HCl, pH 7.5, 150 mM KOAc, 1 mM MgOAc, 0.1% Nonidet-40 and 10% glycerol
SDS-PAGE sample buffer	50 mM Tris-HCl, pH 6.8, 5% SDS, 0.25% bromophenol blue, 25% glycerol
PBS	137 mM NaCl, 2.7 mM KCl, 4.3 mM Na_2HPO_4, 1.4 mM KH_2PO4, pH 7.4

cleared at 11,300 x *g* for 15 min at 4°C. With the exception of GST-Nup170-M, the cleared supernatants were then incubated with pre-equilibrated glutathione sepharose beads at 4°C for 1.5 h. The beads were then washed extensively with Lysis Buffer A (Table 2-3), and each of the fusions was cleaved from GST with PreScission protease (Amersham Bioscience), 2-10 U, in a total volume of 100-500 µl. The GST-Nup170-M construct was largely insoluble and concentrated in inclusion bodies. The inclusion was extracted twice with B-PER Bacterial Protein Extraction Reagent (Pierce) for 15 min on ice, and the extract was used directly for immunization. The integrity and quantity of each recombinant protein was determined by staining with Coomassie Blue Stain (BioRad BioSafe Coomassie) and an initial 200-1000 µg of antigen in Freund's Complete Adjuvant (Sigma) and subsequent boosts of 50-500 µg in Freund's Incomplete Adjuvant (Sigma) were injected into New Zealand White Rabbits. Antibody titres were monitored monthly using wild type, GFP tagged ORFs, with knockouts for positive and negative controls. These antibodies and others used in this thesis are listed in Table 2-3.

Table 2-3. Antibodies

Antibody Reactivity	Antibody name (Rabbit ID)	Antigen	Dilution (Western blot)	Optimal bleed	Reference
Nup170p	1 D 6	GST-Nup170-M (aa 538-1106)	1/500 in PBST, preabsorbed against *nup170Δ* acetone powder	Final	This study
Mad1p	3 I 4	GST-Mad1	1/2000 in PBST	4th-Final	This study
Mad2p	1 E 2	GST-Mad2	1/500 in PBST	3rd	This study
Xpo1p	9_2	Xpo1 (cleaved from GST-Xpo1)	1/1000 in PBST	1st-Final	This study
GFP	3 B 4	GFP (cleaved from GST-GFP)	1/5000 in PBST	3rd-Final	This study
Nup53p	H174	Nup53 (Cleaved from GST-Nup53)	1/5000 in PBST	Final	Marelli et al., 1998
Nup60p	4_5	Nup60 (Cleaved from GST-Nup60)	1/2000 in PBST	Final	D.W. Van de Vosse
Clb2p	Clb2 (y-180): sc-9071	aa 1-180 of Clb2p	1/1000 in PBST	Final	Santa Cruz Biotech

2.4 Protein Purification

2.4.1 GST fusion preparation and Nup53p purification

5 ml cultures of *E. coli* Rosetta* (Lutzmann et al., 2002) transformed with the plasmid pG6P1-NUP53 (pGEX-6P1 backbone) (Lusk et al., 2007) or plasmids expressing GST fusions (GST-Mad1, GST-Mad1-1-325, GST-Mad1-318-749 and GST-Mad1-475-

749) were grown overnight to late log phase and 0.5 ml was subcultured into 50 ml 2YT, grown at 37°C to an OD_{600} of 1.0 and induced with 0.5 mM IPTG for 6 h at 25°C. Cells were collected by centrifugation, resuspended in 15 mL of Lysis Buffer A containing 10 mg lysozyme and swollen on ice. Cells were then lysed, and DNA was sheared by vigorous sonication. The resulting lysate was then clarified by centrifugation at 11,300 x *g* for 15 min at 4°C. The cleared supernatant was then incubated with 50 µl pre-equilibrated glutathione sepharose for 1 h at 4°C with gentle inversion. Following binding, beads were washed 6 times with 1 mL Lysis Buffer A. A final 1 mL wash with Lysis Buffer A supplemented with 12.5 mM $MgSO_4$ and 8.8 mM ATP was incubated at 37°C for 10 min to aid in the release of copurifying heat shock proteins. To produce pure Nup53p, glutathione beads with bound GST-Nup53 were resuspended in a volume of 150 µl and incubated with 10 U of PreScission Protease (Amersham Biosciences), which recognizes a human rhinovirus cleavage site between GST and Nup53p. Cleavage proceeded for 3 h at 4°C. For long-term storage, Nup53p was snap frozen in $N_{2(l)}$.

2.4.2 Nup60p purification for Figure 7-2

Nup60p was purified using the same method as that used for Nup53p except that inductions were conducted for 3 h at 23°C.

2.5 *In vitro* binding experiments

In vitro binding experiments using Nup53p, Nup60p (Fig. 7-2) and immobilized GST-Mad1 fragments were performed as follows: GST, GST-Mad1, GST-Mad1-1-325,

GST-Mad1-318-749 and GST-Mad1-475-749 were purified according to Section 2.4.2. 5 μg of GST or GST-Mad1 fusions immobilized on glutathione sepharose beads (~10 μl) were then incubated with ~ 10 μg of purified recombinant Nup53p or Nup60p for 1 h at 4°C. Following binding, the supernatant was sampled, and the beads were washed extensively with Lysis Buffer A. Bound proteins were eluted with SDS-PAGE sample buffer and resolved by SDS-PAGE. Proteins were visualized with Biosafe Coomassie (BioRad).

2.6 DAPI staining

For experiments monitoring cell cycle progression of nup mutants in nocodazole, cells were arrested in G1-phase with 10 μg/ml α-factor and released into nocodazole at room temperature. Cells were sampled at 20 min intervals and fixed in 70% ethanol. Cells were washed and stained for ~10 min with 1 μg/ml 4',6-diamidino-2-phenylindole (DAPI).

2.7 Western blotting

For western blotting, proteins were initially resolved by SDS-PAGE with 6-12% acrylamide-containing gels in BioRad Mini Protean III units. Proteins were transferred to nitrocellulose membranes using BioRad Mini Trans-Blot cells. Post-transfer membranes were initially stained with 1 x amido black, then washed extensively in H_2O to remove excess amido black. Membranes were then blocked with 5% skim milk powder in PBS-T (PBS containing 0.1% Tween-20) for 1 h. Primary antibodies listed in Table 2-2 were used to detect yeast proteins and GFP by probing membranes for 0.75-1.5 h at room

temperature or overnight at 4°C in PBS-T + 5% skim milk. Membranes were washed extensively in PBS-T following removal of the primary antibody. HRP-conjugated donkey anti-rabbit secondary antibodies were used to detect primary rabbit antibodies (at a 1/10000 dilution in PBS-T + 5% skim milk), and the ECL system was used to amplify HRP luminescence (both from Amersham Biosciences). Exposure times were between 30 sec and 5 min.

2.8 Cell cycle arrest

All cell cycle arrest experiments were performed in YPD media. For G1 arrests, cells were grown to OD_{600} of 0.3 (early log phase) and were arrested with 10 μg/ml α-factor (BioVectra) for 2 h at 30°C. G1 arrest was confirmed microscopically by monitoring schmooing percentage. Cells were harvested by centrifugation and washed twice with one volume of YPD . Cells were released at 23°C either in the presence of absence of nocodazole.

To arrest cells in G2/M with microtubule disruption, cells were treated with nocodazole at a final concentration of 12.5 μg/ml and were incubated at 23°C or 37°C. Arrest efficiency was determined by microscopically monitoring the percentage of large budded cells.

For G2/M arrests using *cdc26Δ* strains, cells were grown to an OD_{600} of 0.5 at 23°C and were shifted to 37°C. Arrests proceeded for 3 h and again, arrest was monitored microscopically. For experiments where nocodazole was added to *cdc26Δ* arrested strains, nocodazole was added at 2.5 h.

2.9 Mps1 overexpression

The plasmid encoding *GAL1-NmycMPS1* (pAFS120) was a gift of Dr. Mark Winey (University of Colorado, Boulder, Colorado). The strain YPH499 was a gift of Dr. Munira Basrai (National Institutes of Health, Bethesda, Maryland). Mps1p overexpression was performed as outlined in Hardwick et al., 1996. Briefly, strains harbouring inducible *GAL1-MPS1* were grown overnight in YP containing 2% raffinose to an OD_{600} of ~0.3. Cells were arrested in G1-phase with 10 μg/ml α-factor for ~2 h and transferred to YP containing 2% raffinose and 3% galactose containing 10 μg/ml α-factor for another 2 h. Cells were released into the cell cycle by washing two times with YP containing 2% raffinose and 3% galactose. Samples were taken every 20 min for the duration of the experiment and fixed in 70% ethanol. Cell morphology was observed using light microscopy.

2.10 Fluorescence microscopy

All images of GFP and RFP fusion proteins were acquired in live cells using either an Olympus BX-50 fluorescence microscope equipped with a SPOT digital camera, an Olympus IX-81 fluorescence microscope equipped with an Olympus IX2-UCB digital camera, or with a confocal microscope (LSM510) (Carl Zeiss MicroImaging). Yeast strains harbouring plasmid-borne fusions were grown to early log phase in the appropriate dropout media and then transferred to YPD for 2-3 h. Cells were then examined directly or following treatment with 12.5 μg/ml nocodazole for 1.5-2.5 h to arrest in G2/M phase. The subcellular distribution of Mad1-NLS-GFP_3 was examined

directly in logarithmically growing cells. Alternatively, cells expressing Mad1-NLS-GFP_3 were treated with 10 mM NaN_3 and 100 mM 2-deoxyglucose for 30 min at 30°C (Shulga et al., 1996; Iouk et al., 2002). Cells were then washed with CM-URA media (without glucose) and examined immediately. To examine the effects of metabolic poisons on the distribution of Mad1-GFP in G2/M-phase arrested cultures, logarithmically growing cells were first arrested in G1-phase with α-factor and released into 12.5 μg/ml nocodazole for 1 h in YPD, washed twice with YP (no glucose), and then incubated for 10 min at 30°C in YP containing 12.5 μg/ml nocodazole, 10 mM NaN_3 and 100 mM 2-deoxyglucose prior to examination.

All images acquired with an LSM510 confocal microscope were acquired as follows: to excite GFP, an Ar/2 (Argon) laser line emitting 488 nm light was used. Fluorescent emission was collected with a long pass filter (LP 505 nm). For colocalization of Mad1-GFP with Mtw-RFP or Xpo1-GFP with Spc42-RFP or Mtw1-RFP, GFP was again excited with the Ar/2 laser's 488 nm light but was collected with a bandpass filter (BP 505-530 nm). RFP was excited with a He (Helium) 543 nm laser, and the resulting fluorescence was collected with a long pass filter (LP 560 nm). The optical depth of all images is 0.7 μm.

2.11 Laser photobleaching of Mad1-GFP

The strain Y3057 was grown to an OD_{600} of ~0.3 and arrested in G1-phase using α-factor for 2 h at 30°C. Cells were harvested and washed in YPD twice before release into YPD containing 12.5 mg/ml nocodazole at room temperature. After 1 h, cells were washed and resuspended in CM-URA containing 12.5 mg/mL nocodazole. 1.2 mL of

cell suspension was applied to a microscope slide with a thin agarose pad (Fagarasanu et al., 2005; Adames et al., 2000) and sealed with valap. The initial scan employed both 488 and 543 nm light lines and was used to colocalize Mad1-GFP with Mtw1-RFP. Subsequent images did not employ the 543 nm laser line (except for the final image). Kinetochore-associated Mad1-GFP was specifically bleached with 50 iterations of full intensity 488 nm light. Images were acquired every 12 sec for the duration of each experiment. Metamorph software was used to delineate concentric regions around both the kinetochore-Mad1-GFP focus and the Mlp-associated Mad1-GFP focus, and integrated fluorescent values were determined and background subtracted. Data were initially logged to Microsoft Excel and then to Kaleidagraph. The first order rate constant, k, corresponds to the slope of a best-fit line through the points described by $-LN[(F_{max}-F_{(t)})/(F_i-F_0)]$, where F_{max} is the bleached region at maximal recovery (Howell et al., 2004). The half-time of fluorescence recovery, $t_{1/2}$, is calculated according to $t_{1/2}=\ln 2/k$. Strains for photobleaching (Y3057, Y3116 and Y3156) were grown to an OD_{600} of ~0.3 and arrested in G1-phase using α-factor for 2 h at 30°C. Cells were harvested and washed in YPD twice before release into YPD containing 12.5 mg/mL nocodazole at room temperature. After 75 min, cells were washed and resuspended in CM-URA containing 12.5 mg/mL nocodazole, except for Y3156 which was treated for an additional 15 min with 100 ng/mL leptomycin B (Sigma-Aldrich, Oakville, Ontario, Canada). 1.2 μL of cell suspension was applied to a microscope slide with a thin agarose pad (Fagarasanu et al., 2005; Adames et al., 2000) and sealed with valap. Y3091 (*prp20-7*) and Y3161 (*kap95-14*) were treated similarly except cells were shifted to 37°C for 30 min in the continued presence of nocodazole to inactivate prp20p or kap95p. Cells were

then placed on a heated stage for imaging. Y3096 (*gsp1-G21V*) cells grown in YP raffinose were arrested in G1 and released into nocodazole for 60 min but were then shifted to YP Raf/Gal to induce *gsp1-G21V* overexpression for 90 min. In all cases, the initial scan used both 488 and 543 nm light lines and was used to colocalize Mad1-GFP with kinetochores (Mtw1-RFP). Subsequent images did not employ the 543 nm laser line. Kinetochore-associated Mad1-GFP was specifically bleached with 15 iterations of full intensity 488 nm light. Images were acquired every 15 sec throughout duration of each experiment.

2.12 Affinity purification of pA fusions

2.12.1 For Figure 3-9

Mlp1p and Mlp2p (YVG5 and YVG7, respectively) were C-terminally tagged with *Staphylococcus aureus* protein A (pA) and immunopurified from yeast whole cell lysates as previously described (Dilworth et al., 2001) with the following modifications: (1) cell disruption was achieved by grinding cell pellets under $N_{2(l)}$ using the procedure described by Schultz et al. (1997); (2) Lysate clarification consisted solely of low-speed centrifugation at 5000 x *g* for 15 min at 4° C; (3) After binding, the IgG sepharose beads were washed 5 times with 10 mL of wash buffer containing 50 mM $MgCl_2$ to remove unbound proteins, and proteins that remained bound were eluted by the addition of SDS-PAGE sample buffer.

2.13 Xpo1p inhibition with Leptomycin B

Yeast cells harbouring the plasmid pKW711 (*xpo1-T539C*) were grown to an OD_{600} of 0.5 in YPD. One mL of cells was harvested and Leptomycin B was added to a final concentration of 100 ng/mL (Neville and Rosbash, 1999). Leptomycin B activity (Xpo1p nuclear export inhibition) was assayed using the NLS-GFP-NES reporter Stade et al., 1997).

2.14 Sequence alignments

Alignments of the PKI and HIV Rev NESs with the NES of Mad1p were done manually and using the online general purpose multiple sequence alignment tool ClustalW at the European Bioinformatics Institute at: http://www.ebi.ac.uk/Tools/clustalw/index.html.

Chapter III: *Interactions between Mad1p and the Nuclear Transport Machinery in the Yeast Saccharomyces cerevisiae**

* This work was reproduced from Scott, R.J., Lusk, C.P., Dilworth, D.J., Aitchison, J.A. and R.W. Wozniak. (2005). **Interactions between Mad1p and the nuclear transport machinery in the yeast Saccharomyces cerevisiae.** *Molecular Biology of the Cell.* 16(9):4362-74 by copyright permission of Garland Publishing, Incorporated.

3.1 Overview

In addition to its role in nucleocytoplasmic transport, the NPC acts as a docking site for proteins whose apparent primary cellular functions are unrelated to nuclear transport, including Mad1p and Mad2p, two proteins of the SAC. To understand this relationship, we have mapped domains of yeast *S. cerevisiae* Mad1p that interact with the nuclear transport machinery, including further defining its interactions with the NPC. We showed that a Kap95p/Kap60p dependent NLS, positioned in the C-terminal third of Mad1p, is required for its efficient targeting to the NPC. At the NPC, Mad1p interacts with Nup53p and a presumed Nup60p/Mlp1p/Mlp2p complex through two coiled-coil regions within its N-terminus. When the SAC is activated, a portion of Mad1p is recruited to kinetochores through an interaction that is mediated by the C-terminal region of Mad1p and requires energy. We showed using photobleaching analysis that in nocodazole-arrested cells, Mad1p rapidly cycles between the Mlp proteins and kinetochores. Our further analysis also showed that only the C-terminus of Mad1p is required for SAC function and that the NPC, through Nup53p, may act to regulate the duration of the SAC response.

3.2 Results

3.2.1 Regions of Mad1p that mediate its interactions with the NPC and kinetochores

Mad1p is a member of a group of proteins that function in the SAC (Lew and Burke, 2003). We have previously shown that the majority of Mad1p localizes to NPCs throughout the cell cycle (Iouk et al., 2002). Notably, Mad1-GFP is excluded from the region of the NE directly overlaying the nucleolus (Appendix Fig. 7-1). In an effort to determine the functional significance of the association of Mad1p with the NPC and other components of the nuclear transport machinery, we constructed a series of Mad1p deletion mutants to define domains responsible for anchoring Mad1p to the NPC and targeting it to kinetochores. Our truncation mutants were, in part, designed to evaluate the function of three predicted coiled-coil domains positioned within amino acid residues 57-221, 264-320, and 390-585 (Fig. 3-1).

The subcellular distributions of the Mad1p truncations were evaluated by C-terminally tagging various deletion mutants with GFP and monitoring their localization using confocal microscopy. The distribution of each of the truncations was evaluated in asynchronous cultures and cells arrested with nocodazole in G2/M-phase (Fig. 3-2A). Nocodazole destabilizes microtubules, causing an activation of the SAC machinery and subsequent cell cycle arrest. Under these conditions, most of the visible Mad1p remains associated with the NPC, while a pool of Mad1p appears to be recruited to kinetochores (Iouk et al., 2002; Gillett et al., 2004). To produce the GFP chimeras of full-length Mad1p and the C-terminal deletions containing amino acid residues 1-250 and 1-325, the

Figure 3-1. Truncation mutants of Mad1p.

A schematic of N- and C-terminal truncations of Mad1p is shown. Amino acid residues are shown on the left. The SMART domain annotation resource (Schultz et al., 1998) predicts Mad1p contains three coiled-coil domains highlighted in black with bordering residues indicated. The amino acid sequence of the Mad1p NLS and its position (hatched region) are shown.

GFP ORF was chromosomally integrated following the appropriate codon into the endogenous *MAD1* gene to produce the Mad1-GFP, 1-250-GFP, or 1-325-GFP fusions. N-terminal deletions of *MAD1* encoding amino acid residues 250-325, 318-749 and 475-749 were fused in frame with the *GFP* ORF, assembled in a yeast *CEN* plasmid, and introduced into a *mad1Δ* strain. Cellular levels of the plasmid encoded fusion proteins were similar or slightly higher than endogenous GFP-tagged Mad1p, while the integrated *1-250-GFP* and *1-325-GFP* chimeras produced higher levels of protein.

As previously shown, Mad1-GFP localized in a punctate pattern along the nuclear periphery, consistent with its NPC association, in both asynchronous and G2/M-arrested cells (Fig. 3-2A) (Iouk et al., 2002). Similarly, we observed that 1-325-GFP, containing the first and second predicted coiled-coil regions of Mad1p, also concentrated at the nuclear periphery. The NPC association of this region was dependent on both predicted coiled-coil regions, as the first (1-250-GFP) or the second (250-325-GFP) coiled-coil region alone exhibited severely reduced or undetectable levels of NE signal, respectively. Instead, these constructs were distributed throughout the cell (Fig. 3-2A).

The NE signal observed with the 1-325-GFP construct also appeared reduced with higher levels of cytoplasmic signal as compared to Mad1-GFP, suggesting that the C-terminus of Mad1p may contribute to its association with the NPC. To evaluate this possibility, we examined the localization of N-terminal deletion mutants. Both 318-749-GFP and 475-749-GFP accumulated in the nucleus, but lacked any obvious NPC association (Fig. 3-2A). Interestingly, 475-749-GFP was also visible at a single intranuclear focus in asynchronous cultures (Fig. 3-2A). This pattern was also visible in cells arrested in G1 using α-factor or in G2/M following SAC activation induced by microtubule

Figure 3-2. *In vivo* localization of Mad1p truncation mutants.

A) The ORF encoding GFP was integrated after specific codons within the endogenous *MAD1* gene in the strain BY4741 to produce chimeric ORFs encoding full-length Mad1-GFP (Y3028), 1-325-GFP (Y3029), and 1-250-GFP (Y3030). *GFP*-tagged N-terminal deletions of *MAD1* encoding the truncation 250-325-GFP (pMad1-250-325-GFP), 318-749-GFP (pMad1-318-749-GFP), or 475-749-GFP (pMad1-475-749-GFP) in a *CEN/URA3* plasmid were introduced into *mad1Δ* cells (Y3021). Strains were grown to mid-log phase at 30°C and viewed directly (asynchronous (AS) cultures) or arrested in G2/M by treatment with 12.5 μg/mL nocodazole (NOC) for ~ 2 and then examined. Arrows indicate intranuclear foci and arrowheads indicate approximate nuclear position in representative cells. Fluorescent images were captured using a confocal microscope. Note, in addition to a diffuse nuclear signal, foci of 318-749-GFP and 475-749-GFP signal colocalized with the kinetochore marker Mtw1-RFP in 13% and 61% of asynchronous cells and 62% and 83% of nocodazole arrested cells, respectively. B) Cells producing the tagged kinetochore protein Mtw1-RFP (Y3031) and either 318-749-GFP or 475-749-GFP were arrested in G1-phase using α-factor or in G2/M-phase by treatment with 12.5 μg/mL nocodazole (Noc). Images of the two fluorescent proteins were obtained as in A. Merged images are shown in the right panels. Bars, 5 μm.

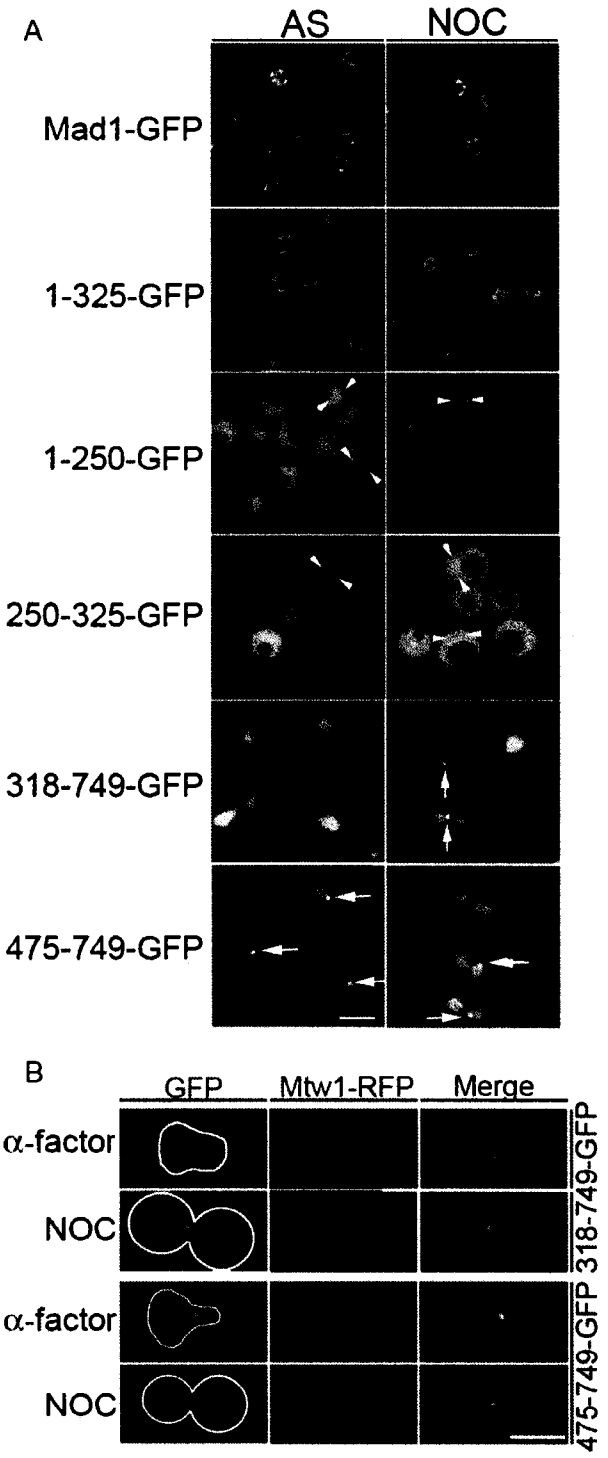

Figure 3-2. *In vivo* localization of Mad1p truncation mutants.

depolymerization using nocodazole (Figs. 3-2A and 3-2B). Coexpression with *MTW1-RFP,* encoding a kinetochore marker (Goshima and Yanagida, 2000), revealed that 475-749-GFP colocalized with kinetochores throughout the cell cycle and upon SAC activation. In contrast, 318-749-GFP was diffusely distributed throughout the nucleoplasm with no visible focal concentration in most cells grown asynchronously or arrested with α-factor (Figs. 3-2A and 3-2B). Upon SAC activation, 318-749-GFP colocalized with kinetochores (Fig. 3-2B). These results suggested that the region contained within residues 318-475 regulates the SAC-induced association of Mad1p with the kinetochores.

3.2.2 Mad1p contains a cNLS that is required for its efficient targeting to the NPC

We hypothesized that an NLS could play a role in the efficiency of Mad1p targeting to the NPC and into the nucleus, in much the same way that an NLS-like region functions in the efficient targeting of Nup53p (Lusk et al., 2002) and the SUMO deconjugating enzyme Ulp1p (Panse et al., 2003) to NPCs. An NLS functioning in a similar manner and positioned in the third coiled-coil region of Mad1p might explain the decrease in NPC targeting of the 1-325 truncation and the nuclear accumulation of both the 318-749 and 475-749 truncations. A potential bipartite NLS (amino acid residues 506-527) was previously recognized by sequence analysis of Mad1p (Hardwick and Murray, 1995). To test whether this region functions as an NLS, a 499-533-GFP_3 chimera containing the NLS and three tandemly repeated *GFP* ORFs was expressed in yeast and the distribution of the fusion protein was evaluated by confocal microscopy. As shown in Fig. 3-3A, this reporter concentrated in the nucleus. Moreover, its nuclear accumulation was dependent

on energy, as treatment of cells with the metabolic poisons 2-deoxy-D-glucose and sodium azide (Shulga et al., 1996) inhibited its nuclear accumulation (Fig. 3A). These data confirmed that this region of Mad1p is capable of functioning as an NLS.

Due to the resemblance of the Mad1-NLS to a consensus bipartite, cNLS (Robbins et al., 1991; Makkerh et al., 1996), we predicted that its cognate kap receptor was the heterodimer Kap60p/Kap95p. To address this possibility, we examined the localization of 499-533-GFP in cells harbouring a temperature-sensitive allele of *KAP95, kap95-14* (Leslie et al., 2002), as well as a separate kap mutant (*kap121-34*) (Leslie et al., 2002). The 499-533-GFP accumulated in the nucleus in wild type and *kap121-34* cells at 23°C and non-permissive temperature (37°C) (Fig. 3-3B). However, it was unable to accumulate in the nucleus of *kap95-14* cells at 37°C, suggesting that the Kap95p/Kap60p complex plays an integral role in its import.

We also examined if the cNLS of Mad1p and the Kap95p/Kap60p complex function in the efficient localization of Mad1p to the NPC. First, we compared the subcellular distribution of Mad1-GFP with a mutant mad1p protein lacking the NLS. Plasmid-borne genes encoding both proteins were introduced into *mad1Δ* cells and Western blotting confirmed that both proteins were produced at similar levels (Fig. 7-6). As shown in Fig. 3-3C, Mad1-GFP was detected exclusively at the nuclear periphery, while mad1ΔNLS-GFP showed increased levels of cytoplasmic fluorescence in addition to that visible at the NE, suggesting that mad1ΔNLS-GFP was inefficiently targeted to NPCs.

If the cNLS region of Mad1p functions in conjunction with kaps to facilitate the association of Mad1p with the NPC, a mutation in Kap95p or Kap60p that inhibits import would also alter Mad1p localization. This was what we observed. In a *kap95-14*

Figure 3-3. Mad1p contains a functional NLS.

A) The nucleotides encoding amino acid residues 499-533 of Mad1p were inserted upstream of the ORFs encoding three tandemly repeated GFPs in the plasmid pMad1-NLS-GFP_3 (Mad1-NLS-GFP_3) and introduced into wild type yeast cells (BY4741). The localization of Mad1-NLS-GFP_3 was then visualized using a confocal microscope before (Untreated) and after treatment with the metabolic poisons 2-deoxy-D-glucose and sodium azide (+2DG/N_3). B) Import of the Mad1p NLS requires Kap95p. pMad1-NLS-GFP_3 plasmid was introduced into a wild type strain (DF5) and the temperature-sensitive kap mutants *kap121-34* and *kap95-14*. Localization of the NLS was examined at 23°C and 2.5 h after shifting cells to 37°C. C) The NLS of Mad1p is required for the efficient localization of Mad1p to the NPC. Plasmids harbouring *MAD1-GFP* (pMad1-GFP; +NLS) or *mad1ΔNLS-GFP* (p*mad1ΔNLS-GFP*; -NLS) were introduced into a *mad1Δ* strain (Y3021) and the localization of the fusion proteins was visualized with a confocal microscope. D) Kap95p is required for the efficient localization of Mad1p to the NPC. A plasmid encoding Mad1-GFP was introduced into *mad1Δ* (YMB1911) and *mad1Δkap94-14* (Y3032) strains. Localization of Mad1-GFP was compared in these two strains at 23°C and after cells were shifted to 37°C for 2.5 h. Bars, 5 μm.

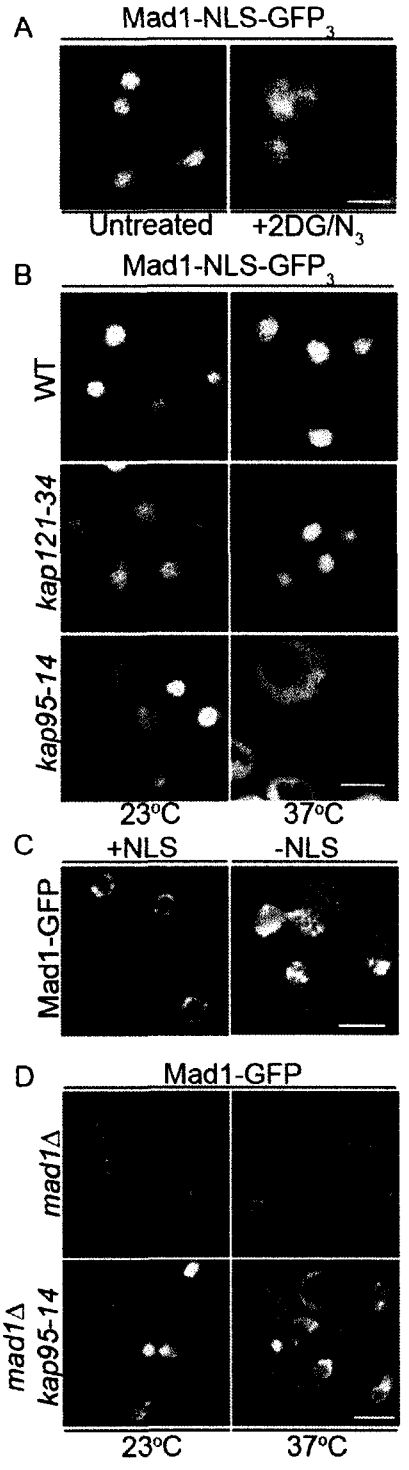

Figure 3-3. Mad1p contains a functional NLS.

strain, which exhibits import defects at both permissive (23°C) and non-permissive temperatures (37°C) (Leslie et al., 2002), Mad1-GFP showed a similar distribution as that observed with the mad1ΔNLS-GFP protein, including increased cytoplasmic fluorescence (Fig. 3-3D). Moreover, we observed significant numbers of cells where Mad1-GFP had accumulated in the nucleus, suggesting that a loss of Kap95p function did not completely prevent its access to the nucleoplasm, but clearly altered its ability to concentrate at the nuclear periphery.

3.2.3 Binding sites for Mad1p at the NPC

Once targeted to the NPC, the N-terminal regions of Mad1p (residues 1-325) mediated its interactions with the NPC. We have previously shown that the interactions of Mad1p with the NPC are, in part, mediated by its physical interactions with a subcomplex of nups containing Nup53p (Iouk et al., 2002). Using *in vitro* binding assays, we examined whether Mad1p and its truncations were capable of interacting directly with Nup53p. For these experiments, recombinant GST-Mad1p, GST-1-325, GST-318-479, GST-475-749, and GST alone were synthesized in *E. coli*, purified, and immobilized on glutathione-Sepharose beads. With the exception of the GST-Mad1p fusion, which was partially degraded, the bead-bound fraction consisted predominantly of a single species. As shown in Fig. 3-4A, recombinant Nup53p bound to GST-Mad1p and GST-1-325, but only weakly to GST-318-749. Nup53p failed to bind GST-475-749 and GST alone (Figs. 3-4A and B). Moreover, GST-Mad1p failed to bind recombinant Nup170p, another member of the Nup53p-containing subcomplex in similar experiments. We conclude

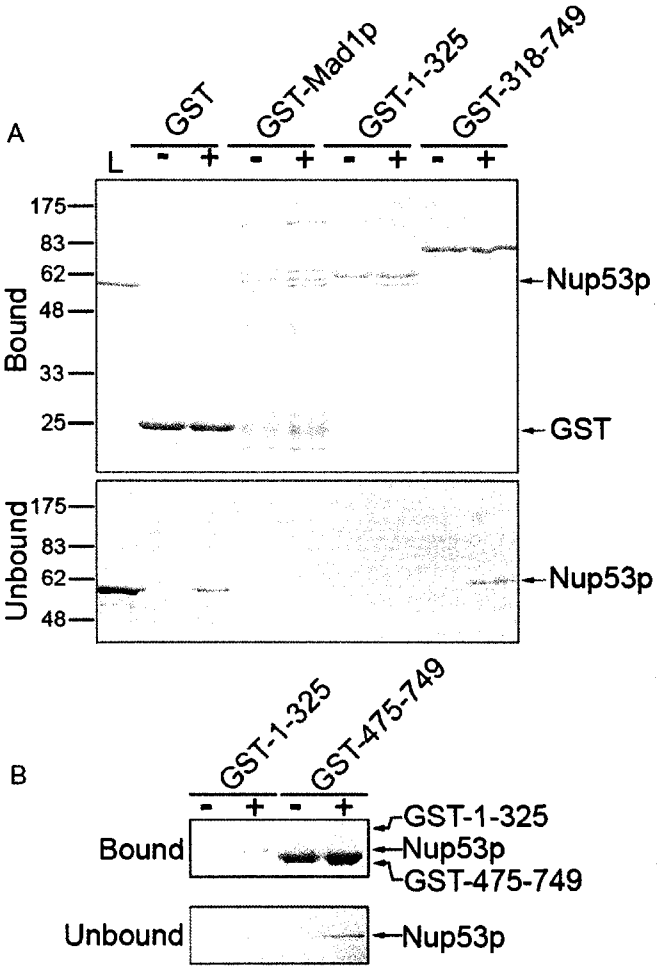

Figure 3-4. Nup53p binds directly to Mad1p.

A) The recombinant proteins GST, GST-Mad1p, GST-1-325 or GST-318-749 were synthesized in *E. coli* (BL21) and purified using glutathione sepharose beads. The bead-bound proteins were incubated with (+) or without (-) purified, recombinant Nup53p (L). Following this, the unbound fraction was collected, the beads were washed, and the bound fraction was eluted with SDS-PAGE sample buffer. Proteins present in equivalent proportions of the bound and unbound fractions were resolved using SDS-PAGE and visualized with Coomassie blue staining. Molecular mass markers in kilodaltons are shown on the left. B) Binding experiments were conducted using GST, GST-1-325 or GST-475-749 and Nup53p as described in (A). Note, GST-475-749 failed to bind Nup53p and was present in the unbound fraction. The lack of Nup53p in the bound fractions was only visible after extended periods of electrophoresis when the mobility of Nup53p is sufficiently different from that of GST-475-749 protein.

from these results that the 1-325 region of Mad1p that binds the NPC (Fig. 3-2A) is also capable of binding Nup53p.

Neither Nup53p nor a structurally related nup, Nup59p, function as the sole binding site for Mad1p at the NPC. We have shown that null mutations of *NUP53* or *NUP59* contain NPC-associated Mad1p at slightly reduced (Iouk et al., 2002) or near wild type levels (Fig. 3-5A). In an attempt to define other nups that bind to Mad1p, we examined the localization of Mad1p in various nup null mutants. Of the ~30 *NUP* genes in yeast, the majority can be individually deleted without resulting in a lethal phenotype (Giaever et al., 2002). Of these, we detected a subset of nup and NPC-associated mutants that exhibited altered growth characteristics on media containing the microtubule-destabilizing drug benomyl. These data are summarized in Table 3-1. In each case, these null mutants showed an increased resistance to the growth inhibition caused by benomyl. One possible explanation for these results is that the SAC is altered in these mutants. In addition to mutations in genes that encode members of the Nup53p-containing complex (Iouk et al., 2002), three mutant strains, *nup60Δ*, *nup2Δ*, and *pom34Δ*, showed an increased resistance to growth inhibition caused by benomyl. Using these results as a guide, we focused on examining the effects of these null mutations on the localization of Mad1p. Deletion of the *POM34* or *NUP2* gene had no obvious effect on the association of Mad1p with the NPC (Fig. 3-5A). In contrast, the NE concentration of the Mad1-GFP was eliminated in the *nup60Δ* mutant. The localization of Nup53p, however, was not affected in these cells. Mad1-GFP was instead concentrated at a single intranuclear focus, which did not colocalize with the kinetochore marker Mtw1-RFP in asynchronous cultures (Fig. 3-5B).

Figure 3-5 The localization of Mad1-GFP is altered in mutants of *nup60Δ*, *mlp1Δ* and *mlp2Δ*.

A) The *GFP* ORF was integrated following the last amino acid codon of the chromosomal copy of *MAD1* in haploid strains containing null mutations in *NUP53* (*nup53Δ*), *POM34* (*pom34Δ*), *NUP2* (*nup2Δ*), *NUP60* (*nup60Δ*), *MLP1* (*mlp1Δ*), *MLP2* (*mlp2Δ*) and the *MLP1 MLP2* double mutant (*mlp1Δmlp2Δ*) to produce the strains Y3067, Y3037, Y3036, Y3040, Y3065, Y3066, and Y3061, respectively. Logarithmically growing cultures of these strains and an isogenic wild type counterpart (Y3028) were examined by fluorescence microscopy and images were acquired using a confocal microscope. B) The localization of Mad1-GFP was examined in the *nup60Δ* strain. Logarithmically growing asynchronous (AS) *nup60Δ* cells expressing genomically integrated *MAD1-GFP* and *MTW1-RFP* (Y3057) were directly visualized. Note, RFP and GFP foci did not colocalize. Y3057 cells were also synchronized in G1 with α-factor and then released into media containing 12.5 μg/mL nocodazole at 25°C. Cells were examined 60 min after addition of nocodazole. Arrows in the merged panel point to foci where Mtw1-RFP colocalizes with Mad1p-GFP. In cells containing two GFP and two RFP foci, colocalization of two foci is observed in 94% of cells. C) In asynchronous cell cultures of the *nup60Δ* mutant, Mad1p colocalizes with Mlp2p. Logarithmically growing *nup60Δ* cells expressing genomically integrated *MAD1-GFP* and *MLP2-RFP* (Y3062) were visualized using fluorescence microscopy. Arrows indicate colocalization of Mad1-GFP with Mlp2-RFP in the merged panel. D) Localization of Mad1-GFP in a *mlp1Δmlp2Δ* mutant. The plasmid pMad1-GFP was introduced into an *mlp1Δmlp2Δ* double mutant containing a genomically integrated *MTW1-RFP* (Y3064). Mad1-GFP and Mtw1-RFP were visualized in this background in both asynchronous (AS) and in cells treated with 12.5 μg/mL nocodazole for 2 h. Bars, 5 μm.

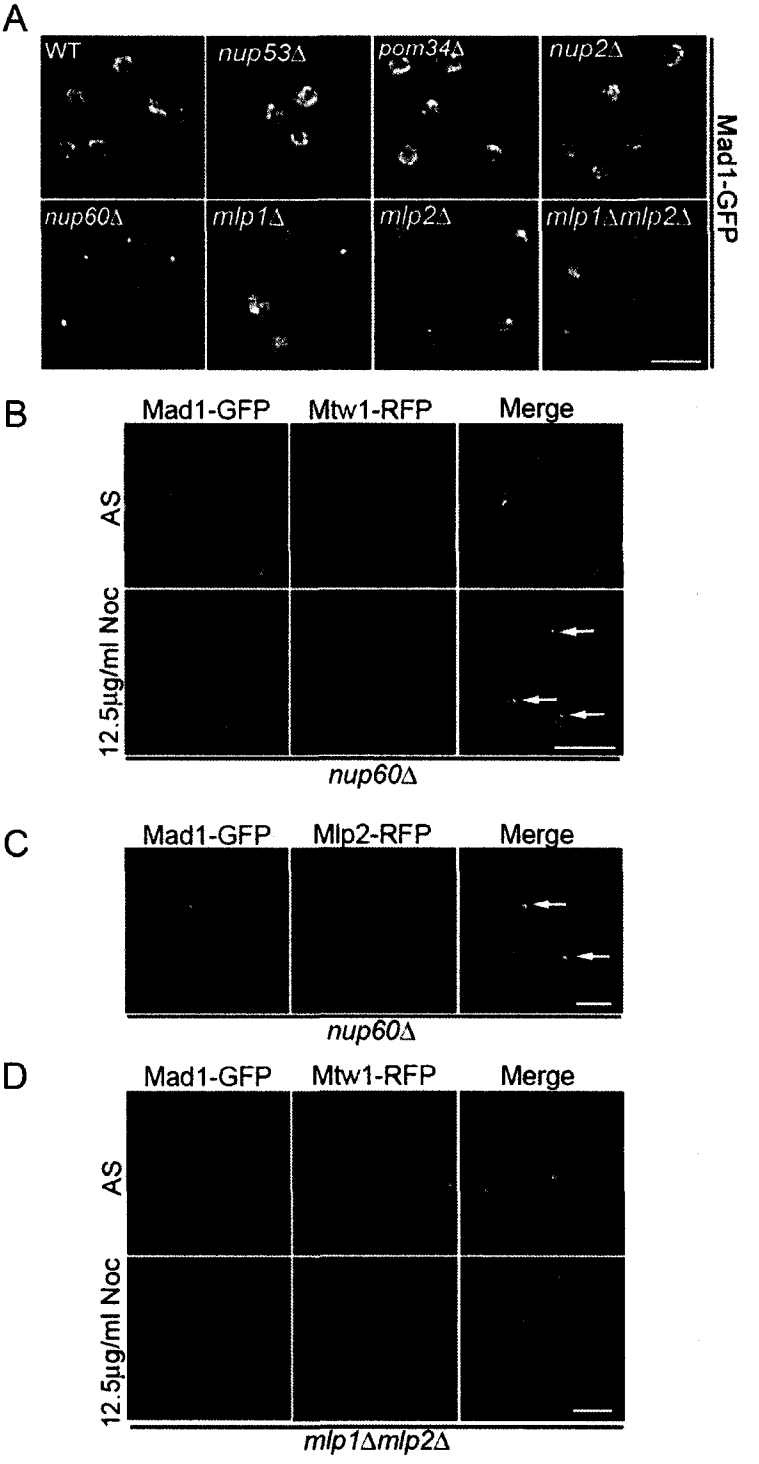

Figure 3-5. The localization of Mad1-GFP is altered in mutants of *nup60*Δ, *mlp1*Δ and *mlp2*Δ.

Table 3-1.

Phenotypes of *nupΔ* and *mlpΔ* mutants on benomyl

Mutant	Query mutant sensitivity Wild type sensitivity	Reference
nup53Δ	Resistant	Iouk et al., 2002
nup59Δ	Resistant	Iouk et al., 2002
nup170Δ	Resistant	Iouk et al., 2002
nup157Δ	Resistant	Iouk et al., 2002
nup60Δ	Resistant	This study
nup2Δ	Resistant	This study
pom34Δ	Resistant	This study
gle1Δ	N/C	This study
nup42Δ	N/C	This study
gle2Δ	N/C	This study
nup120Δ	N/C (slow growth)	This study
nup100Δ	N/C	This study
nup188Δ	N/C	This study
nup116Δ	N/C	This study
pom152Δ	N/C	Iouk et al., 2002
nup133Δ	N/C	This study
nup84Δ	N/C	This study
mlp1Δ	N/C	This study
mlp2Δ	N/C	This study
mlp1Δmlp2Δ	Resistant	This study

The intranuclear Mad1-GFP foci observed in the *nup60Δ* mutant cells were reminiscent of the localization of Mlp1p and Mlp2p previously reported in this mutant (Feuerbach et al., 2002). These two structurally related proteins are attached to the nucleoplasmic face of the NPC and are believed to form fibers that extend into the interior of the nucleus (Strambio-de-Castillia et al., 1999). Removal of Nup60p causes Mlp1p and Mlp2p to be released from their NPC attachment and concentrate at a single undefined focus in the nucleoplasm that does not colocalize with SPBs or kinetochores. An examination of Mad1-GFP and Mlp2-RFP in the *nup60Δ* mutant revealed that these proteins colocalize (Fig. 3-5C, arrows). To assess whether Mlp1p and Mlp2p act as a binding site for Mad1p, we investigated the localization of Mad1-GFP in mutants lacking these nonessential proteins (*mlp1Δ*, *mlp2Δ*, and *mlp1Δ mlp2Δ*). As shown in Fig. 3-5A, the NE concentration of Mad1-GFP was altered in each strain. Both the *mlp1Δ* and *mlp2Δ* mutants exhibited foci of concentrated Mad1-GFP as well as a diffuse nucleoplasm distribution, while only a diffuse intranuclear signal was present in the *mlp1Δ mlp2Δ* mutant. These results are consistent with the conclusion that Mlp proteins act as binding sites for Mad1p.

The concentration of Mad1p at the Mlp1p/Mlp2p foci in the *nup60Δ* strain allowed us to clearly visualize the recruitment of Mad1p from these structures to kinetochores upon SAC activation. As shown in Fig. 3-5B, following arrest of *nup60Δ* cells with nocodazole, Mad1-GFP was visible at two distinct nuclear foci (arrows). One of these two foci colocalized with one of two kinetochore foci detected with Mtw1-RFP. The Mad1-GFP-associated kinetochores likely represent those that have been dislodged from

microtubules, while those lacking Mad1-GFP have not been released from the spindle (Gillett et al., 2004). Similar experiments were also conducted in the *mlp1Δ mlp2Δ* mutant. We observed that the diffuse nuclear Mad1-GFP concentrated at a single kinetochore cluster following treatment with nocodazole (Fig. 3-5D). These observations are consistent with the results of the truncation analysis from which we concluded that the NPC-binding domain of Mad1p is not required for kinetochore binding.

3.2.4 Mad1p is dynamically associated with the Mlps.

When the SAC is activated, two separate populations of Mad1p can be defined on the basis of their association with kinetochores and the NPC-associated Mlp proteins. In the *nup60Δ* strain these two pools are easily distinguishable. We have taken advantage of this phenotype to examine the dynamics of Mad1p movement between these two locations using FRAP analysis. For these experiments, *nup60Δ* cells producing Mad1-GFP and Mtw1-RFP were arrested in nocodazole-containing media, and the position of the Mad1p-containing unattached kinetochores was located and photobleached. Images were then acquired at 12 sec intervals (Figs. 3-6A and 3-6B). Intensity measurements were collected from the bleached kinetochore and unbleached Mlp-associated Mad1-GFP. We observed that more than 60% of the kinetochore-associated Mad1-GFP signal recovered with a $t_{1/2}$ = 30 sec. The less than 40% that failed to recover may have a slow turnover rate and/or there was an insufficient fluorescent pool for full recovery. The recovery of the kinetochore-associated Mad1-GFP signal was accompanied by a corresponding decay of the Mlp-associated Mad1-GFP (Fig. 3-6B), which was not detected in unbleached

Figure 3-6. Mad1p dynamically associates with nocodazole-treated kinetochores and requires energy for this association.

A) The strain Y3057 was arrested in G1-phase with α-factor and released into media containing 12.5 μg/mL nocodazole at 25°C. After 60 min, cells were harvested and placed on agarose slides. The kinetochore-associated Mad1-GFP was identified based on colocalization with Mtw1-RFP (Pre-bleach). Kinetochore Mad1-GFP was bleached by applying 50 iterations of full intensity 488 nm light. GFP images only were acquired every 12 sec. At the end of the experiment, Mtw1-RFP was once again visualized (8'). Arrows point to the bleached focus. Note, bleached Mtw1-RFP did not recover during the time course of the experiments. Bar, 2 μm. B) Plots of the integrated fluorescent intensities at both kinetochore (circles) and Mlp protein foci (squares) are shown on the left and the natural log plot of kinetochore recovery against time is shown on the right. The normalized fluorescent recovery of Mad1-GFP at kinetochores fits a single exponential function. The natural log plot was used to calculate the first order rate constant, k, and the $t_{1/2}$ of Mad1-GFP recovery. C) Y3057 cells were arrested in nocodazole-containing medium (12.5 μg/mL) for 60 min. The culture was then split, and harvested cells were suspended in medium containing nocodazole and glucose (Noc + Glucose) or with nocodazole, 2-deoxy-D-glucose and sodium azide (Noc + 2DG/N_3) for 10 min. Images were collected using a confocal microscope. Bar, 5 μm.

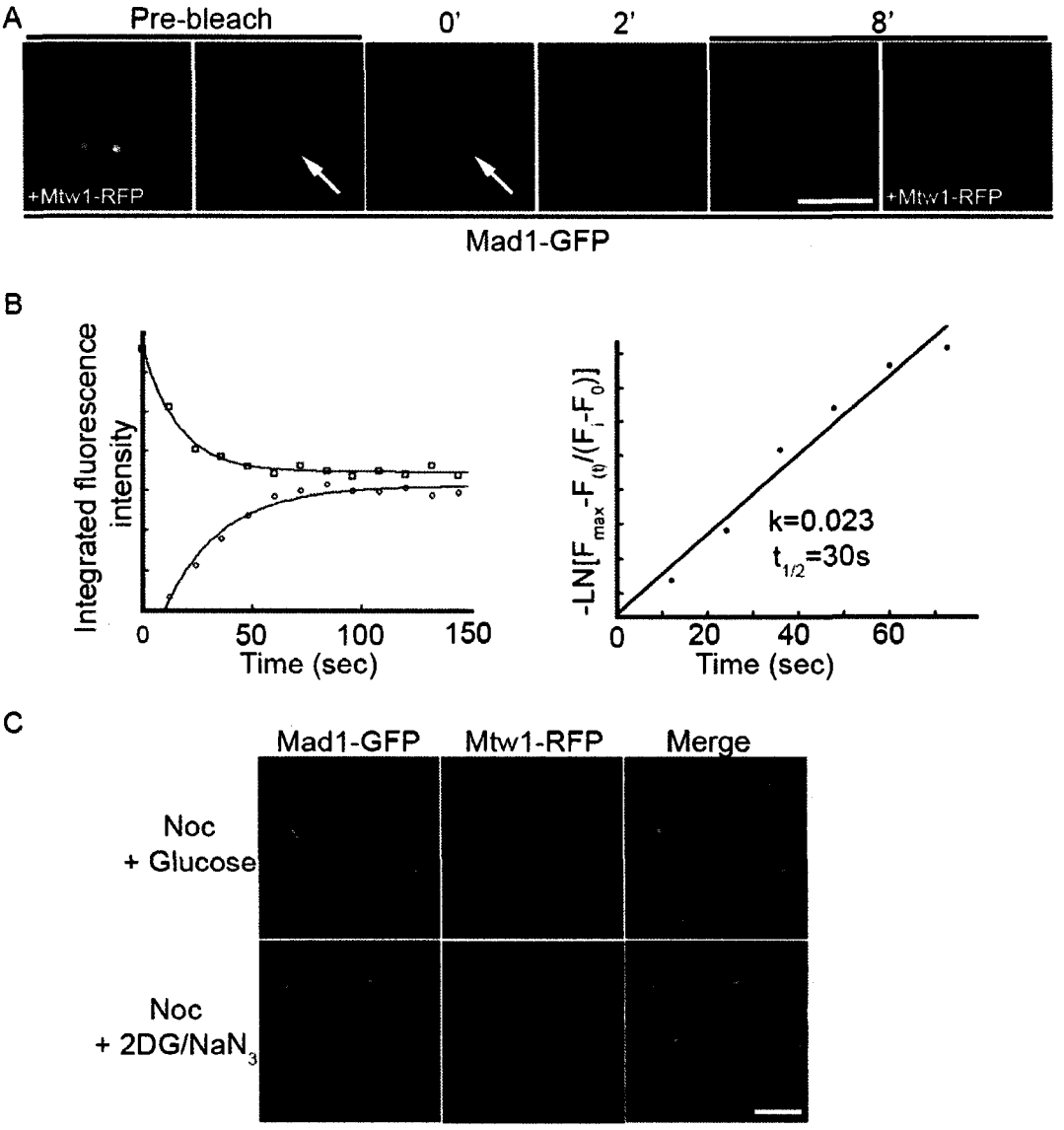

Figure 3-6. Mad1p dynamically associates with nocodazole-treated kinetochores and requires energy for this association.

control cells. In contrast, we detected no recovery of the Mtw1-RFP at the bleached kinetochore, consistent with previous observations that this protein is a component of the inner kinetochore (Pinsky et al., 2003; De Wulf et al., 2003). We interpret these results to reflect an exchange of bleached Mad1-GFP from kinetochores with unbleached Mad1-GFP associated with Mlp proteins.

The dynamic movement of Mad1p between the Mlp proteins and kinetochores prompted us to examine whether the association of Mad1p with these structures was dependent on energy. For these experiments we again utilized *nup60Δ* cells producing Mad1-GFP and Mtw1-RFP. Following arrest with nocodazole, cells were treated for 10 min with the metabolic poisons 2-deoxyglucose and sodium azide to deplete cellular ATP and GTP (Shulga et al., 1996), and the distributions of Mad1-GFP and Mtw1-RFP were examined. Neither the distribution of Mtw1-RFP nor the Mlp protein-associated Mad1-GFP was affected in treated cells (Fig. 3-6C). However, the localization of Mad1-GFP at kinetochores was abolished. Similarly, the association of the C-terminal constructs of Mad1p (318-749 and 475-749) with kinetochores in arrested cells was also disrupted by metabolic poisons. These results are consistent with the idea that the association of Mad1p with the kinetochores is dynamic and requires energy.

3.2.5 Role of the nuclear transport machinery in Mad1p function

We have used the various truncation mutants discussed above to evaluate the functional significance of the interactions of Mad1p with the nuclear transport machinery. To do this, we tested the ability of the various truncations to complement the benomyl sensitivity of a *mad1Δ* strain (Li and Murray, 1991). Like other spindle checkpoint

mutants, *mad1* null mutants are sensitive to benomyl and cannot delay cell division in response to spindle depolymerization, a phenotype visualized as an inability to grow on benomyl-containing plates. Plasmids encoding various Mad1p truncations, both untagged and GFP-tagged, were introduced into a *mad1Δ* strain, and the resulting strains were serially diluted and plated onto YPD plates containing 12.5 μg/ml benomyl and grown at 25°C to evaluate their ability to rescue wild type growth rates. As previously shown, growth on benomyl-containing plates of the *mad1Δ* strain can be equally complemented by a plasmid-borne copy of the *MAD1* or the *MAD1-GFP* gene (Figs. 3-7A and 3-7B) (Iouk et al., 2002). We observed that the NPC binding region of Mad1p alone (residues 1-325), or smaller truncations of this region, did not complement the benomyl sensitivity of the *mad1Δ* strain (Figs. 3-7A and 3-7B). Truncations lacking the NPC-binding N-terminus, including the 318-749 and 475-749 constructs, rescued growth suggesting that the C-terminus of Mad1p contained regions sufficient for SAC function. Of these truncations, we also detected a reproducible difference between the ability of the 318-749 and the 475-749 constructs to complement the *mad1Δ* benomyl sensitivity. Cells containing the 318-749 construct were more resistant to benomyl than those containing either the 475-749 construct or the full-length protein (Fig. 3-7A and 3-7B). This phenotype was similar to those observed in various nup null mutants (see above).

Each of the constructs that rescued the SAC function of the *mad1Δ* strain contained the cNLS peptide. Therefore, we tested whether the deletion of the NLS altered the function of the C-terminal constructs or full-length Mad1p. We observed that removal of the NLS from the full-length protein (mad1ΔNLS-GFP) did not appear to cause a

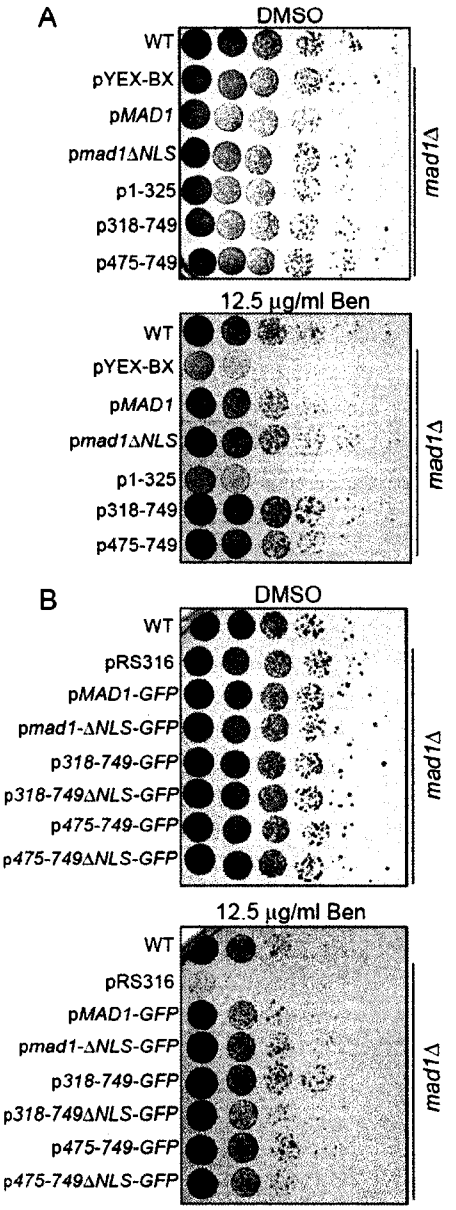

Figure 3-7. The C-terminus of Mad1p is required for SAC function.

Plasmids encoding Mad1p or the indicated truncations, either alone (A) or as fusions with GFP (B), were introduced into the *mad1Δ* strain Y3021. Following overnight growth in liquid cultures, equal amounts of cells were serially diluted ten-fold onto YPD plates containing vehicle alone (DMSO) or 12.5 μg/ml benomyl and grown at 25°C for 2-3 days. The growth characteristics of these strains were compared to wild type (WT) cells (BY4741) and the *mad1Δ* strain containing the empty vector pYEX-Bx (A) or pRS316 (B). The ΔNLS constructs lack the coding region for amino acid residues 506-527 of Mad1p.

reproducible change in its ability to complement the benomyl sensitivity of the *mad1Δ* strain (Figs. 3-7A and 3-7B). However, we did detect a difference in the 318-749ΔNLS and the 475-749ΔNLS constructs, which failed to fully restore benomyl resistance to the *mad1Δ* strain to that observed with their NLS-containing counterparts (Figs. 3-7A and 3-7B). These differences were not explained by differences in expression levels. These results suggest that the cNLS contributes to the efficiency of the spindle checkpoint functions of these mutants.

The analysis of the Mad1p truncation mutants suggests that NPC binding is not required for the SAC function of Mad1p. These data are consistent with our observations that none of the NPC mutants we have implicated in binding Mad1p exhibit an increased sensitivity to benomyl. Instead their more robust growth in the presence of this drug has led us to speculate that the association of Mad1p with the NPC could function to modulate its activity, potentially influencing exit from SAC arrest. To address this, wild type BY4741 and various isogenic null mutant strains were arrested with α-factor and then released into media containing moderate levels of nocodazole (12.5 μg/ml). Under these conditions, BY4741 cells progress to M-phase and are temporarily delayed in metaphase by the SAC machinery until they release into anaphase. Beginning at ~100 min after nocodazole treatment, cells began to overcome arrest and an increasing number proceeded to telophase and were visible as large budded cells with two nuclei. However, we observed that progression from metaphase to telophase was strikingly delayed in the *nup53Δ* mutant. Whereas 50% of wild type, *nup59Δ*, and *nup60Δ* large budded cells contained two nuclei at 160 min, only 20% of the *nup53Δ* cells displayed this phenotype

(Fig. 3-8A), suggesting they are delayed in their progression through anaphase. This delay could be rescued by a plasmid-borne copy encoding wild type Nup53p, but not a Nup53p mutant lacking its Kap121p binding domain.

The response of *nup53Δ* strains to SAC activation was also examined in cells overproducing the kinase Mps1p. Overexpression of Mps1p following release from α-factor arrest induces a SAC-dependent M-phase arrest (Hardwick et al., 1996). As shown in Fig. 3-8B, under these conditions *mad1Δ* cells failed to arrest and exhibited only a transient increase in the number of large budded cells before exiting mitosis (Hardwick et al., 1996) (Fig. 3-8B). In contrast, wild type, *nup53Δ* and *nup59Δ* cultures accumulated as large budded cells until ~200 min post α-factor release, at which point the number of large budded wild type and *nup59Δ* cells began to decrease as cells exited mitosis and progressed into G1-phase. However, as we observed with nocodazole-arrested cells, *nup53Δ* cultures remained arrested for an extended period, staying large budded through time points extending to 240 min (Fig. 3-8B). These results are consistent with the conclusion that Nup53p plays a role in terminating the SAC. Of note, we also attempted similar experiments using the *nup60Δ* strain. However, this strain failed to accumulate elevated levels of Msp1p and thus we were unable to employ this assay.

3.3 Discussion

An accumulating body of evidence has established that the NPC acts as a docking site for a variety of proteins whose apparent primary cellular functions are unrelated to nuclear transport. Two examples are the SAC proteins Mad1p and Map2p, which have

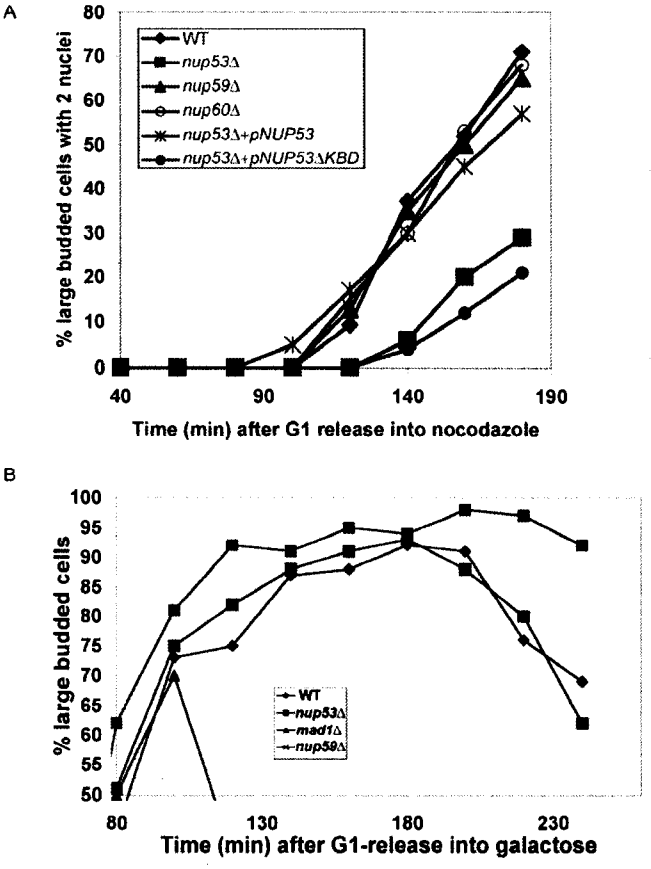

Figure 3-8. Termination of the SAC is delayed in *nup53Δ* cells.

A) WT (BY4741) cells and the mutant strains *nup53Δ* (CPL32), *nup59Δ* (Y3068), *nup60Δ* (3058), *nup53Δ* + pNUP53 (CPL32 containing pNUP53), and *nup53Δ* + pNUP53ΔKBD (CPL32 containing pNUP53ΔKBD) were synchronized in G1-phase using α-factor and released into media containing 12.5 μg/ml of nocodazole. At the indicated time points, cells were fixed with 70% ethanol and stained with DAPI to visualize nuclei and monitor progression from metaphase to telophase. The number of large budded (G2/M) cells containing two DAPI-staining bodies were scored and are presented graphically as a percentage of total cells verses time (min) after release into nocodazole-containing media. (B) WT (CPL61), *nup53Δ* (CPL62), *nup59Δ* (CPL63) and *mad1Δ* (CPL64) strains containing an extra copy of the *MPS1* ORF chromosomally integrated behind a galactose-inducible promoter were grown in media containing 2% raffinose. The cells were synchronized in G1-phase with α-factor at 30°C and released into media containing 2% raffinose and 3% galactose in the presence of α-factor to induce the synthesis of excess Mps1p. After 2 h, cells were released from G1, and G2/M-phase arrest was monitored by scoring the number of large budded cells at the indicated time points (min). These numbers are shown graphically as a percentage of total cells versus time.

been detected in association with NPCs in species from yeast to humans (Campbell et al., 2001; Iouk et al., 2002). These proteins bind tightly to one another (Chen et al., 1999) and, through Mad1p, this complex interacts with the NPC (Iouk et al. 2002). To understand the mechanisms that govern its association with the NPC and the kinetochores, we have mapped domains of Mad1p that interact with the nuclear transport machinery and further defined its interactions with NPC-associated binding sites. In addition to Nup53p, these binding sites include a presumed Nup60p/Mlp1p/Mlp2p complex from which we propose Mad1p cycles to kinetochores when the SAC is activated. The interaction of Mad1p with the NPC occurs through an N-terminal region, which can be separated from a C-terminal region that controls both its SAC activity and kinetochore binding.

The efficient targeting of Mad1p to the NPC requires the kap Kap95p and a cNLS positioned between residues 506-527 (Fig. 3-3). Removing the cNLS from Mad1p or inhibiting Kap95p function reduces the efficiency with which Mad1p is targeted to the NPC (Figs. 3-3C and 3-3D). Kap-assisted assembly of components of the NPC has previously been observed for both *bona fide* nups, such as Nup53p (Lusk et al. 2002), and other NPC-associated proteins, including Ulp1p (Panse et al., 2003). In the case of Ulp1p, its association with the NPC is proposed to be directly mediated by kaps. It is also possible that Kap95p/Kap60p performs a similar function for Mad1p or, perhaps more likely, the kaps facilitate the movement of Mad1p into the NPC and its nucleoplasmic face where it interacts with specific nups. Removal of the nup-binding domain, as in the 318-749 and 475-749 Mad1p constructs, appears to bypass this

deposition step and leads to the release of the Mad1p truncations into the nucleoplasm (Fig. 3-2A).

Once targeted to the NPC the association of Mad1p with the NPC is largely mediated by two predicted coiled-coil domains within its N-terminal 325 residues (Fig. 3-2A). On the basis of detected physical associations and *in vivo* evidence, we predict that Mad1p is likely to interact directly with specific nups, including Nup53p (Fig. 3-4A and 3-5A) (Iouk et al., 2002). Similarly, vertebrate Nup53 and Nup153, a potential vertebrate counterpart of Nup60p, play a role in the attachment of Mad1 to the NPC (Hawryluk-Gara et al., 2005) (L. Hawryluk-Gara and R.W. Wozniak, unpublished data). In yeast, these interactions may be transient *in vivo* and precede the eventual association of Mad1p with Mlp1p and Mlp2p. We have shown that strains lacking both Mlp1p and Mlp2p fail to concentrate Mad1p at the nuclear periphery (Figs. 3-5A and 3-5D). Moreover, in cells lacking Nup60p, Mad1p colocalizes with intranuclear clusters of Mlp proteins (Fig. 3-5C).

A model where Mad1p interacts with Nup53p prior to its association with the Mlp proteins is consistent with accumulating data suggesting that these proteins lie within close proximity in the NPC. Nup53p is a member of a complex of nups, which includes its binding partners Nup157p and Nup170p, that is part of the core structures of the NPC (Marelli et al., 1998). This subcomplex interacts with Nup145Np (Lutzmann et al., 2005). The C-terminus of this latter nup is required for the NPC association of Nup60p, which in turn is proposed to anchor the Mlp proteins to the NPC (Feuerbach et al., 2002). We have also obtained further data that support this hierarchical model. Mass spectrometry was used to identify proteins associated with affinity-purified, protein A-

tagged Mlp1p and Mlp2p (see Fig. 3-9). The most abundant species identified included Nup170p, Nup157p, and Nup145p (both N- and C-terminal regions), supporting the idea that these nups are positioned near the Mlp proteins. Our analysis of the Mlp-associated proteins, however, did not detect Mad1p, suggesting this interaction may be labile under the conditions of these experiments. Nup60p and Nup53p were also not detected. However, this was not surprising, as they are predicted to migrate in a region of the gel not analyzed due to contamination with the heavy chain of IgG.

The association of Mad1p with the NPCs throughout the cell cycle and upon SAC activation, as well as the close proximity of kinetochores to the NE, precluded an unambiguous visual detection of Mad1p at kinetochores in our strain backgrounds. However, deletion of the NPC binding domain from Mad1p and the corresponding decrease in NE localization allowed us to clearly detect Mad1p truncations at kinetochores (Figs. 3-2A and 3-2B). Similarly, we could visualize the recruitment of full-length Mad1p to unattached kinetochores following activation of the SAC in the *nup60Δ* strain (Fig. 3-5B). These observations are consistent with chromatin immunoprecipitation experiments and data suggesting a partial colocalization of the Mad1-GFP with kinetochore markers (Gillett et al., 2004).

The phenotype of the *nup60Δ* mutants also allowed us to follow the dynamics of Mad1p association with kinetochores using photobleaching techniques. Our data show a rapid ($t_{1/2}$~30 sec at 23°C) exchange of Mad1p at kinetochores, which is accompanied by similar movements of Mad1-GFP at the Mlp protein foci (Figs. 3-6A and 3-6B). The results of these experiments are consistent with the idea that Mad1p actively cycles

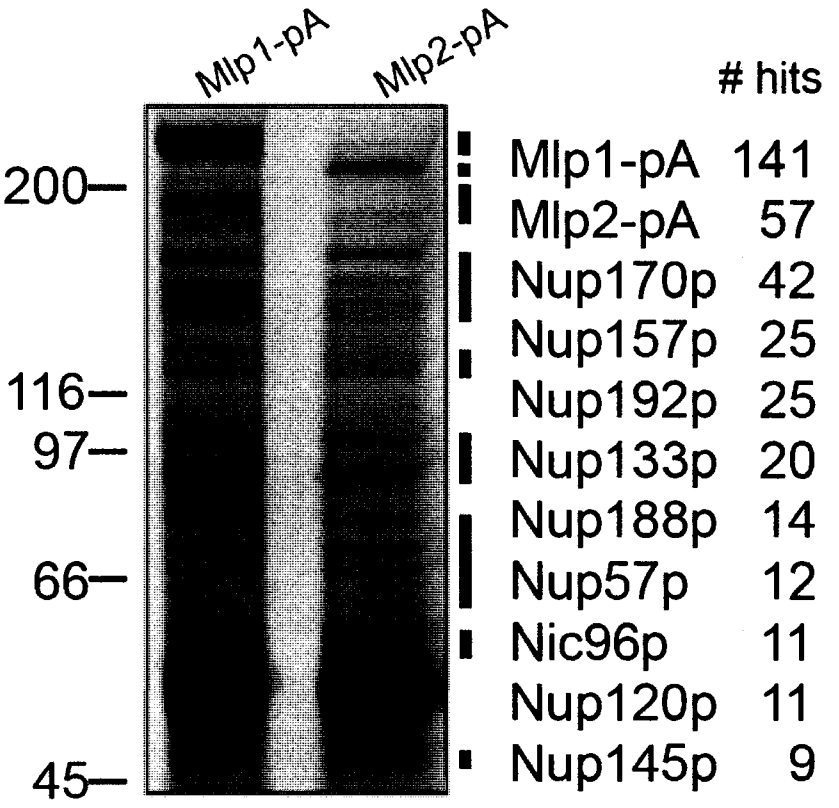

Figure 3-9. Mlp1p and Mlp2p physically interact with Nup145p and members of the Nup53p-containing complex.

Mlp1-pA and Mlp2-pA-associated protein complexes were immunopurified from yeast whole cell lysates, resolved by SDS-PAGE and stained with Coomassie blue (left). The vertical black bars indicate gel sections containing prominent protein bands of molecular weight greater than 45 kDa that were excised and used to identify peptides by LCQ-MS/MS following in-gel trypsin digestion. The identified peptides in each of the gel slices were compiled, and this list was then thresholded to contain only the Mlp proteins and nups for which 9 or more peptides were identified (right). This revealed an enrichment of several NPC core proteins in these immunopurification eluates.

between binding sites at the Mlp proteins and kinetochores. Since the *nup60Δ* strain does not exhibit a detectable SAC defect, it is likely that this cycling event occurs in wild type cells where the Mlp proteins are associated with the NPC. Moreover, similar measurements performed in vertebrates have also detected that 20-30% of Mad1 exchanges on unattached kinetochores at a similar rate ($t_{1/2}$ = ~16 s) (Shah et al., 2004: Howell et al., 2004). However, the majority of Mad1 in this system appears to be largely immobile and believed to be stably associated with unattached kinetochores where it is thought to function as a catalytic platform for the SAC signal. Our results suggest that a larger percentage of Mad1p (>60%) is rapidly mobile in yeast and capable of cycling between kinetochores and NPC-associated structures. The functional relevance of this is unclear, but the prevalence of the mobile pool may suggest that it also plays a role in inhibiting progression into anaphase.

Strikingly, we observed that the association of Mad1p with the kinetochores, but not with the Mlp proteins (Fig. 3-6C), was energy-dependent. This does not appear to be the results of an inhibition of release of Mad1p from the Mlp proteins, as we have observed a similar release from unattached kinetochores of Mad1p truncations that fail to associate with the NPC. Moreover, it seems unlikely that the loss of kinetochore association is due to depletion of nuclear Mad1p caused by nuclear import inhibition, since the Mlp protein-bound pool of Mad1p is not affected (Fig. 3-6C). Thus, the most likely explanation is that the kinetochore binding site of the cycling pool of Mad1p is dependent on energy through an, as yet, undefined mechanism. It is important to note that the release of Mad1p from kinetochores was observed in experiments performed on nocodazole-treated cell cultures (Fig. 3-6C), suggesting microtubules do not play a role in this process. This

is in contrast to observations examining the energy-dependent association of Mad2 with kinetochores in rat Ptk cells where release induced by metabolic poisons requires spindle microtubules (Howell et al., 2000).

We also noted that both full-length and the 318-749 region of Mad1p were recruited to kinetochores only upon activation of the SAC, while a further truncated fragment lacking residues 318-474 (truncation 475-749) was associated with kinetochores in asynchronous cultures, independent of activation of the SAC (Figs. 3-2A and 3-2B). A likely explanation is that residues 318-474 can inhibit kinetochore association by masking binding sites for kinetochore constituents that are present nearer the C-terminus between residues 475-749. SAC activation is predicted to induce conformational changes in Mad1p or release a binding partner and expose the kinetochore binding site within residues 475-749. Which kinetochore-associated proteins act to anchor the Mad1p truncations to these structures is unclear. Our results would suggest that the Mad1p binding site is a constitutive kinetochore component. One candidate is the Ndc80p complex, which has been suggested to link the Mad1p-interacting protein Mad2p to kinetochores when the SAC is activated (Gillett et al., 2004).

Deletion mutations of Mad1p discussed above were also used to evaluate the contribution of the nuclear transport apparatus to the function of Mad1p in the SAC. The benomyl sensitivity of *mad1Δ* strains could be suppressed by truncations containing the C-terminal, cNLS-containing region of Mad1p (318-749 or 475-749), but not by the N-terminal NPC binding domain (residues 1-325). The apparent requirement of the C-terminus of Mad1p for SAC function was also supported by FACS analysis, showing that

in the presence of nocodazole these mutants arrest in G2/M similarly to wild type cells. The importance of this C-terminal domain in the SAC is likely linked to its ability to target to kinetochores (Fig. 3-2) and bind Mad2p (Chen et al., 1999). Consistent with this idea, we have noted that introduction of the 318-749 and 475-749 truncations into *mad1Δ* cells, which normally contain a diffuse cellular pool of Mad2p (Iouk et al., 2002), induces the nuclear accumulation of Mad2p.

The degree to which the C-terminal constructs were capable of rescuing the benomyl sensitivity of the *mad1Δ* strain was reduced, but not eliminated, when the cNLS was deleted (Fig. 3-7B). These ΔNLS constructs are diffusely distributed throughout the cell (Fig. 3-10), presumably entering the nucleoplasm by diffusion in sufficient amounts for them to function in the SAC. However, they fail to accumulate at kinetochores, suggesting threshold nuclear levels of the constructs must be reached for this event. Interestingly, inclusion of the NPC binding domain (*e.g.* the Mad1-ΔNLS construct) restored binding to unattached kinetochores. Cumulatively, these results have led us to conclude that sequence elements that mediate the NPC association and kap binding of Mad1p can function independently to establish a nuclear pool necessary for kinetochore recruitment.

The NPC may also play other roles in modulating SAC activity. Several pieces of data suggest that the NPC may negatively regulate the SAC, perhaps limiting the duration of the SAC. This function would explain the observation that a *nup53Δ* strain remains arrested in M-phase for significantly longer periods of time than wild type cells in the presence of moderate concentration levels of nocodazole (Fig. 8A). Moreover, strains

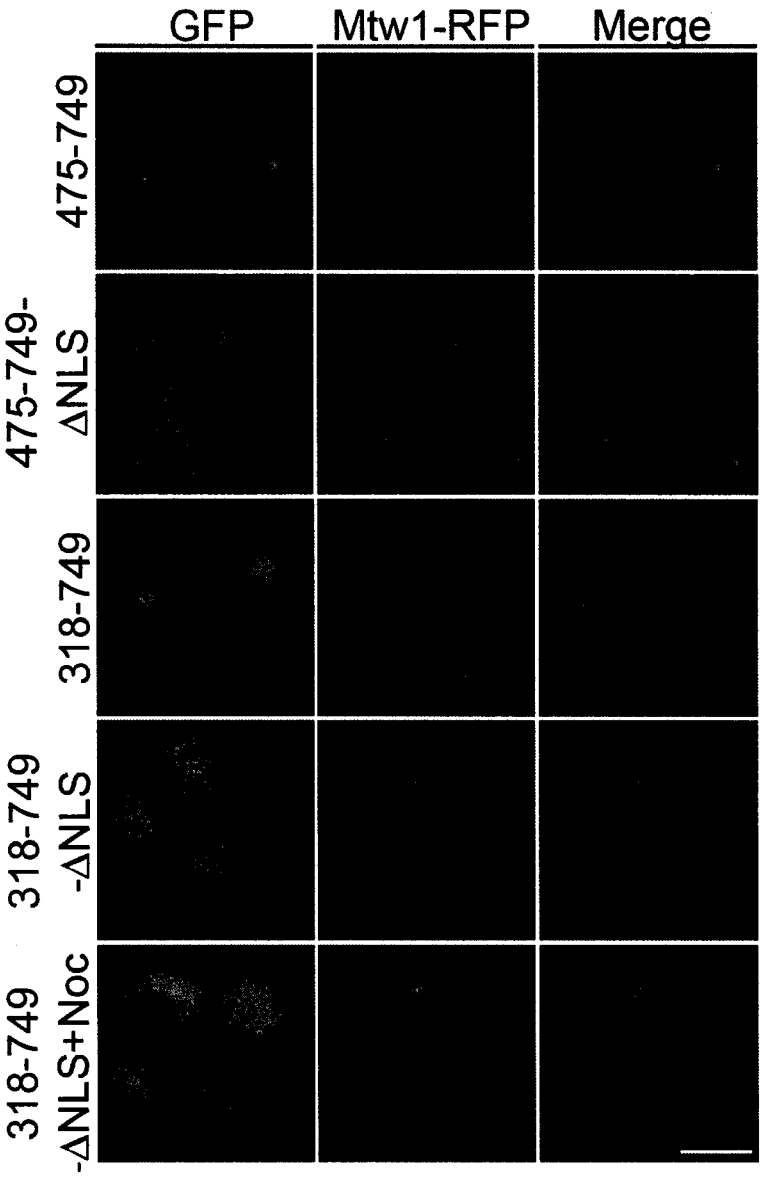

Figure 3-10. The kinetochore association of the C-terminal region of Mad1p is dependent on its NLS.

Plasmids expressing 475-749-GFP (p475-749-GFP), 475-749-ΔNLS-GFP (p475-749-ΔNLS-GFP), 318-749-GFP (p318-749-GFP), or 318-749-ΔNLS-GFP (p318-749-ΔNLS-GFP) were introduced into a *mad1Δ* strain expressing Mtw1-RFP (Y3031). Asynchronous cultures or cells arrested with 12.5 μg/mL nocodazole at 30°C for 1.5 h (+Noc) were examined using a confocal microscope to visualize the GFP and RFP fusion proteins. Merged images are shown on the right.

expressing the Mad1p 318-749 truncation, whose binding to the NPC and Nup53p is compromised, reproducibly exhibit an increased resistance to benomyl similar to that observed in *nup53Δ* strains (Fig. 3-7). These phenotypes could be a consequence of extending the length of the SAC.

The involvement of Nup53p in SAC duration can be envisioned as occurring by different mechanisms. In one case, Nup53p, and possibly other NPC-associated proteins, may modulate the function of Mad1p, and possibly that of its binding partner Mad2p, by either directly regulating their interactions with other SAC components or by physically segregating them away from their sites of action, including kinetochores. Recruitment of Mad2p back to the NPC is in fact what is observed following exit from the SAC (Iouk et al., 2002). Alternatively, it is possible that a regulatory role for Nup53p is linked to its ability to control Kap121p-mediated import in SAC-arrested cells and thus potentially the nuclear localization of key SAC control proteins (Makhnevych et al., 2003). This idea is consistent with our observation that a Nup53p mutant lacking the Kap121p binding site is unable to complement the SAC duration defect of the *nup53Δ* strain (Fig. 3-8A). However, we are careful to interpret these data, as this mutation also inhibits the incorporation of Nup53p into the NPC (Lusk et al., 2002).

In conclusion, we envisage that the NPC, beyond its established role in nuclear transport, acts as a macromolecular hub from where the functions of a diverse spectrum of proteins, including SAC components, are modulated. This role for the NPC could be accomplished by it acting as a reaction platform or through it functioning as a distribution center that controls access of proteins to their locations of action (*e.g.* accessibility of Mad1p or Mad2p to other elements of the SAC machinery and kinetochores). In addition

to the SAC proteins, this role for the NPC is likely to extend to other classes of proteins. In species ranging from vertebrates to yeast, NPCs interact with proteins involved in diverse functions including, for example, the desumoylating enzyme Ulp1p (Panse et al., 2003) and a poly-(ADP-ribose) polymerase tankyrase (Scherthan et al., 2000). The degree to which the dynamic interactions of these proteins with the NPC and kaps regulate their function represents a major challenge in understanding the role of the NPC in cellular physiology.

Chapter IV: *The Export Karyopherin Xpo1p Regulates the Targeting and Turnover of the Spindle Assembly Checkpoint Protein, Mad1p*

4.1 Overview

NPCs are strategically positioned along the surface of the NE where they control the exchange of macromolecules between the cytoplasm and the nucleoplasm. However, several proteins interact with the NPC but play no obvious role in transport suggesting that the NPC is involved in other cellular processes. These proteins include Mad1p and Mad2p, which function in the SAC. These proteins are bound to the NPC during interphase and are recruited onto mitotic kinetochores during SAC activation. In Chapter III, I showed that *S. cerevisiae* Mad1p dynamically associates with both NPCs and kinetochores during SAC activation and that its association with kinetochores is energy-dependent. Here, I show that the cycling of Mad1p on and off kinetochores and the NPC is dependent on the GTPase Ran and the soluble nuclear export factor, Xpo1p. In mutants of the yeast RanGEF, *PRP20*, Mad1p turnover at the kinetochores is inhibited during SAC activation. Similarly, overexpression of a dominant-negative mutant of Ran incapable of GTP hydrolysis allows association of Mad1p with kinetochores but prevents its turnover. Kinetochore turnover of Mad1p and normal cell cycle progression is also inhibited by mutations in Xpo1p. Consistent with this idea, Xpo1p is present in the nucleus and at spindle pole bodies throughout the cell cycle, but is recruited to kinetochores during SAC activation. Furthermore, I have identified a NES within the primary sequence of Mad1p and have shown that this sequence is required for the efficient targeting of Mad1p to kinetochores during SAC arrest. Finally, the targeting of

Xpo1p to kinetochores during SAC arrest is dependent on Mad1p itself, suggesting that Mad1p and Xpo1p interact with kinetochores interdependently.

4.2 Results

4.2.1 The NPC-associated SAC protein Mad1p contains a functional NES.

We have previously shown that the SAC protein Mad1p is docked at NPCs throughout unperturbed cell cycles in budding yeast (Iouk et al., 2002) (Chapter III). The association of Mad1p with the NPC is dependent on a subset of nups including, Nup60p, and two proteins, Mlp1p and Mlp2p, that form fibers that extend from the nucleoplasmic face of the NPC. Removal of Nup60p dislodges both Mlp1p and Mlp2p into a single intranuclear focus that retains Mad1p binding (Feuerbach et al., 2002) (Chapter III) (Fig. 4-1A, i-ii). Activation of the SAC in *nup60Δ* strains results in a redistribution of Mad1p from the Mlp-associated focus onto a kinetochore-associated focus (Fig. 4-1A, iii-iv and Fig. 4-2). Mad1p associates with unattached kinetochores but not kinetochores that have achieved microtubule attachments, resulting in two kinetochore populations (Gillett et al., 2004). The *nup60Δ* strain thus provides a valuable background in which to study the movement of Mad1p during SAC activation. This has allowed us to show that Mad1p is capable of cycling between the NPC kinetochores with a $t_{1/2}$ on kinetochores of ~ 30 sec. Moreover, this event is energy-dependent (Iouk et al., 2002) (Chapter III).

Mad1p contains a Kap60p/Kap95p dependent NLS within its C-terminus that is required for its efficient movement to NPCs (Chapter III). We postulated that the nuclear

Figure 4-1. The NPC resident protein Mad1p contains a functional Xpo1p-dependent NES within its C-terminus.

The NPC resident protein Mad1p contains a functional Xpo1p-dependent NES within its C-terminus. (A) Mad1-GFP was visualized in either wild type (Y3028, i) or *nup60Δ* mutant cells (Y3040, ii and iii). Mad1-GFP localizes to the NE in a punctate pattern (i) and is mislocalized to a single intranuclear focus in the absence of Nup60p (ii). *nup60Δ* cells were treated with 12.5 μg/mL nocodazole for 75 min before Mad1-GFP visualization (iii). Mad1-GFP is recruited to a second intranuclear focus (iii) coincident with kinetochores as indicated by Mtw1-RFP colocalization (iv) Bars, 2 μm. (B) Mad1p amino acids 563-576 contain a predicted Xpo1p NES. A prediction algorithm (la Cour et al., 2004) was used to identify a putative NES within the primary sequence of Mad1p and manual sequence alignment was used to align Mad1p with both the Rev and PKI NESs. Numbers indicate residue numbers of the respective proteins. Black boxes indicate conserved residues that when mutagenized abolish NES function (C) The SV40 large T NLS was introduced in tandem with the predicted Mad1p NES upstream of GFP for use in a nuclear transport competition assay (Stade et al., 1997) to confirm its functionality as an Xpo1p-dependent NES (SV40-NLS/Mad1-NES-GFP). This construct was visualized in the presence or absence of leptomycin B in a strain expressing *xpo1 T539C*, a leptomycin B sensitive strain (Y3105). SV40-NLS/PKI-NES-GFP was used as a control (upper panels) Bars, 5 μm. (D) SV40-NLS/Mad1-NES-GFP was introduced into the *xpo1-1* temperature sensitive strain (Y3105) and observed at the permissive (23°C) and restrictive temperatures (37°C, 30 min) Bars, 5 μm.

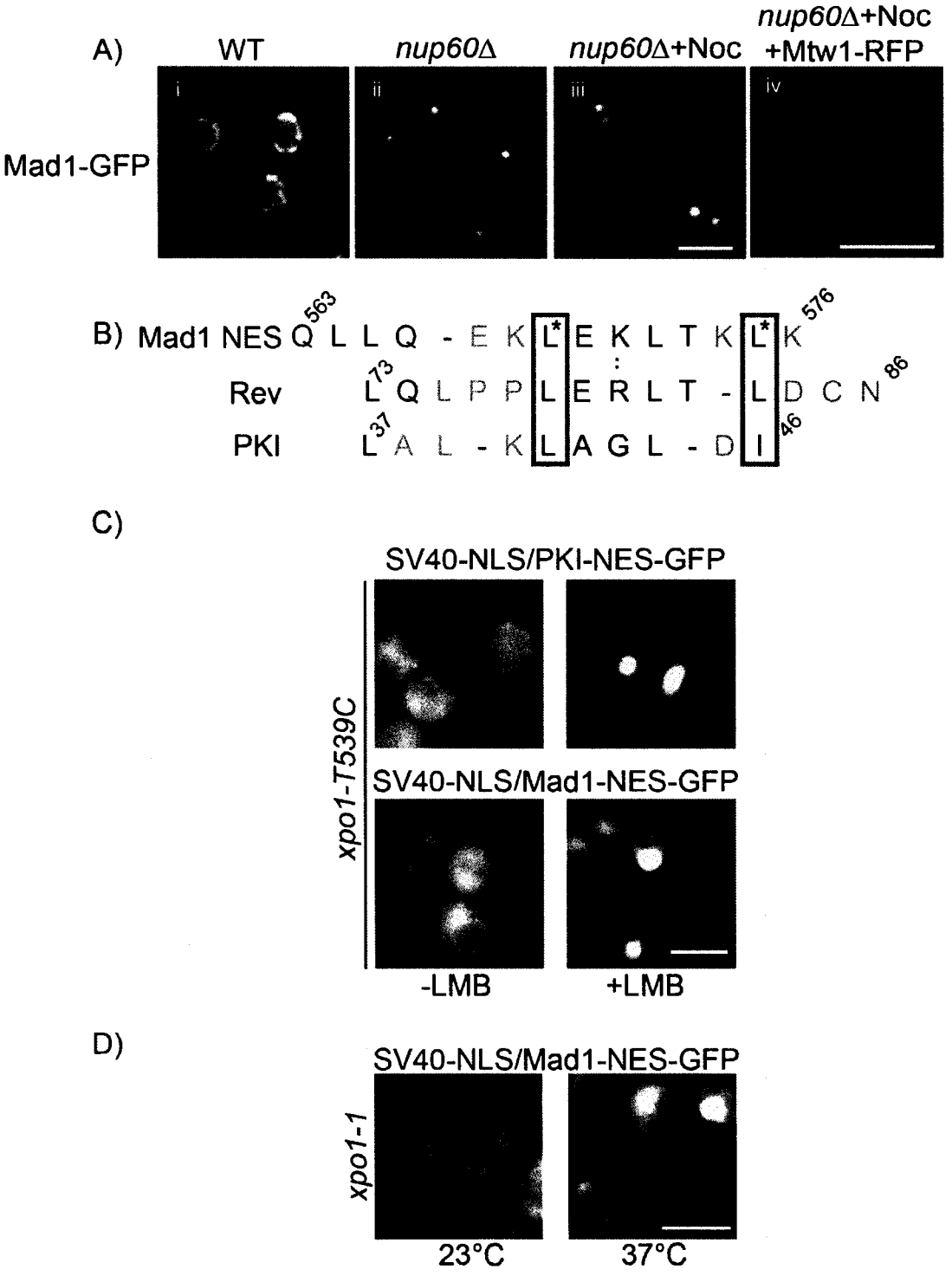

Figure 4-1. The NPC resident protein Mad1p contains a functional Xpo1p-dependent NES within its C-terminus.

transport machinery might also play a role in its movement from the NPC to kinetochores. To further explore this possibility, we examined the primary sequence of Mad1p to determine whether it contained regions that conformed to consensus sequences for nuclear import (NLS) or nuclear export (NES) signals. Mad1p residues 563-576 were found to align well with the known NESs of HIV Rev and heat stable inhibitor of cAMP-dependent protein kinase (PKI) (Fig. 4-1B) (Fischer et al., 1995; Wen et al., 1995). To test the functionality of the predicted Mad1p NES, we employed a nuclear transport competition assay in which both an NLS and an NES are fused to GFP (Stade et al., 1997). In this assay, NLS-NES-GFP is equilibrated between the nuclear and cytoplasmic compartments. Inactivation of the cognate importin or exportin results in a shift in the localization of the reporter from the nucleus or cytoplasm, respectively, due to dominant effects of the wild type kap. To test whether Mad1$^{563\text{-}576}$ can function as an NES, we constructed a SV40-NLS/Mad1$^{563\text{-}576}$-GFP fusion and examined its localization in an xpo1-T539C mutant. The xpo1-T539C mutant functions like the wild type protein but unlike wild type yeast Xpo1p, it is sensitive to the fungal toxin leptomycin B (Neville and Rosbash, 1999). As shown in Fig. 4-1C, both a control reporter, SV40-NLS/PKI-NES-GFP, and SV40-NLS/ Mad1$^{563\text{-}576}$-GFP are visible throughout the cell (Fig 4-1C, upper left panel). Upon addition of leptomycin B to cells, the control reporter accumulated in the nucleus, consistent with an inhibition of xpo1-T539C. Similarly, SV40-NLS/ Mad1$^{563\text{-}576}$-GFP also accumulated in the nucleus of leptomycin B-treated cells suggesting that Xpo1p recognizes Mad1$^{563\text{-}576}$ as an NES (Fig. 4-1C, lower right panel). In further support of this, we observed similar results in experiments using the temperature sensitive mutant, *xpo1-1*. At the permissive temperature, SV40-NLS/

Mad1$^{563-576}$-GFP was localized throughout *xpo1-1* cells. However, following a shift to the non-permissive temperature (37°C), the reporter accumulated within the nucleus. This suggests that Mad1$^{563-576}$ encodes a functional Xpo1p-dependent NES.

4.2.2 SAC-induced targeting of Mad1p to kinetochores is dependent on functional Xpo1p and RanGEF (Prp20p)

We have demonstrated that Mad1p contains sequences recognized by Xpo1p (Fig. 4-1) and Kap60p/Kap95p (Chapter III) motifs for both the nuclear import and export machinery and suggest that it may use them as a way of regulating its activity. With this in mind, we tested the effects of mutations in these and other kaps on the ability of Mad1p to target to and associate with kinetochores in response to SAC activation. In these experiments, we analyzed Mad1-GFP kinetochore targeting in a *nup60Δ* strain containing mutations in one of three kaps, *KAP95* (*kap95-14*), *MSN5* (*msn5Δ*) or *XPO1* (*xpo1-T539C*). Cultures were grown to mid-log phase, shifted to their non-permissive condition (excluding wild type and *msn5Δ*) and directly treated with nocodazole to induce SAC arrest. Kinetochore position was established in these strains by colocalization with Mtw1-RFP. In both wild type and the *msn5Δ* strain, we detected Mad1-GFP recruitment to kinetochores (Fig. 4-2A). Similarly, Mad1-GFP targeting to kinetochores was unaffected by the *kap95-14* mutation at both the permissive and non-permissive temperatures. In contrast, inhibition of Xpo1p function inhibited recruitment of Mad1-GFP to kinetochores. As shown in Fig. 4-2A, activation of the SAC by treatment with nocodazole did not induce the association of Mad1-GFP with kinetochores when *xpo1-T539C* cells were previously treated with leptomycin B. These results are

Figure 4-2. Xpo1p-dependent Madp1 kinetochore targeting.

Mad1-GFP and Mtw1-RFP were introduced into *nup60Δ* strains harbouring mutations in *KAP95* (*kap95-14*), *MSN5* or *XPO1* (*xpo1-T539C* and *xpo1-1*). Strains, except wild type and *msn5Δ*, were imaged at both their permissive and restrictive conditions (100 ng/mL Leptomycin B or 37°C, respectively) to inactivate Kap95p, Xpo1p (A) or Prp20p (B). 12.5 μg/mL nocodazole was then added to the media for 90 min to activate the SAC and strains were visualized. Arrows show Mad1-GFP overlap with Mtw1-RFP. Arrowheads show kinetochores devoid of Mad1-GFP. Bars, 2 μm.

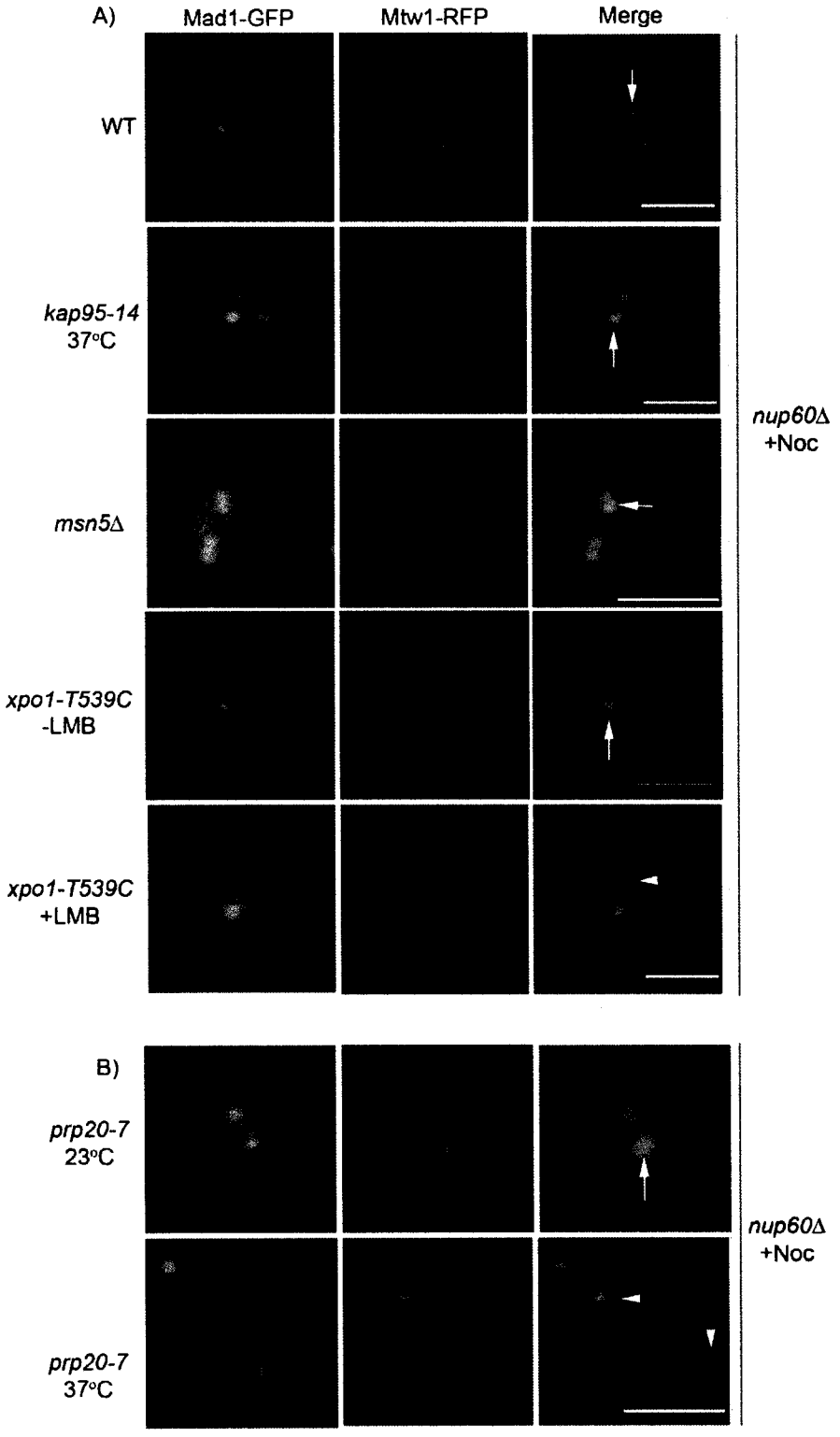

Figure 4-2. Xpo1p-dependent Madp1 kinetochore targeting.

consistent with a role for Xpo1p in mediating intranuclear Mad1p targeting to kinetochores during SAC arrest.

Xpo1p, its cargo and RanGTP form cooperative complexes with RanGTP within the nucleus (Fornerod et al., 1997; Petosa et al., 2004). The presence of an Xpo1-dependent NES within Mad1p combined with the finding that Mad1p fails to target to kinetochores in *XPO1* mutants suggests that these proteins interact and raises the question of what role RanGTP plays in kinetochore targeting of Mad1p. To test this, we introduced a *nup60Δ* mutation into a temperature sensitive *prp20-7* strain expressing both integrated Mad1-GFP and the kinetochore protein, Mtw1-RFP. The prp20-7 mutant protein rapidly mislocalizes from the nucleoplasm to the cytoplasm at 37°C, leading to decreased nuclear levels of RanGTP (Amberg et al., 1993; Dilworth et al., 2001). At 23°C, nocodazole treatment of the *prp20-7* strain induces recruitment of Mad1-GFP to kinetochores. However, when the *prp20-7* strain is shifted to the non-permissive temperature (37°C) for 30 min prior to treatment with nocodazole, subsequent targeting of Mad1-GFP to kinetochores was inhibited (Fig. 4-2B). These findings are consistent with a role for both nuclear RanGTP and Xpo1p in the targeting of Mad1p to kinetochores during SAC activation.

4.2.3 The NES of Mad1p is required for its efficient targeting to kinetochores during SAC arrest

To assess whether the requirement of Xpo1p in the targeting of Mad1p to kinetochores is directly linked to their association *in vivo*, we examined the consequence of mutating the NES region of Mad1p. Mad1p NES point mutants were designed based

on single mutants in both the Rev and PKI NESs that have been shown to abolish NES function (Malim et al., 1991; Wen et al., 1995). Two mutants were constructed changing leucine 569 to alanine and leucine 575 to alanine. To test the effects of these mutations on nuclear export, theses mutations were introduced into the construct encoding the SV40-NLS/Mad1-NES-GFP reporter. As shown in Fig. 4-3A, the SV40-NLS/Mad1-NES-GFP reporter equilibrates between the nucleus and the cytoplasm. However, introduction of either the L569A or the L575A mutation resulted in a redistribution of the reporter to the nucleus, indicating that both of these individual mutations attenuate Mad1p NES function.

To test the effects of the NES mutants on Mad1p kinetochore targeting, we introduced the L569A or L575A mutations into endogenous *MAD1*. These mutants were then tagged at their 3' ends with the GFP ORF. *MAD1-GFP*, *mad1-L569A-GFP* and *mad1-L575A-GFP* expressing strains were arrested in G1 with α-factor and released into nocodazole containing media. After 75 min in nocodazole, cells were visualized on a fluorescent microscope. GFP-tagged wild type Mad1p targeted efficiently to kinetochores during SAC arrest (Fig. 4-3B). However, both mad1-L569A-GFP and mad1-L575A-GFP failed to efficiently target to kinetochores during SAC arrest (Fig. 4-3B). These effects could not be attributed to a decrease in cellular levels of the Mad1p mutants. These findings support the conclusion that Xpo1p interacts with Mad1p via an NES and that this interaction is required for the efficient targeting of Mad1p kinetochores.

To test whether the NES mutants in *MAD1* resulted in lesions in the SAC, we plated each mutant on YPD plates containing the microtubule destabilizing drug,

Figure 4-3. Inactivation of the Mad1p NES dramatically reduces Mad1p's kinetochore targeting ability.

(A) GFP fusions of the wild type Mad1p NES or mutant versions in which the codons for either leucine 569 or 575 have been mutated to alanine (L569A *mad1*-NES or L575A *mad1*-NES) was introduced in tandem downstream of the SV40 large T NLS and visualized in wild type cells. Bars, 5 μm. (B) A *nup60Δ* yeast strain expressing the kinetochore protein Mtw1-RFP in which the *MAD1* gene has been replaced by *MAD1-GFP*, *mad1-L569A-GFP* or *mad1-L575A-GFP* was synchronized in G1 with α-factor and released into YPD containing 12.5 μg/mL nocodazole for 75 min and imaged. Arrows show Mad1-GFP overlap with Mtw1-RFP. Arrowheads show kinetochores devoid of Mad1-GFP. Bars, 2 μm. (C) *MAD1, mad1-L569A* or *mad1-L575A* was integrated into a *mad1Δ* strain at the endogenous *MAD1* locus and spotted in 10-fold serial dilutions onto YPD+DMSO or YPD+12.5 μg/mL benomyl plates. Plates were scanned after growth at 25°C for 3 days.

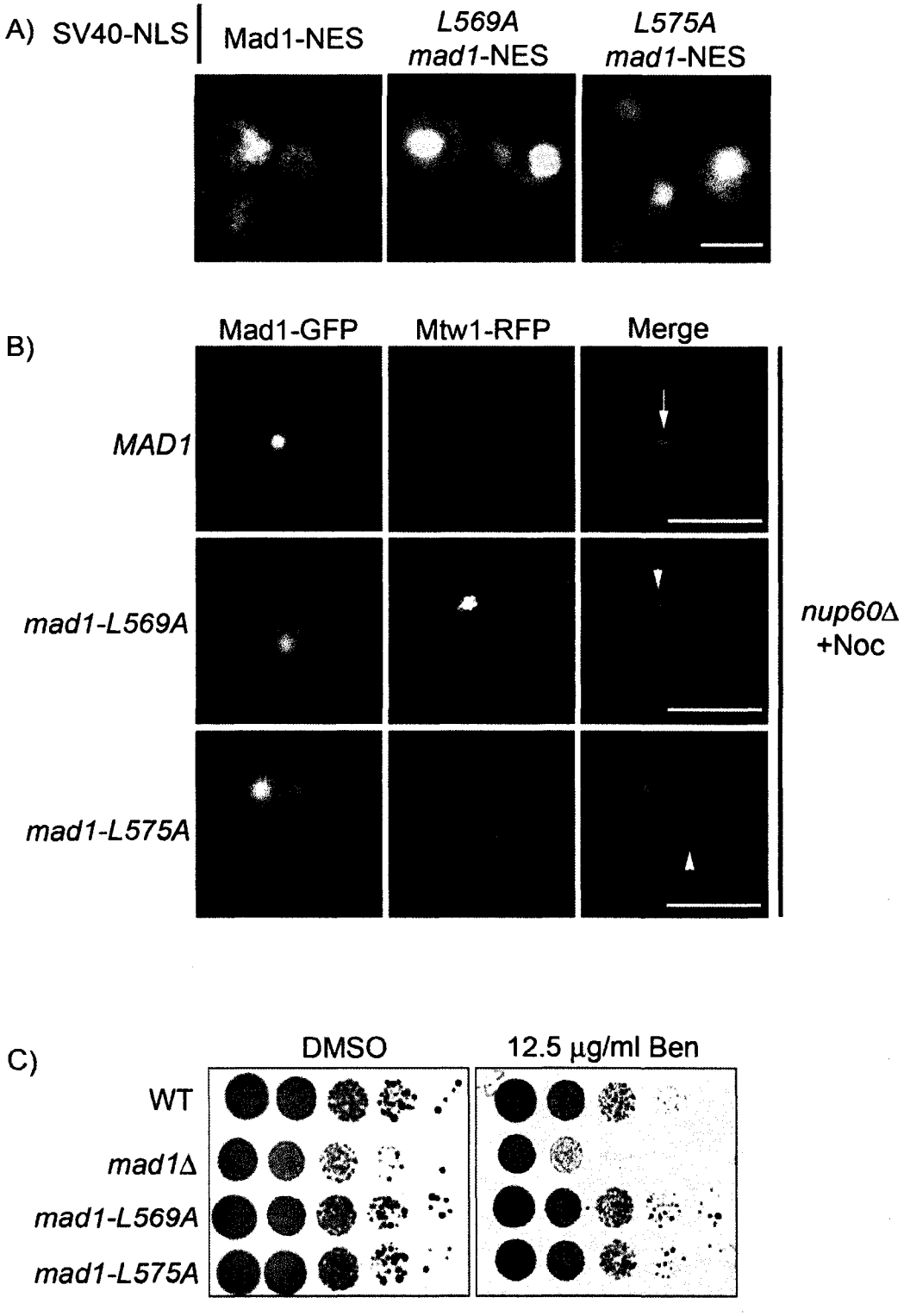

Figure 4-3. Inactivation of the Mad1p NES dramatically reduces Mad1p's kinetochore targeting ability.

benomyl. As shown in Fig. 3C, both the *mad1-L569A* and *mad1-L575A* strains grew similarly to the wild type counterpart and did not show an increased benomyl sensitivity characteristic of mutations in SAC components including null mutants of *MAD1* (*mad1Δ*, Fig. 4-3C). We conclude from these results that while these mutants inhibit kinetochore association of Mad1p, they remain functional in the SAC.

4.2.4 Xpo1p is targeted to kinetochores during SAC arrest

Our data support the hypothesis that Xpo1p, through its interaction with the Mad1p NES, targets the protein to kinetochores where the SAC is activated. This raises the question of whether Xpo1p also is recruited to kinetochores. It has previously been shown that Xpo1p displays a predominantly nuclear localization and that the protein shuttles between the nucleus and the cytoplasm (Stade et al., 1997). Consistent with the results of Stade et al., we observed nuclear accumulation of Xpo1-GFP in logarithmically growing cultures (Fig. 4-4A)(Stade et al., 1997). However, in addition to its nuclear localization, we were also able to detect the accumulation of Xpo1-GFP at either one focus or two foci per nucleus. These Xpo1-GFP foci did not appear to coincide with kinetochores. Actively growing, asynchronous cultures producing both Xpo1-GFP and the kinetochore marker Mtw1-RFP exhibited distinct non-overlapping foci (Fig. 4-4A). Instead, these foci colocalized with the SPB. Coexpression of *XPO1-GFP* and *SPC42-RFP* revealed both proteins localized in foci that overlapped with one another (Fig. 4-4B), both in G1 when one SPB is present and following SPB duplication in S-phase. As the movement of Mad1p from NPCs to kinetochores is only visible following activation of the SAC, we examined whether SAC activation would also alter the localization of

Figure 4-4. Xpo1p associates with SPBs in logarithmically growing cells and redistributes to kinetochores during SAC arrest.

Logarithmically growing cells synthesizing Xpo1-GFP and Mtw1-RFP (A) or Xpo1-GFP and Spc42-RFP (B), all expressed from their endogenous promoters, were harvested and imaged on an epifluorescence microscope. (C) Xpo1-GFP- and Mtw1-RFP-producing cells were arrested in nocodazole containing media and analyzed microscopically. A *cdc26Δ* mutant was introduced into this strain, cells were shifted to 37°C, and the localization of Mtw1-RFP and Xpo1-GFP was assessed in the absence (D) and presence (E) of nocodazole.

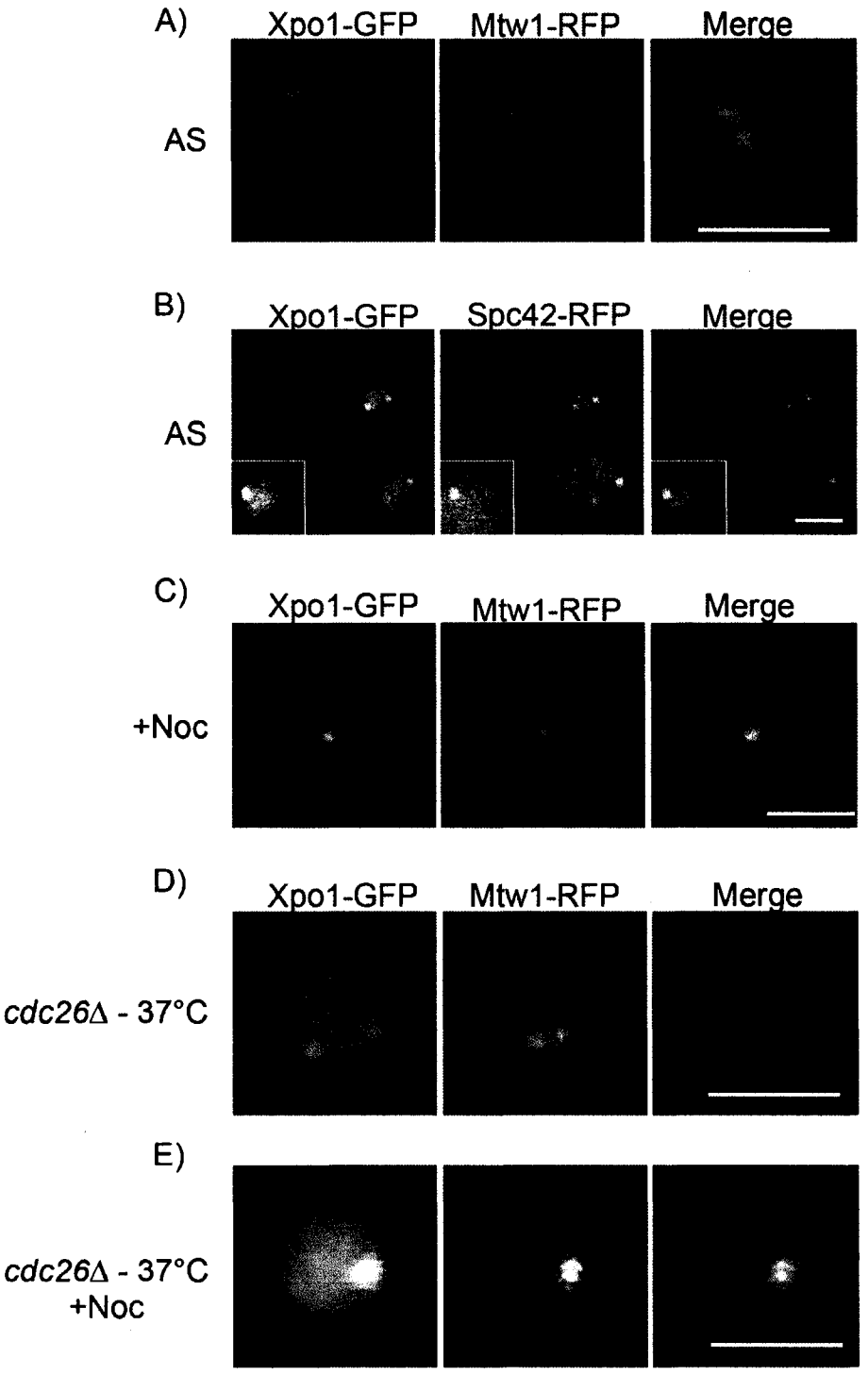

Figure 4-4. Xpo1p associates with SPBs in logarithmically growing cells and redistributes to kinetochores during SAC arrest.

Xpo1-GFP. In these experiments, cells producing Xpo1-GFP and Spc42-RFP or Xpo1-GFP and Mtw1-RFP were treated with nocodazole to induce SAC arrest. Under these conditions, colocalization of Xpo1-GFP with Spc42-RFP was no longer detected and instead, Xpo1-GFP was detected at kinetochores, as indicated by an overlapping signal with Mtw1-RFP (Fig. 4-4C). We also assessed the localization of Xpo1-GFP in a *cdc26Δ* mutant. Cdc26p is a heat shock protein of the APC that is required for growth at 37°C, and *cdc26Δ* mutants at this temperature arrest at the metaphase-anaphase transition without activating the SAC (Hwang and Murray, 1997; Zachariae et al., 1996). Using *cdc26Δ* cells arrested at 37°C, we further assessed whether SAC activation is required for Xpo1p recruitment to kinetochores. As shown in Fig. 4-4D, arresting this strain in metaphase did not induce the movement of Xpo1-GFP to kinetochores, suggesting that this event requires activation of the SAC.

4.2.5 Mad1p turnover on kinetochores during SAC arrest requires Xpo1p

We previously demonstrated that Mad1p cycles between NPCs and kinetochores during SAC arrest (Chapter III). Having established that Xpo1p is required for Mad1p targeting to kinetochores (Fig. 4-2), we directly examined the role of this kap in the turnover of Mad1p at kinetochores. We again made use of mutants in *XPO1, KAP95* or *MSN5*, in *nup60Δ* strain backgrounds expressing both Mad1-GFP and Mtw1-RFP. For these experiments, cells were arrested in G1 and released into nocodazole-containing media to activate the SAC and allow Mad1-GFP to target to kinetochores. We then shifted each strain to their non-permissive condition for the appropriate times and monitored Mad1-GFP turnover at kinetochores by FRAP analysis. In a wild type

background strain, the Mad1-GFP signal at post-photobleached kinetochores recovered completely by 5 min consistent with our previous findings that Mad1p dynamically associates with kinetochores (Chapter III). Similarly, Mad1-GFP recovered on kinetochores following bleaching in both the *kap95-14* strain at 37°C and the *msn5Δ* strain suggesting that these kaps were not required for normal Mad1-GFP kinetochore turnover (Fig. 4-5A). In contrast, photobleaching of kinetochore-associated Mad1-GFP failed to recover in the *xpo1-T539C* strain treated with leptomycin B. These data, together with those discussed above, suggest that Xpo1p is required for both Mad1p's initial targeting onto kinetochores and for subsequent kinetochore turnover during SAC arrest.

4.2.6 RanGTP and its conversion to RanGDP are required for Mad1p turnover on kinetochores

Because Mad1p kinetochore targeting and turnover are influenced by Xpo1p, we investigated the role of the Ran cycle in regulating these events. As discussed above, RanGTP is required for the association of Mad1p with kinetochores following SAC activation, raising the question of whether RanGTP is also required for the turnover of Mad1p at kinetochores. To address this, a *prp20-7 nup60Δ* strain producing Mad1-GFP and Mtw1-RFP was synchronized in G1 phase and then arrested in the subsequent G2/M phase at 23°C with nocodazole. Under these conditions, Mad1-GFP is targeted to unattached kinetochores (Fig. 4-5B, Pre-bleach). The cells were then shifted to the non-permissive temperature for an additional 30 min and the subcellular distribution of Mad1-

Figure 4-5. Mutations in *XPO1* and the Ran cycle abrogate the turnover of Mad1p on kinetochores during SAC arrest.

Wild type (WT), *kap95-14*, *msn5Δ* or *xpo1-T539C* (A), *prp20-7* (B) or *gsp1-G21V* (C) strains deleted for *NUP60* and expressing Mad1-GFP and Mtw1-RFP were arrested in G1 using α-factor and released into 12.5 μg/mL nocodazole for 75 min. Cells were then shifted to their non-permissive condition (+LMB, *xpo1-1* and *prp20-7*, 37°C for 30 min; *gsp-g21V*, +Gal for 90 min) and visualized on a confocal microscope. Kinetochore-associated Mad1-GFP was initially identified by colocalization with Mtw1-RFP (Pre-bleach, arrows). Mad1-GFP was photobleached with 15 iterations of full intensity 488 nm light. Arrows point to the bleached focus, and small arrowheads point to the Mlp-associated focus of Mad1-GFP. Images were acquired immediately following bleaching (Post-bleach, 0') and followed at 12 sec intervals. In (C), the unbleached focus migrated toward the bleached focus during the time course. Bars, 2 μm.

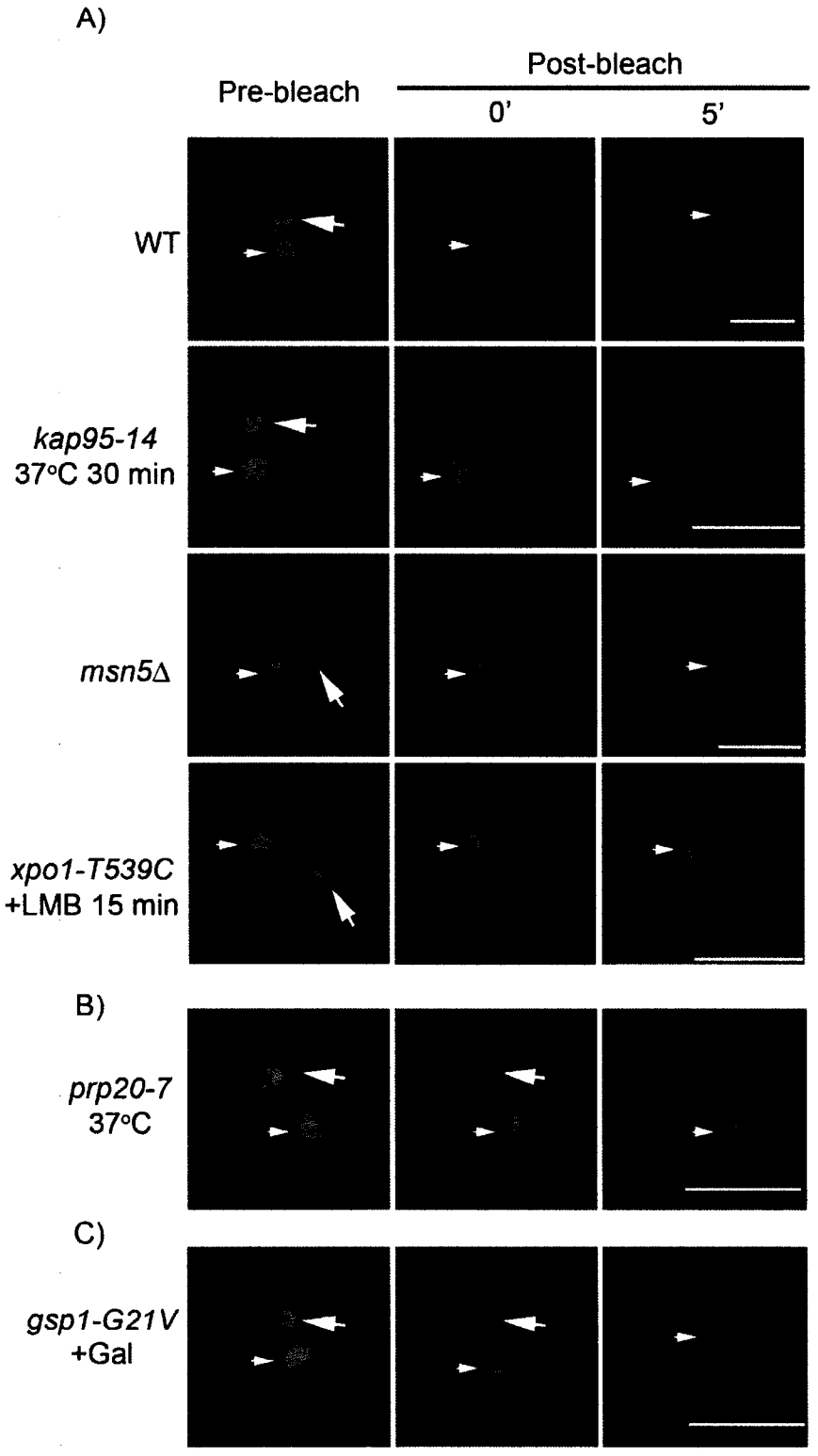

Figure 4-5. Mutations in *XPO1* and the Ran cycle abrogate the turnover of Mad1p on kinetochores during SAC arrest.

GFP was then monitored using confocal microscopy. Interestingly, Mad1-GFP kinetochore localization was maintained at the non-permissive temperature, as evidenced by overlap with Mtw1-RFP. Similarly, the Mlp-associated focus of Mad1-GFP was unaffected (Fig. 4-5B, Pre-bleach). These results suggest that depletion of RanGTP either did not affect the dynamic association of Mad1p with kinetochores or that the kinetochore-associated pool of Mad1-GFP was immobile under these conditions. To distinguish between these two possibilities, we employed FRAP analysis. The kinetochore-associated pool of Mad1-GFP was identified by colocalization with Mtw1-RFP, photobleached and fluorescent recovery was monitored. Inspection of the bleached focus revealed that the Mad1-GFP signal in the *prp20-7* strain failed to recover across the time course of the experiment (Fig. 4-5B). On the basis of these results, we suggest that nuclear RanGTP is required for the cycling of Mad1p on and off unattached kinetochores.

Having observed that nuclear RanGTP levels are important for Mad1p kinetochore turnover, we investigated whether GTP hydrolysis by Ran plays a role in this process. To do this, we employed a dominant-negative mutant of yeast Ran, Gsp1p, the *gsp1-G21V* (Ran-G21V) mutation that stabilizes Ran in its GTP bound form (Schlenstedt et al., 1995). In these experiments, the Ran-G21V gene under the control of the GAL1/10 promoter was integrated into the genome in a *nup60Δ* strain synthesizing Mad1-GFP and Mtw1-RFP. Asynchronous cultures of this strain were grown to an OD_{600} of 0.5 in raffinose-containing media and arrested with nocodazole for 90 min. Following this arrest, cells were shifted to galactose-containing media for an additional 90 min in the maintained presence of nocodazole to induce expression of the dominant negative Ran mutant. We then visualized the cells and, similar to nocodazole-arrested

prp20-7 cells, we observed that Mad1-GFP remained associated with unattached kinetochores under these conditions. However, upon photobleaching of the kinetochore-associated pool, Mad1-GFP was no longer capable of recovering on unattached kinetochores (Fig. 4-5C). Cumulatively, these results are consistent with a model in which RanGTP and its conversion to RanGDP is required for the turnover of Mad1-GFP at unattached kinetochores.

4.3 Discussion

As a better understanding of the NPC and the nuclear transport machinery has emerged, it has become increasingly clear that the NPC machinery serves roles beyond nuclear transport and that some non-transport activities are orchestrated from the NPC. The SAC proteins Mad1p and Mad2p are among the proteins docked at NPCs, an interaction conserved from yeast to humans (Campbell et al., 2001; Iouk et al., 2002) (Chapter III). In yeast, Mad1p is docked at the nucleoplasmic face of NPCs through a presumed complex of Nup60/Mlp1/Mlp2 (Fig. 4-1A). From this complex Mad1p, is dynamically recruited onto kinetochores during SAC arrest in an energy-dependent fashion (Chapter III). Here, we have defined an Xpo1p-dependent NES in Mad1p that is required for its targeting to kinetochores during SAC arrest and have implicated the Ran cycle in Mad1p kinetochore targeting and turnover.

The efficient targeting of Mad1p to kinetochores requires functional Xpo1p and an intact NES within Mad1p (Figs. 4-2A and 4-3B). This suggests that Xpo1p is required for the intranuclear targeting of Mad1p but not necessarily for its nuclear export. Kap mediated intranuclear targeting has previously been suggested for the TATA-binding

protein. Import of TATA-binding protein into the nucleus requires Kap114p, and a subsequent intranuclear targeting step requires both Kap114p and TATA-containing double-stranded DNA to stimulate its deposition on promoters (Pemberton et al., 1999). In our situation, Mad1p is imported into the nucleus in association with Kap60p/Kap95p and deposited at NPCs at the Nup60/Mlp1/Mlp2 complex. Here, Mad1p is associated with NPCs throughout unperturbed cell cycles until depolymerization of microtubules stimulates activation of the SAC. During SAC activation, Mad1p and Mad2p are recruited in an Xpo1p-dependent fashion onto kinetochores. It is unclear whether a putative Mad1p/Xpo1p complex is dissociated on kinetochores and if so, if centromeric DNA or a high affinity kinetochore binding site provides the stimulus for release of Mad1p at kinetochores.

At kinetochores, Mad1p, along with the closed form of Mad2p (C-Mad2), is suggested to act as a template for recruitment and conversion of unbound open Mad2 (O-Mad2p) to C-Mad2p that is competent to bind to and inhibit Cdc20p, preventing APC activation (Musacchio and Salmon, 2007; Nezi et al., 2006). While we have shown that Mad1p and Mad2p exist in a complex at the NPC during interphase (Iouk et al., 2002), it is unclear whether this complex consists of Mad1p/C-Mad2p. In budding yeast, the SAC is not activated during every cell cycle, and consistent with this, Mad1p and Mad2p maintain their association with the NPC during unperturbed cell cycles. This implies that the Mad1p/Mad2p complex that is found at NPCs is inactive and suggests that the C-Mad2p conformer is inactive for APC^{CDC20} inhibition. Alternatively, it is possible that the Mad1p/C-Mad2p complex is not able to impair the SAC until it is associated with unattached kinetochores. It is intriguing to speculate about the nature of the signal

emanating from kinetochores to NPCs that results in a redistribution of Mad1p/C-Mad2p to kinetochores and what prevents this complex from being recruited to kinetochores and activating the SAC during every cell cycle.

During SAC activation, Mad1p is targeted to, and cycles on and off of kinetochores in exchange with the NPC-associated pool of Mad1p (Chapter III). Xpo1p is required for this targeting (Figs. 4-2 and 4-5), and is itself relocated from SPBs to kinetochores during SAC arrest (Fig. 4-4). This is consistent with the formation of a Mad1p/Xpo1p complex specifically during SAC arrest; however, we have thus far been unable to identify such a complex both *in vivo* and *in vitro*. Interestingly, Arnaoutov and colleagues have also shown that HsXpo1 (Crm1) is recruited to mitotic kinetochores in HeLa cells, suggesting that Xpo1 may play a role in targeting other proteins to kinetochores in metazoans (Arnaoutov et al., 2005). Notably, the authors found that Xpo1p was not required for the association of Mad1p with kinetochores following microtubule depolymerization. This result could be a consequence of their experimental design wherein cells were first treated with nocodazole (allowing Mad1 to target to kinetochores) and then treated with leptomycin B. This would prevent Xpo1p turnover on kinetochores and, consequently, Mad1p turnover. A prediction of this would be that Mad1-GFP would be associated with kinetochores but would not display normal turnover kinetics in cells treated with nocodazole then leptomycin B, similar to what we observe in yeast (Fig. 4-5) (Arnaoutov et al., 2005; Howell et al., 2004; Shah et al., 2004). It should be noted that in both *bub1Δ* and *mad1Δ* strains but not *mad2Δ* strains Xpo1p fails to associate with kinetochores during SAC arrest suggesting that Xpo1p requires Mad1p and Mad1p's upstream binding partner Bub1p (Gillett et al., 2004) for binding to

kinetochores (Fig. 4-6). This conforms to a scenario in which Mad1p and Xpo1p associate with kinetochores co-dependently (Figs. 4-2A, 4-5 and 4-6).

Consistent with a role for the export kap, Xpo1p, in Mad1p kinetochore targeting, Mad1p contains an Xpo1p NES positioned between residues 563 and 576 (Figs. 4-1B and 4-3). Mutation of the Mad1p NES results in both a mislocalization of the NLS/NES reporter in a nuclear transport competition assay and in the inability of Mad1p to target to kinetochores in the context of the full-length protein (Figs. 4-3A and 4-3B). Interestingly, while both mutations within the NES, L569A and L575A, dramatically altered the ability of Mad1p to target to kinetochores, no growth inhibition was observed when cells were plated on benomyl (Figs. 4-3B and 4-3C) indicating that the SAC is functional. It has been shown that one kinetochore lacking microtubule occupancy is sufficient to induce SAC arrest (Li and Nicklas, 1995; Rieder et al., 1995). This lends itself to the suggestion that these mutations greatly reduce Mad1p kinetochore targeting (below the limit of detection), as opposed to completely inhibiting targeting, which would be predicted to inactivate the SAC.

In addition to its requirement for Xpo1p in targeting, the small G-protein Ran, specifically in its GTP-bound state, is also required for Mad1p kinetochore targeting and turnover (Figs. 4-2 vi and 4-5). Again, this is consistent with the formation of a complex of Xpo1p, Mad1p and Gsp1p-GTP (Ran) forming during M-phase. This complex would typically be referred to as a nuclear export complex however; I suggest that an export complex cannot be defined as such until it encounters the RanGAP (Rna1p in yeast) in the cytoplasm. Here, following RanGTP-GDP conversion, the complex would be dissociated and define a nuclear export cycle. For Mad1p, it is possible that

Figure 4-6. Xpo1p requires Mad1p and Bub1p for normal kinetochore localization.

Deletions in SAC components *MAD1*, *MAD2* and *BUB1* were introduced into a *cdc26Δ* strain. Strains were grown to midlog phase at 23°C then shifted to 37°C for 2 h. Cells were then visualized directly (top panel set of each strain) or shifted to nocodazole containing media to induce the SAC. Cells were maintained at 37°C for 0.5 h during the nocodazole treatment to ensure continued metaphase arrest (bottom panel set of each strain).

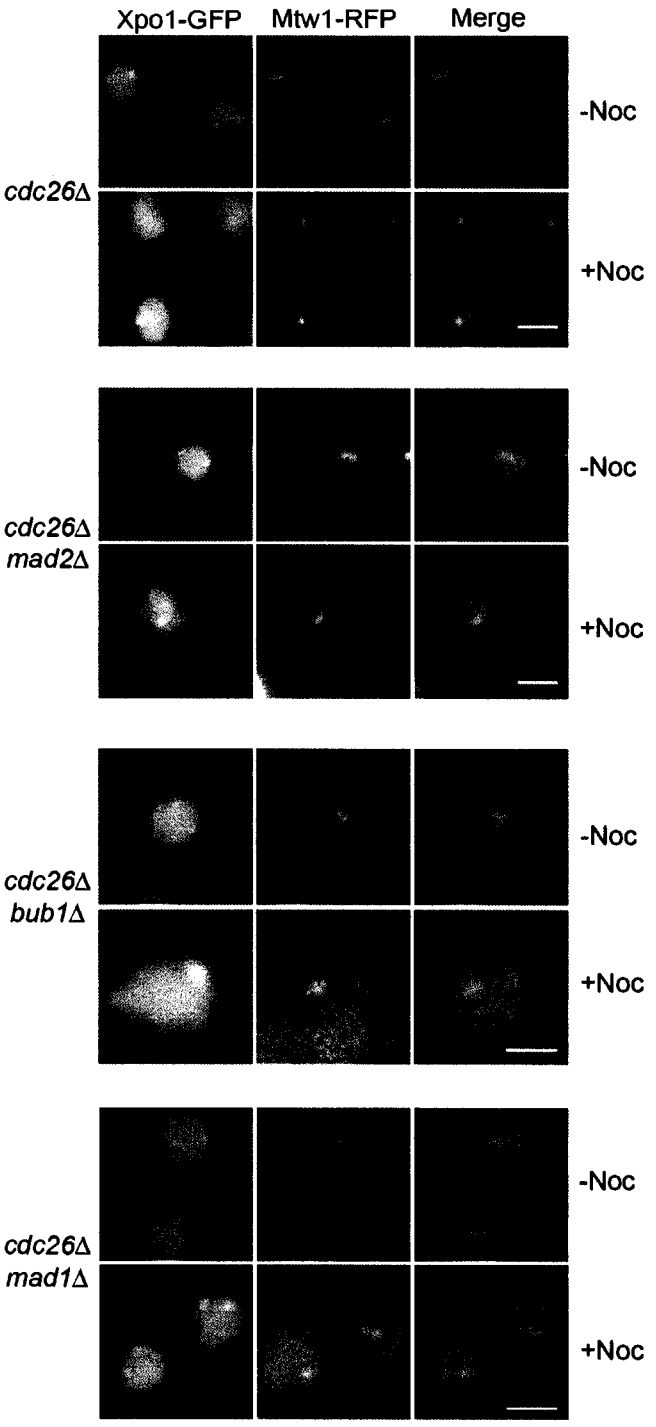

Figure 4-6. Xpo1p requires Mad1p and Bub1p for normal kinetochore localization.

export through the NPC is inhibited by high affinity sites provided by the Nup60/Mlp1/Mlp2 (or other nups) docking complex at the nucleoplasmic faces of NPCs. As such, the presumed Xpo1/Mad1/Gsp1 complex would be confined to the nucleus and to intranuclear targeting events, including to kinetochores.

The finding that Mad1p targeting to kinetochores not only requires nuclear RanGTP but that it appears to require Ran-mediated GTP hydrolysis is an intriguing result. On its surface, the suggestion that Ran-mediated GTP hydrolysis occurs within the nucleus is confounding. The gradient established for nuclear transport relies on high concentrations of nuclear RanGTP maintained by the RanGEF (Prp20p in yeast) and the presence of RanGDP in the cytoplasm maintained by RanGAP (Rna1p in yeast). For this reason, it is thought that the RanGAP and RanGEF are strictly compartmentalized to the cytoplasm and nucleoplasm, respectively. In metazoans, however, recent studies have shown that following NEBD, RanGAP can be found in association with kinetochores during M-phase (Arnaoutov and Dasso, 2003; Joseph et al., 2002; 2004). How RanGAP may access kinetochores during the closed mitosis of yeast is less clear, but evidence has been provided in both *S. cerevisiae* and in *S. pombe* that RanGAP can associate with chromatin and moreover that *S. cerevisiae* RanGAP contains both an NLS and an NES, indicating that the protein may shuttle between the nucleus and cytoplasm (Feng et al., 1999; Nishijima et al., 2006). Whether shuttling is cell cycle-regulated requires further investigation and could provide insight about how the cell regulates the SAC.

In metazoans, attenuation of the SAC is at least partially mediated by $p31^{comet}$ (Habu et al., 2002; Vink et al., 2006; Xia et al., 2004). A functional homologue of this protein has yet to be identified in *S. cerevisiae* (Nezi et al., 2006), suggesting that other

mechanisms exist to aid in SAC attenuation. The rapid rate of Mad1p turnover on kinetochores provides one possible mechanism for SAC shutoff in *S. cerevisiae*. In this scenario, Mad1p, with the aid of Xpo1p, shuttles between the NPC and kinetochores until each kinetochore is occupied by microtubules, preventing this complex from associating with kinetochores. Whether microtubule occupancy, an active inhibitor such as $p31^{comet}$ or other mechanisms, including NPC-mediated ones, are required to attenuate the SAC in yeast remains unclear.

The NPC and kaps, in addition to their roles in nuclear transport, can be thought of as a way station and delivery apparatus from which alternative cellular processes, including the SAC, can be regulated. How signalling from kinetochores to NPCs, or *vice versa*, impinge on cellular processes remains to be resolved. Of note, the NPC undergoes dramatic structural rearrangements during SAC arrest. Specifically, a Kap121p binding site on Nup53p is uncovered resulting in mitosis-specific inhibition of the Kap121p import pathway (Makhnevych et al., 2003). It is intriguing to speculate if and how kinetochores could signal to NPCs to induce these dramatic changes and if the movement of Xpo1p, and Mad1p, between these two locations could be responsible for transducing this signal.

Chapter V: *Perspectives*

5.1 Synopsis

The SAC genes were initially uncovered in genetic screens designed to identify components required for cell survival in the presence of microtubule-destabilizing drugs (Li and Murray, 1991; Hoyt et al., 1991). It has since been shown that two of the SAC proteins, Mad1p and Mad2p, are found in association with interphase NPCs and from there, are targeted onto kinetochores during mitosis. At kinetochores, Mad1p and Mad2p participate the in formation of an inhibitory signal that halts cell cycle progression at the metaphase to anaphase transition. Here we have defined a subset of nups required for Mad1p localization to NPCs and have defined the domains of Mad1p required for NPC and kinetochore localization. We have shown that Mad1p is dynamically associated with kinetochores and NPCs and that its movement between these locales requires an Xpo1p-specific NES. Here, I will discuss our results in the context of their implications regarding the NPC and nuclear processes, including the SAC. I will also speculate about how these three processes may be interwoven to endow cells with mechanisms to coordinate chromosome segregation with NPC processes during mitosis.

5.2 NPCs as sites of convergence for nuclear processes

Following proteomic analyses of yeast and vertebrate NPCs, the apparent complement of proteins was determined (Rout et al., 2000; Cronshaw et al., 2002). These proteins, *bona fide* nups, are thought to constitute the stationary phase of nuclear transport (Marelli et al., 2001). However, several lines of evidence prior to and since these studies have suggested that NPCs are dynamic in their own structure and that additional components reside at NPCs. An excellent example of a mobile nucleoporin is

Nup2p. Nup2p is associated with the nucleoplasmic face of the NPC but does not co-enrich with NPCs in fractionation experiments (Rout et al., 2000). Interestingly, Nup2p interacts with Kap60p/Kap95p and is mobile (Dilworth et al., 2001). The mobility of Nup2p along with RanGEF (Prp20p) are proposed to delimit boundaries between active and inactive chromatin regions (Dilworth et al., 2005). Another example of nups with functions outside of the NPC and nuclear transport is the Nup107-160 complex. The Nup107-160 complex associates with metazoan kinetochores during mitosis and is required for normal mitotic progression (Zuccolo et el., 2007) (Section 1.7.2). These examples highlight the dynamic nature of nups and the potential for their involvement in non-transport related activities.

In addition to nups with secondary non-transport functions, the NPC also hosts proteins that are not *bona fide* nups. Dbp5p is one of these and is anchored at NPCs through an interaction with Nup159p (Strahm et al., 1999; Weirich et al., 2004). The localization of Dbp5p is likely not temporally regulated and constitutively participates in mRNA export. However, other NPC-associated proteins, including Mad1p and Mad2p, are temporally regulated in their NPC association. The NPC association of the SUMO isopeptidase Ulp1p is also temporally regulated. During mitosis, Ulp1p is transiently released from the NPC and mediates septin ring desumoylation in a Kap121p-dependent fashion (Makhnevych et al., 2007).

The Mlp proteins are another example of NPC-associated proteins with unique characteristics. While nups are evenly distributed along the NE, Mlp anchorage at NPCs is limited to regions of the NE that do not overlay the nucleolus (Galy et al., 2004). This is similar to what we observe for the localization of Mad1p to NPCs (Appendix, Fig. 7-1)

and is also the case for Ulp1p (Zhao et al., 2004). Interestingly, Mad1p, Mlp1p, Mlp2p and Ulp1p are all dependent on Nup60p for their normal localization to NPCs yet Nup60p itself localizes to NPCs, that overlay the nucleolus (Feuerbach et al., 2002; Galy et al., 2004; Zhao et al., 2004) (Chapter III). Notably, and consistent with this, Mad1p and Nup60p interact directly in using *in vitro* binding assays (Appendix, Fig. 7-2). The asymmetric NPC-associated protein distribution along the NE suggests that NPCs themselves are compositionally distinct and may perform distinct non-homogenous functions. This may highlight the ability of the NPC to serve as a distribution center in specific nuclear regions for the function of these proteins and others in cellular processes.

5.3 Karyopherins as kinetochore targeting factors

The mechanisms that govern protein transport into and out of the nucleus are well studied and generally well understood. A less appreciated aspect of protein targeting concerns protein targeting to subdomains of a given organelle. Most characterized nuclear signal sequences are indeed organellar-targeting sequences, and few examples exist of signals that specify discrete domain localization. Notably, two examples of NLSs that aid in subnuclear targeting have been identified (Section 1.5.2) (Hatanaka, 1990; Pemberton et al., 1999). Both the TATA-binding protein and regulatory proteins of HIV-I are targeted to their subnuclear domains using their NLSs. Here, we have shown that Mad1p contains an Xpo1p-specific NES that is required for its targeting and turnover on SAC-arrested kinetochores. Together, these data suggest that nuclear signal sequences and nuclear transport receptors may be involved in targeting events beyond simple nuclear localization or export.

The use of nuclear transport receptors for subnuclear targeting has important consequences for transport complexes. As discussed in Section 1.5, nuclear import complexes are dissociated in the nucleus as a consequence of RanGTP-mediated conformational changes of import kaps. This dissociation is thought to occur at the nuclear basket, effectively releasing import cargos at their earliest encounter with the nuclear compartment (Marelli et al., 2001; Dilworth et al., 2001). The ability of an import complex to bypass cargo release on nuclear entry would predict that certain kap/cargo complexes are incapable of binding RanGTP. The complex could prevent RanGTP binding in several ways. The simplest explanation for this is that the cargo molecule itself blocks the Ran-binding site on the kap. The Ran binding domain of kaps and the cargo interacting domains are located N- and C- terminally respectively; however, the superhelical kap twist could feasibly place the cargo over the kap Ran binding domain (Chi et al., 1997a; 1997b; Kutay et al., 1997; Cingolani et al., 1999). Only once the cargo reaches its final binding destination (*e.g.* TATA-containing DNA) would the Ran binding domain be uncovered. Another possibility is that specific kap-NLS interactions are insensitive to dissociation by Ran-GTP. Recombinant chimeric Kapβ2 NLSs display this property (Cansizoglou et al., 2007). In this case as in the first possibility, kap-NLS complexes may only be dissociated once cargo interacts with a high affinity binding partner or a conformational change is induced through cargo binding.

The intranuclear targeting of Mad1p by Xpo1p presumably requires the formation of a nuclear export-like complex. This trimeric complex including RanGTP would be subject to the same transport rules as other nuclear export complexes. Whether the complex shuttles between the cytoplasm and nucleus is unclear although the presence of

both NLS and NES in Mad1p is suggestive. It is possible that a high affinity interaction between Mad1p and the Mlp1p/Mlp2p/Nup60p complex or with Nup53p at NPCs prevents the Mad1p/Xpo1p complex from being exported. Alternatively, the NPC itself may induce dissociation of the Mad1p/Xpo1p complex. Dissociation of a nuclear export complex in the nucleus, specifically at kinetochores, would likely require the function of a Ran-specific GAP. Interestingly, in the *xpo1-1* mutant strain, Mad1-GFP is mislocalized to intranuclear foci reminiscent of SPBs at the non-permissive temperature (Appendix, Fig. 7-3). The mislocalization of Mad1-GFP in this background is strong evidence suggesting that Mad1p and Xpo1p form a complex *in vivo* and supports the possibility that they form a stable nuclear export-like complex in the nucleus.

5.3.1 RanGAP at kinetochores

In order for an Xpo1/Mad1p/RanGTP complex to be released on kinetochores, we predict that RanGTP would be converted to RanGDP. This is supported by our experimental evidence showing that inhibition of RanGTP to RanGDP conversion impairs Mad1p turnover on kinetochores during SAC activation (Fig. 4-5). This implies that the intrinsic GTPase activity of Ran would be increased in the kinetochore vicinity, likely by RanGAP. We have been unable to detect RanGAP (Rna1-GFP) on kinetochores or in the nucleus of asynchronous and nocodazole-arrested cells (Appendix, Fig. 7-4A). We suggest that RanGAP could interact with kinetochores during yeast mitosis, as it does in vertebrates, but at levels below our detection limits (Joseph et al., 2002; 2004; Arnaoutov et al., 2005). Support for this comes from studies demonstrating that yeast RanGAP contains functional NLS and NES sequences and accumulates in the

nucleus of *xpo1-1* temperature sensitive cells at the non-permissive temperature (Feng et al., 1999). Moreover, RanGAP was shown to accumulate in the nucleus of both *S. pombe* and *Aspergillus nidulans* nuclei, suggesting that its movement into the nucleus is required for an important and possibly conserved process (De Souza et al., 2004; Kusano et al., 2004; Nishijima et al., 2006). It is possible then that in M-phase-arrested *XPO1* mutants at their non-permissive condition, RanGAP would be detected on kinetochores. It is also possible that the RanGAP NES would be required for kinetochore targeting, consistent with the mechanism proposed here. This raises the possibility that other proteins are targeted to kinetochores in an Xpo1p-dependent fashion.

5.4 NESs for kinetochore targeting

The SAC protein Mad1p of yeast and RanGAP1, Nup358 and the chromosomal passenger complex (CPC) of vertebrates are targeted to kinetochores during mitosis in a Xpo1p-dependent fashion (Chapter IV) (Arnaoutov et al., 2005; Knauer et al., 2006). This raises the possibility that Xpo1p-mediated kinetochore targeting is a more general mechanism employed by cells in building kinetochores. It follows that other kinetochore proteins would be predicted to contain NESs. In a coarse survey of both yeast and vertebrate kinetochore proteins, predicted NESs were found in several notable proteins (la Cour et al., 2004). Among these were the yeast SAC protein, Bub1p, and the resident kinetochore protein, Ndc80p. Ndc80p has been suggested to be required for the assembly of SAC proteins on kinetochores during yeast SAC activation (Gillett et al., 2004). In vertebrates both ZW10 and ROD contained predicted NESs (Appendix, Fig. 7-4B). This is also significant, as ZW10, together with Nuf2 and Ndc80 (Hec1) are required for the

stable association of Mad1 and Mad2 at unattached kinetochores (Martin-Lluesma et al., 2002; DeLuca et al., 2003; Kops et al., 2005). Further investigation is required to determine if these NESs are functional and whether they are necessary for kinetochore targeting. Kap-mediated targeting of NES-containing proteins to kinetochores would provide cells with a mechanism by which they could sample the kinetochore environment and relay that information back to NPCs, completing a signalling loop. In this way, kinetochores could sample NPCs and coordinate NEBD and NPC disassembly with chromosome congression and segregation.

5.5 Kinetochore signalling to the NPC

The apparent primary function of Mad1p is to provide a signalling platform at kinetochores from which the SAC can inhibit the APC. Interestingly, our work shows that Mad1p is not stably associated with yeast kinetochores and rapidly shuttles between kinetochores and NPCs during SAC arrest (Fig. 3-6). This shuttling is consistent with a signal transduction function for Mad1p from kinetochores to NPCs (Fig. 5-1). During mitosis, kinetochore architecture must be altered to accommodate both the loss of stable microtubule interactions and also to allow for the recruitment of SAC proteins. In parallel with these changes, the yeast NPC also undergoes structural rearrangements during mitosis. Specifically, the Nup53-containing complex is reorganized and releases its binding partner, Nup170p, uncovering a binding site specific for Kap121p. The Kap121p binding site on Nup53p is thought to slow the movement of this kap through the NPC effectively inhibiting Kap121p-mediated nuclear import during M-phase (Makhnevych et al., 2003). Similarly, the fungus *A. nidulans*, which also proceeds

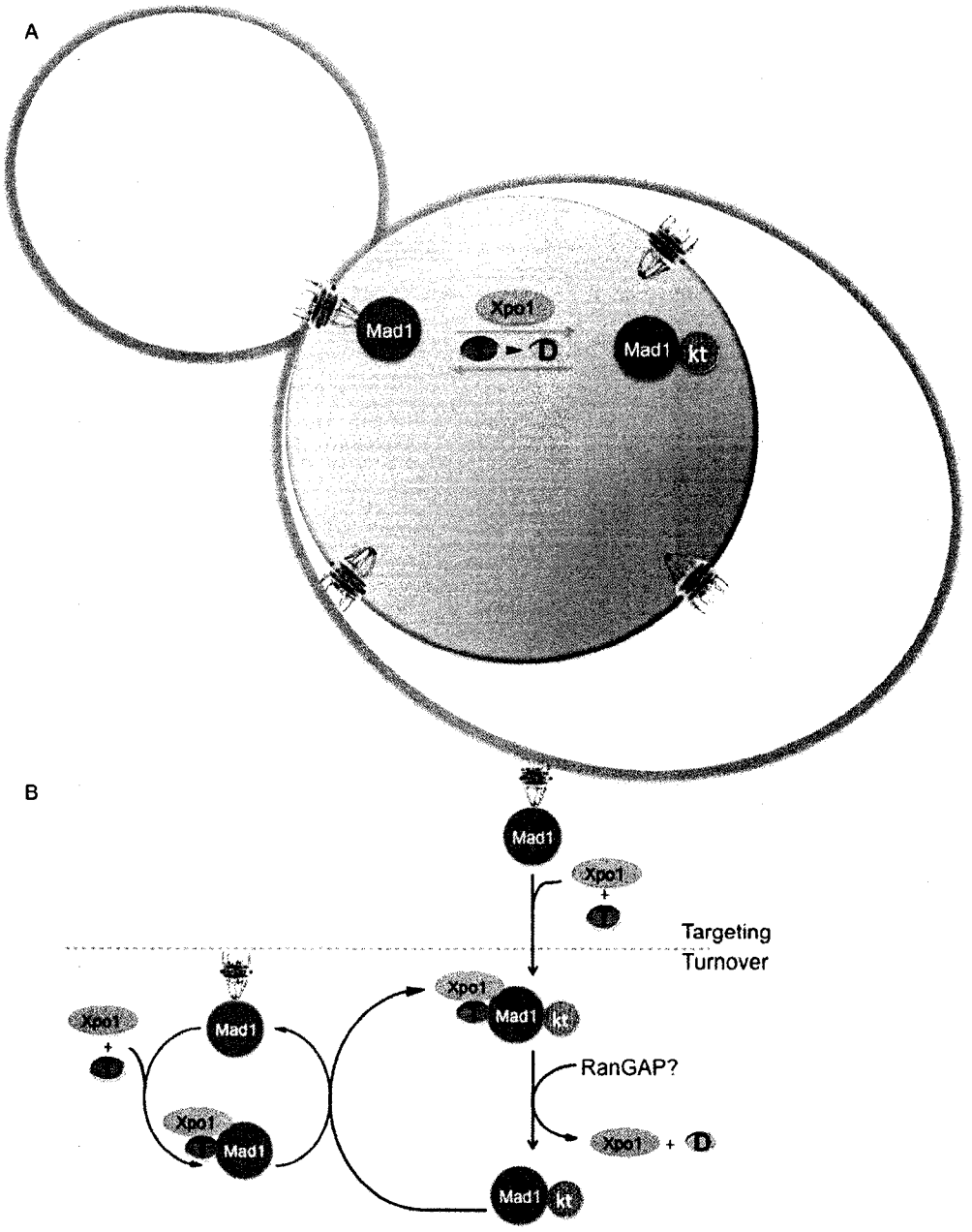

Figure 5-1. Xpo1p-mediated communication between kinetochores and NPCs.

A) During SAC arrest, Mad1p (dark grey sphere) is redistributed from NPCs to kinetochores (red sphere, labelled kt) in an Xpo1p (light grey oval) and RanGTP dependent manner. Additionally, the conversion of RanGTP (T) to RanGDP (D) is required for the turnover of Mad1p at kinetochores. B) Mad1p targeting (upper portion) and turnover at kinetochores (lower portion) requires Xpo1p and RanGTP. A Ran-specific GAP is proposed to function at kinetochores.

through a closed mitosis, also undergoes a partial rearrangement of its NPCs during M-phase (De Souza et al., 2004). The signal that triggers NPC rearrangement is unclear; however, one possibility is that this signal may emanate from kinetochores. In yeast, where the NE remains intact, it is possible that a signal to trigger NPC rearrangements is the movement of Mad1p from kinetochores to NPCs during mitosis. Consistent with this, recent work in our laboratory has demonstrated that deletion of *MAD1* alleviates the Kap121p-mediated nuclear import inhibition during mitosis (L. Cairo and R. Wozniak, personal communication). Further experiments have shown that the C-terminus of the protein, which is competent for rescuing the SAC but does not bind the NPC, is not capable of recovering import inhibition. This suggests that the interaction between Mad1p and the NPC, and not the SAC itself, is critical for inducing structural rearrangements during mitosis that lead to the inhibition of Kap121p-mediated nuclear import (Fig. 5-1). This also implies that the kap-mediated targeting and turnover of Mad1p to kinetochores and NPCs by Xpo1p could itself serve to modulate another kap pathway, the Kap121p import pathway. In vertebrates, CENP-F migrates from kinetochores and transiently associates with NPCs immediately preceding NEBD in prometaphase. While CENP-F is a potential source of a signal to the vertebrate NPCs and NE for disassembly and breakdown, `RNAi studies have shown that NEBD progresses normally in its absence (Zuccolo et al., 2007) (M. Zuccolo and V. Doye, personal communication). Interestingly, HsMad1 appears to associate with a fraction of kinetochores during prophase prior to NEBD (Campbell et al., 2001). It is possible that in vertebrates, this early association of Mad1 with kinetochores may transduce a signal to NPCs and the NE. This signal could be a cue to induce NPC disassembly and NEBD.

5.6 Mad1p and Mad2p during interphase

We have shown that Mad1p and Mad2p are docked at NPCs in interphase and from here dynamically exchange with kinetochores during SAC arrest (Iouk et al., 2002) (Chapter III and IV). Several groups have shown that Mad1p and Mad2p form a stable complex throughout the cell cycle and that this complex is essential for SAC function (Chen et al., 1999; Chung and Chen, 2002). It has also been shown that both Mad1-bound and Mad1-free Mad2 are required for SAC function. All of these findings, along with photobleaching data, have been incorporated into the Mad2 template model (Chung and Chen, 2002; De Antoni et al., 2005a; Nezi et al., 2006). In this model, Mad1-bound Mad2 adopts a closed conformation (C-Mad2). This heterodimer of Mad1 and C-Mad2 is then capable of recruiting the open form of Mad2 (O-Mad2) and converting it into C-Mad2 that is competent for Cdc20 inhibition. Interestingly, while Mad1p and Mad2p are complexed throughout the cell cycle, the SAC activating properties of this complex appear to be reserved for mitosis only. How this is accomplished is unclear. In metazoans, $p31^{comet}$ is required for silencing the SAC (Xia et al., 2004). $p31^{comet}$ forms a complex specifically with the Cdc20-bound form of Mad2. Because $p31^{comet}$ binds specifically to Cdc20-bound Mad2, it seems unlikely that it would also function as an inhibitor of the Mad1/C-Mad2 heterodimer at NPCs (Xia et al., 2004). A more intriguing possibility is that a nucleoporin is responsible for preventing O-Mad2 recruitment and conversion. A potential nucleoporin is Nup53p. Deletion of *NUP53* results in a mitotic delay similar to that observed in $p31^{comet}$ RNAi experiments (Section 3.2.5) (Xia et al., 2004). SAC activation and Mad1/Mad2 release from NPCs would spatially alleviate this

inhibition and allow O-Mad2 recruitment. Another possibility is that kinetochores sensitize the Mad1/C-Mad2 complex for O-Mad2 conversion and SAC function. This would imply that only when the Mad1/C-Mad2 complex is bound to kinetochores following Xpo1-mediated targeting would it then be competent for SAC signalling. This is analogous to the MCC, which can be purified from interphase cells in an active form but only functions from kinetochores (Sudakin et al., 2001).

5.7 Xpo1 kinetochore targeting of Mad1 in metazoans

Collectively, our data show that yeast Mad1p is localized to NPCs during interphase and that it is redistributed to kinetochores during yeast SAC arrest in an Xpo1p-dependent fashion. We predict that this mechanism of kinetochore targeting would be conserved and that similar results could be expected in metazoans. In a study investigating the targeting of Nup358 and RanGAP1 to kinetochores, the complex was found anchored at kinetochores through Nup358. RNAi depletion of Nup358 resulted in a loss of RanGAP1 at kinetochores (Joseph et al., 2004). Interestingly, in the absence of Nup358, Mad1 and Mad2 were also mislocalized, indicating that it is required for their normal association with kinetochores. Unexpectedly, experiments showing that Nup358 and RanGAP1 are targeted in an Xpo1-dependent manner did not similarly mislocalize Mad1 or Mad2 from unattached kinetochores in the absence of functional Xpo1 (Arnaoutov et al., 2005). This discrepancy can be explained by examining the experimental setup employed. Asynchronous cell populations were treated with leptomycin B to inhibit Xpo1 function, pre-extracted, fixed and prepared for immunofluorescence. Under these conditions, Mad1 and Mad2 would have been targeted

to kinetochores prior to Xpo1 inhibition. To resolve this discrepancy, photobleaching experiments on live cells expressing Mad1-GFP such as those presented here in yeast and by Shah et al. and Howell et al. in vertebrates could be employed (Shah et al., 2004; Howell et al., 2004).

The lack of a NE during metazoan mitosis results in the redistribution of Ran and its modulators. RanGAP1 localizes to kinetochores and RanGEF along chromosomes, suggesting that only in the vicinity of chromosomes would Ran have its nucleotide-bound state altered (Joseph et al., 2002). Kalab et al. have indeed visualized this collapsed Ran gradient with localized high concentrations of RanGTP in the vicinity of condensed chromosomes (Kalab et al., 2002). This then raises the question of where in metazoans Xpo1 is forming a RanGTP-dependent complex with its kinetochore-directed cargos such as the CPC and Nup358/RanGAP1. It is possible that this complex forms very close to chromosomes only. In yeast, the situation is compounded by the lack of an NE, and consequent collapse of the Ran gradient during mitosis and a Xpo1p/Mad1p/RanGTP complex could readily form in the nucleoplasm.

A paradoxical finding is that RanGAP1 itself is transported to kinetochores in a RanGTP-dependent Xpo1-mediated fashion (Joseph et al., 2002; Arnaoutov et al., 2005). What prevents the GAP activity of RanGAP is unclear. It is possible that upon deposition of this complex at kinetochores, RanGAP1 activity is recovered, allowing these complexes to be dissociated. This would imply that Xpo1p would be released from this complex at kinetochores potentially releasing it for turnover. Whether Xpo1p is mobile on yeast or metazoan kinetochores remains to be seen.

Our studies have revealed that Mad1p is associated with the yeast NPC during interphase and that it is recruited to mitotic kinetochores from NPCs using an Xpo1p-dependent targeting pathway. We have suggested that other kinetochore proteins, both resident and more transient occupiers such as SAC components, could employ this mechanism of kinetochore targeting. Our studies have suggested that the nuclear transport machinery, including the NPC and kaps, is important for modulating the activity of Mad1p spatially and temporally.

Chapter VI: *References*

Adachi, Y., and M. Yanagida. 1989. Higher order chromosome structure is affected by cold-sensitive mutations in a Schizosaccharomyces pombe gene crm1+ which encodes a 115-kD protein preferentially localized in the nucleus and its periphery. *J Cell Biol.* 108:1195-207.

Adames, N.R., and J.A. Cooper. 2000. Microtubule interactions with the cell cortex causing nuclear movements in *Saccharomyces cerevisiae*. *J Cell Biol.* 149:863-74.

Adams, A., D.E. Gottschling, C.A. Kaiser, and T. Stearns. 1997. Methods in Yeast Genetics. *Cold Spring Harbor Laboratory*:177.

Aitchison, J.D., G. Blobel, and M.P. Rout. 1995a. Nup120p: a yeast nucleoporin required for NPC distribution and mRNA transport. *J Cell Biol.* 131:1659-75.

Aitchison, J.D., G. Blobel, and M.P. Rout. 1996. Kap104p: a karyopherin involved in the nuclear transport of messenger RNA binding proteins. *Science.* 274:624-7.

Aitchison, J.D., M.P. Rout, M. Marelli, G. Blobel, and R.W. Wozniak. 1995b. Two novel related yeast nucleoporins Nup170p and Nup157p: complementation with the vertebrate homologue Nup155p and functional interactions with the yeast nuclear pore-membrane protein Pom152p. *J Cell Biol.* 131:1133-48.

Aitchison, J.D., and R.W. Wozniak. 2007. Cell biology: pore puzzle. *Nature.* 450:621-2.

Akey, C.W., and M. Radermacher. 1993. Architecture of the Xenopus nuclear pore complex revealed by three-dimensional cryo-electron microscopy. *J Cell Biol.* 122:1-19.

Alber, F., S. Dokudovskaya, L.M. Veenhoff, W. Zhang, J. Kipper, D. Devos, A. Suprapto, O. Karni-Schmidt, R. Williams, B.T. Chait, M.P. Rout, and A. Sali. 2007a. Determining the architectures of macromolecular assemblies. *Nature.* 450:683-94.

Alber, F., S. Dokudovskaya, L.M. Veenhoff, W. Zhang, J. Kipper, D. Devos, A. Suprapto, O. Karni-Schmidt, R. Williams, B.T. Chait, A. Sali, and M.P. Rout. 2007b. The molecular architecture of the nuclear pore complex. *Nature.* 450:695-701.

Alcazar-Roman, A.R., E.J. Tran, S. Guo, and S.R. Wente. 2006. Inositol hexakisphosphate and Gle1 activate the DEAD-box protein Dbp5 for nuclear mRNA export. *Nat Cell Biol.* 8:711-6.

Amberg, D.C., M. Fleischmann, I. Stagljar, C.N. Cole, and M. Aebi. 1993. Nuclear PRP20 protein is required for mRNA export. *Embo J.* 12:233-41.

Andrade, M.A., and P. Bork. 1995. HEAT repeats in the Huntington's disease protein. *Nat Genet.* 11:115-6.

Andrulis, E.D., D.C. Zappulla, A. Ansari, S. Perrod, C.V. Laiosa, M.R. Gartenberg, and R. Sternglanz. 2002. Esc1, a nuclear periphery protein required for Sir4-based plasmid anchoring and partitioning. *Mol Cell Biol.* 22:8292-301.

Antonin, W., C. Franz, U. Haselmann, C. Antony, and I.W. Mattaj. 2005. The integral membrane nucleoporin pom121 functionally links nuclear pore complex assembly

and nuclear envelope formation. *Mol Cell.* 17:83-92.

Arnaoutov, A., Y. Azuma, K. Ribbeck, J. Joseph, Y. Boyarchuk, T. Karpova, J. McNally, and M. Dasso. 2005. Crm1 is a mitotic effector of Ran-GTP in somatic cells. *Nat Cell Biol.* 7:626-32.

Arnaoutov, A., and M. Dasso. 2003. The Ran GTPase regulates kinetochore function. *Dev Cell.* 5:99-111.

Arts, G.J., S. Kuersten, P. Romby, B. Ehresmann, and I.W. Mattaj. 1998. The role of exportin-t in selective nuclear export of mature tRNAs. *Embo J.* 17:7430-41.

Beck, M., F. Forster, M. Ecke, J.M. Plitzko, F. Melchior, G. Gerisch, W. Baumeister, and O. Medalia. 2004. Nuclear pore complex structure and dynamics revealed by cryoelectron tomography. *Science.* 306:1387-90.

Becker, D.M., and L. Guarente. 1991. High-efficiency transformation of yeast by electroporation. *Methods Enzymol.* 194:182-7.

Belgareh, N., G. Rabut, S.W. Bai, M. van Overbeek, J. Beaudouin, N. Daigle, O.V. Zatsepina, F. Pasteau, V. Labas, M. Fromont-Racine, J. Ellenberg, and V. Doye. 2001. An evolutionarily conserved NPC subcomplex, which redistributes in part to kinetochores in mammalian cells. *J Cell Biol.* 154:1147-60.

Belgareh, N., C. Snay-Hodge, F. Pasteau, S. Dagher, C.N. Cole, and V. Doye. 1998. Functional characterization of a Nup159p-containing nuclear pore subcomplex. *Mol Biol Cell.* 9:3475-92.

Ben-Efraim, I., and L. Gerace. 2001. Gradient of increasing affinity of importin beta for nucleoporins along the pathway of nuclear import. *J Cell Biol.* 152:411-7.

Bickel, T., and R. Bruinsma. 2002. The nuclear pore complex mystery and anomalous diffusion in reversible gels. *Biophys J.* 83:3079-87.

Biggins, S., and A.W. Murray. 2001. The budding yeast protein kinase Ipl1/Aurora allows the absence of tension to activate the spindle checkpoint. *Genes Dev.* 15:3118-29.

Bischoff, F.R., and H. Ponstingl. 1991. Catalysis of guanine nucleotide exchange on Ran by the mitotic regulator RCC1. *Nature.* 354:80-2.

Bischoff, F.R., and H. Ponstingl. 1995. Catalysis of guanine nucleotide exchange of Ran by RCC1 and stimulation of hydrolysis of Ran-bound GTP by Ran-GAP1. *Methods Enzymol.* 257:135-44.

Blobel, G. 1985. Gene gating: a hypothesis. *Proc Natl Acad Sci U S A.* 82:8527-9.

Brachmann, C.B., A. Davies, G.J. Cost, E. Caputo, J. Li, P. Hieter, and J.D. Boeke. 1998. Designer deletion strains derived from *Saccharomyces cerevisiae* S288C: a useful set of strains and plasmids for PCR-mediated gene disruption and other applications. *Yeast.* 14:115-32.

Burke, B., and J. Ellenberg. 2002. Remodelling the walls of the nucleus. *Nat Rev Mol Cell Biol.* 3:487-97.

Byrd, D.A., D.J. Sweet, N. Pante, K.N. Konstantinov, T. Guan, A.C. Saphire, P.J. Mitchell, C.S. Cooper, U. Aebi, and L. Gerace. 1994. Tpr, a large coiled coil protein whose amino terminus is involved in activation of oncogenic kinases, is localized to the cytoplasmic surface of the nuclear pore complex. *J Cell Biol.* 127:1515-26.

Cabal, G.G., A. Genovesio, S. Rodriguez-Navarro, C. Zimmer, O. Gadal, A. Lesne, H. Buc, F. Feuerbach-Fournier, J.C. Olivo-Marin, E.C. Hurt, and U. Nehrbass. 2006. SAGA interacting factors confine sub-diffusion of transcribed genes to the nuclear envelope. *Nature.* 441:770-3.

Callan, H.G., and S.G. Tomlin. 1950. Experimental studies on amphibian oocyte nuclei. I. Investigation of the structure of the nuclear membrane by means of the electron microscope. *Proc R Soc Lond B Biol Sci.* 137:367-78.

Campbell, M.S., G.K. Chan, and T.J. Yen. 2001. Mitotic checkpoint proteins HsMAD1 and HsMAD2 are associated with nuclear pore complexes in interphase. *J Cell Sci.* 114:953-63.

Cansizoglu, A.E., B.J. Lee, Z.C. Zhang, B.M. Fontoura, and Y.M. Chook. 2007. Structure-based design of a pathway-specific nuclear import inhibitor. *Nat Struct Mol Biol.* 14:452-4.

Carazo-Salas, R.E., O.J. Gruss, I.W. Mattaj, and E. Karsenti. 2001. Ran-GTP coordinates regulation of microtubule nucleation and dynamics during mitotic-spindle assembly. *Nat Cell Biol.* 3:228-34.

Casolari, J.M., C.R. Brown, S. Komili, J. West, H. Hieronymus, and P.A. Silver. 2004. Genome-wide localization of the nuclear transport machinery couples transcriptional status and nuclear organization. *Cell.* 117:427-39.

Castillo, A.R., J.B. Meehl, G. Morgan, A. Schutz-Geschwender, and M. Winey. 2002. The yeast protein kinase Mps1p is required for assembly of the integral spindle pole body component Spc42p. *J Cell Biol.* 156:453-65.

Chan, G.K., S.A. Jablonski, D.A. Starr, M.L. Goldberg, and T.J. Yen. 2000. Human Zw10 and ROD are mitotic checkpoint proteins that bind to kinetochores. *Nat Cell Biol.* 2:944-7.

Chan, G.K., S.T. Liu, and T.J. Yen. 2005. Kinetochore structure and function. *Trends Cell Biol.* 15:589-98.

Chen, R.H., D.M. Brady, D. Smith, A.W. Murray, and K.G. Hardwick. 1999. The spindle checkpoint of budding yeast depends on a tight complex between the Mad1 and Mad2 proteins. *Mol Biol Cell.* 10:2607-18.

Chen, R.H., A. Shevchenko, M. Mann, and A.W. Murray. 1998. Spindle checkpoint protein Xmad1 recruits Xmad2 to unattached kinetochores. *J Cell Biol.* 143:283-95.

Chen, R.H., J.C. Waters, E.D. Salmon, and A.W. Murray. 1996. Association of spindle assembly checkpoint component XMAD2 with unattached kinetochores. *Science.*

274:242-6.

Chi, N.C., E.J. Adam, and S.A. Adam. 1997. Different binding domains for Ran-GTP and Ran-GDP/RanBP1 on nuclear import factor p97. *J Biol Chem.* 272:6818-22.

Chi, N.C., and S.A. Adam. 1997. Functional domains in nuclear import factor p97 for binding the nuclear localization sequence receptor and the nuclear pore. *Mol Biol Cell.* 8:945-56.

Chial, H.J., M.P. Rout, T.H. Giddings, and M. Winey. 1998. *Saccharomyces cerevisiae* Ndc1p is a shared component of nuclear pore complexes and spindle pole bodies. *J Cell Biol.* 143:1789-800.

Chook, Y.M., and G. Blobel. 1999. Structure of the nuclear transport complex karyopherin-beta2-Ran x GppNHp. *Nature.* 399:230-7.

Chung, E., and R.H. Chen. 2002. Spindle checkpoint requires Mad1-bound and Mad1-free Mad2. *Mol Biol Cell.* 13:1501-11.

Cingolani, G., J. Bednenko, M.T. Gillespie, and L. Gerace. 2002. Molecular basis for the recognition of a nonclassical nuclear localization signal by importin beta. *Mol Cell.* 10:1345-53.

Cingolani, G., C. Petosa, K. Weis, and C.W. Muller. 1999. Structure of importin-beta bound to the IBB domain of importin-alpha. *Nature.* 399:221-9.

Ciosk, R., W. Zachariae, C. Michaelis, A. Shevchenko, M. Mann, and K. Nasmyth. 1998. An ESP1/PDS1 complex regulates loss of sister chromatid cohesion at the metaphase to anaphase transition in yeast. *Cell.* 93:1067-76.

Conti, E., C.W. Muller, and M. Stewart. 2006. Karyopherin flexibility in nucleocytoplasmic transport. *Curr Opin Struct Biol.* 16:237-44.

Cordes, V.C., S. Reidenbach, H.R. Rackwitz, and W.W. Franke. 1997. Identification of protein p270/Tpr as a constitutive component of the nuclear pore complex-attached intranuclear filaments. *J Cell Biol.* 136:515-29.

Cronshaw, J.M., A.N. Krutchinsky, W. Zhang, B.T. Chait, and M.J. Matunis. 2002. Proteomic analysis of the mammalian nuclear pore complex. *J Cell Biol.* 158:915-27.

D'Angelo, M.A., D.J. Anderson, E. Richard, and M.W. Hetzer. 2006. Nuclear pores form de novo from both sides of the nuclear envelope. *Science.* 312:440-3.

Dasso, M. 2002. The Ran GTPase: theme and variations. *Curr Biol.* 12:R502-8.

De Antoni, A., C.G. Pearson, D. Cimini, J.C. Canman, V. Sala, L. Nezi, M. Mapelli, L. Sironi, M. Faretta, E.D. Salmon, and A. Musacchio. 2005a. The Mad1/Mad2 complex as a template for Mad2 activation in the spindle assembly checkpoint. *Curr Biol.* 15:214-25.

De Antoni, A., V. Sala, and A. Musacchio. 2005b. Explaining the oligomerization properties of the spindle assembly checkpoint protein Mad2. *Philos Trans R Soc*

Lond B Biol Sci. 360:637-47, discussion 447-8.

De Souza, C.P., A.H. Osmani, S.B. Hashmi, and S.A. Osmani. 2004. Partial nuclear pore complex disassembly during closed mitosis in Aspergillus nidulans. *Curr Biol.* 14:1973-84.

De Wulf, P., A.D. McAinsh, and P.K. Sorger. 2003. Hierarchical assembly of the budding yeast kinetochore from multiple subcomplexes. *Genes Dev.* 17:2902-21.

Delorme, E. 1989. Transformation of *Saccharomyces cerevisiae* by electroporation. *Appl Environ Microbiol.* 55:2242-6.

DeLuca, J.G., B.J. Howell, J.C. Canman, J.M. Hickey, G. Fang, and E.D. Salmon. 2003. Nuf2 and Hec1 are required for retention of the checkpoint proteins Mad1 and Mad2 to kinetochores. *Curr Biol.* 13:2103-9.

Denning, D.P., S.S. Patel, V. Uversky, A.L. Fink, and M. Rexach. 2003. Disorder in the nuclear pore complex: the FG repeat regions of nucleoporins are natively unfolded. *Proc Natl Acad Sci U S A.* 100:2450-5.

Denning, D.P., V. Uversky, S.S. Patel, A.L. Fink, and M. Rexach. 2002. The *Saccharomyces cerevisiae* nucleoporin Nup2p is a natively unfolded protein. *J Biol Chem.* 277:33447-55.

Devos, D., S. Dokudovskaya, F. Alber, R. Williams, B.T. Chait, A. Sali, and M.P. Rout. 2004. Components of coated vesicles and nuclear pore complexes share a common molecular architecture. *PLoS Biol.* 2:e380.

Devos, D., S. Dokudovskaya, R. Williams, F. Alber, N. Eswar, B.T. Chait, M.P. Rout, and A. Sali. 2006. Simple fold composition and modular architecture of the nuclear pore complex. *Proc Natl Acad Sci U S A.* 103:2172-7.

Dilworth, D.J., A. Suprapto, J.C. Padovan, B.T. Chait, R.W. Wozniak, M.P. Rout, and J.D. Aitchison. 2001. Nup2p dynamically associates with the distal regions of the yeast nuclear pore complex. *J Cell Biol.* 153:1465-78.

Dilworth, D.J., A.J. Tackett, R.S. Rogers, E.C. Yi, R.H. Christmas, J.J. Smith, A.F. Siegel, B.T. Chait, R.W. Wozniak, and J.D. Aitchison. 2005. The mobile nucleoporin Nup2p and chromatin-bound Prp20p function in endogenous NPC-mediated transcriptional control. *J Cell Biol.* 171:955-65.

Drivas, G.T., A. Shih, E. Coutavas, M.G. Rush, and P. D'Eustachio. 1990. Characterization of four novel ras-like genes expressed in a human teratocarcinoma cell line. *Mol Cell Biol.* 10:1793-8.

Engelsma, D., R. Bernad, J. Calafat, and M. Fornerod. 2004. Supraphysiological nuclear export signals bind CRM1 independently of RanGTP and arrest at Nup358. *Embo J.* 23:3643-52.

Englmeier, L., J.C. Olivo, and I.W. Mattaj. 1999. Receptor-mediated substrate translocation through the nuclear pore complex without nucleotide triphosphate hydrolysis. *Curr Biol.* 9:30-41.

Enninga, J., A. Levay, and B.M. Fontoura. 2003. Sec13 shuttles between the nucleus and the cytoplasm and stably interacts with Nup96 at the nuclear pore complex. *Mol Cell Biol.* 23:7271-84.

Enquist-Newman, M., I.M. Cheeseman, D. Van Goor, D.G. Drubin, P.B. Meluh, and G. Barnes. 2001. Dad1p, third component of the Duo1p/Dam1p complex involved in kinetochore function and mitotic spindle integrity. *Mol Biol Cell.* 12:2601-13.

Fabre, E., and E. Hurt. 1997. Yeast genetics to dissect the nuclear pore complex and nucleocytoplasmic trafficking. *Annu Rev Genet.* 31:277-313.

Fagarasanu, M., A. Fagarasanu, Y.Y. Tam, J.D. Aitchison, and R.A. Rachubinski. 2005. Inp1p is a peroxisomal membrane protein required for peroxisome inheritance in Saccharomyces cerevisiae. *J Cell Biol.* 169:765-75.

Famulski, J.K., and G.K. Chan. 2007. Aurora B Kinase-Dependent Recruitment of hZW10 and hROD to Tensionless Kinetochores. *Curr Biol.* 17:2143-9.

Fang, G. 2002. Checkpoint protein BubR1 acts synergistically with Mad2 to inhibit anaphase-promoting complex. *Mol Biol Cell.* 13:755-66.

Fatica, A., and D. Tollervey. 2002. Making ribosomes. *Curr Opin Cell Biol.* 14:313-8.

Feng, W., A.L. Benko, J.H. Lee, D.R. Stanford, and A.K. Hopper. 1999. Antagonistic effects of NES and NLS motifs determine S. cerevisiae Rna1p subcellular distribution. *J Cell Sci.* 112 (Pt 3):339-47.

Feuerbach, F., V. Galy, E. Trelles-Sticken, M. Fromont-Racine, A. Jacquier, E. Gilson, J.C. Olivo-Marin, H. Scherthan, and U. Nehrbass. 2002. Nuclear architecture and spatial positioning help establish transcriptional states of telomeres in yeast. *Nat Cell Biol.* 4:214-21.

Fischer, U., J. Huber, W.C. Boelens, I.W. Mattaj, and R. Luhrmann. 1995. The HIV-1 Rev activation domain is a nuclear export signal that accesses an export pathway used by specific cellular RNAs. *Cell.* 82:475-83.

Fischer, U., J. Huber, W.C. Boelens, I.W. Mattaj, and R. Luhrmann. 1995. The HIV-1 Rev activation domain is a nuclear export signal that accesses an export pathway used by specific cellular RNAs. *Cell.* 82:475-83.

Fletcher, L., T.J. Yen, and R.J. Muschel. 2003. DNA damage in HeLa cells induced arrest at a discrete point in G2 phase as defined by CENP-F localization. *Radiat Res.* 159:604-11.

Fornerod, M., M. Ohno, M. Yoshida, and I.W. Mattaj. 1997. CRM1 is an export receptor for leucine-rich nuclear export signals. *Cell.* 90:1051-60.

Fraschini, R., A. Beretta, L. Sironi, A. Musacchio, G. Lucchini, and S. Piatti. 2001. Bub3 interaction with Mad2, Mad3 and Cdc20 is mediated by WD40 repeats and does not require intact kinetochores. *Embo J.* 20:6648-59.

Frey, S., and D. Görlich. 2007. A saturated FG-repeat hydrogel can reproduce the permeability properties of nuclear pore complexes. *Cell.* 130:512-23.

Frey, S., R.P. Richter, and D. Görlich. 2006. FG-rich repeats of nuclear pore proteins form a three-dimensional meshwork with hydrogel-like properties. *Science.* 314:815-7.

Fried, H., and U. Kutay. 2003. Nucleocytoplasmic transport: taking an inventory. *Cell Mol Life Sci.* 60:1659-88.

Fromont-Racine, M., B. Senger, C. Saveanu, and F. Fasiolo. 2003. Ribosome assembly in eukaryotes. *Gene.* 313:17-42.

Fukuhara, N., E. Fernandez, J. Ebert, E. Conti, and D. Svergun. 2004. Conformational variability of nucleo-cytoplasmic transport factors. *J Biol Chem.* 279:2176-81.

Gall, J.G. 1967. Octagonal nuclear pores. *J Cell Biol.* 32:391-9.

Galy, V., O. Gadal, M. Fromont-Racine, A. Romano, A. Jacquier, and U. Nehrbass. 2004. Nuclear retention of unspliced mRNAs in yeast is mediated by perinuclear Mlp1. *Cell.* 116:63-73.

Galy, V., J.C. Olivo-Marin, H. Scherthan, V. Doye, N. Rascalou, and U. Nehrbass. 2000. Nuclear pore complexes in the organization of silent telomeric chromatin. *Nature.* 403:108-12.

Gerace, L., and G. Blobel. 1982. Nuclear lamina and the structural organization of the nuclear envelope. *Cold Spring Harb Symp Quant Biol.* 46 Pt 2:967-78.

Giaever, G., A.M. Chu, L. Ni, C. Connelly, L. Riles, S. Veronneau, S. Dow, A. Lucau-Danila, K. Anderson, B. Andre, A.P. Arkin, A. Astromoff, M. El-Bakkoury, R. Bangham, R. Benito, S. Brachat, S. Campanaro, M. Curtiss, K. Davis, A. Deutschbauer, K.D. Entian, P. Flaherty, F. Foury, D.J. Garfinkel, M. Gerstein, D. Gotte, U. Guldener, J.H. Hegemann, S. Hempel, Z. Herman, D.F. Jaramillo, D.E. Kelly, S.L. Kelly, P. Kotter, D. LaBonte, D.C. Lamb, N. Lan, H. Liang, H. Liao, L. Liu, C. Luo, M. Lussier, R. Mao, P. Menard, S.L. Ooi, J.L. Revuelta, C.J. Roberts, M. Rose, P. Ross-Macdonald, B. Scherens, G. Schimmack, B. Shafer, D.D. Shoemaker, S. Sookhai-Mahadeo, R.K. Storms, J.N. Strathern, G. Valle, M. Voet, G. Volckaert, C.Y. Wang, T.R. Ward, J. Wilhelmy, E.A. Winzeler, Y. Yang, G. Yen, E. Youngman, K. Yu, H. Bussey, J.D. Boeke, M. Snyder, P. Philippsen, R.W. Davis, and M. Johnston. 2002. Functional profiling of the *Saccharomyces cerevisiae* genome. *Nature.* 418:387-91.

Gillett, E.S., C.W. Espelin, and P.K. Sorger. 2004. Spindle checkpoint proteins and chromosome-microtubule attachment in budding yeast. *J Cell Biol.* 164:535-46.

Goldfarb, D.S., A.H. Corbett, D.A. Mason, M.T. Harreman, and S.A. Adam. 2004. Importin alpha: a multipurpose nuclear-transport receptor. *Trends Cell Biol.* 14:505-14.

Goldman, R.D., Y. Gruenbaum, R.D. Moir, D.K. Shumaker, and T.P. Spann. 2002. Nuclear lamins: building blocks of nuclear architecture. *Genes Dev.* 16:533-47.

Gorbsky, G.J. 1995. Kinetochores, microtubules and the metaphase checkpoint. *Trends Cell Biol.* 5:143-8.

Görlich, D., M. Dabrowski, F.R. Bischoff, U. Kutay, P. Bork, E. Hartmann, S. Prehn, and E. Izaurralde. 1997. A novel class of RanGTP binding proteins. *J Cell Biol.* 138:65-80.

Görlich, D., and U. Kutay. 1999. Transport between the cell nucleus and the cytoplasm. *Annu Rev Cell Dev Biol.* 15:607-60.

Goshima, G., and M. Yanagida. 2000. Establishing biorientation occurs with precocious separation of the sister kinetochores, but not the arms, in the early spindle of budding yeast. *Cell.* 100:619-33.

Grandi, P., V. Doye, and E.C. Hurt. 1993. Purification of NSP1 reveals complex formation with 'GLFG' nucleoporins and a novel nuclear pore protein NIC96. *Embo J.* 12:3061-71.

Grunstein, M., A. Hecht, G. Fisher-Adams, J. Wan, R.K. Mann, S. Strahl-Bolsinger, T. Laroche, and S. Gasser. 1995. The regulation of euchromatin and heterochromatin by histones in yeast. *J Cell Sci Suppl.* 19:29-36.

Gruss, O.J., R.E. Carazo-Salas, C.A. Schatz, G. Guarguaglini, J. Kast, M. Wilm, N. Le Bot, I. Vernos, E. Karsenti, and I.W. Mattaj. 2001. Ran induces spindle assembly by reversing the inhibitory effect of importin alpha on TPX2 activity. *Cell.* 104:83-93.

Habu, T., S.H. Kim, J. Weinstein, and T. Matsumoto. 2002. Identification of a MAD2-binding protein, CMT2, and its role in mitosis. *Embo J.* 21:6419-28.

Hallberg, E., R.W. Wozniak, and G. Blobel. 1993. An integral membrane protein of the pore membrane domain of the nuclear envelope contains a nucleoporin-like region. *J Cell Biol.* 122:513-21.

Hallberg, E., R.W. Wozniak, and G. Blobel. 1993. An integral membrane protein of the pore membrane domain of the nuclear envelope contains a nucleoporin-like region. *J Cell Biol.* 122:513-21.

Hardwick, K.G., R.C. Johnston, D.L. Smith, and A.W. Murray. 2000. MAD3 encodes a novel component of the spindle checkpoint which interacts with Bub3p, Cdc20p, and Mad2p. *J Cell Biol.* 148:871-82.

Hardwick, K.G., and A.W. Murray. 1995. Mad1p, a phosphoprotein component of the spindle assembly checkpoint in budding yeast. *J Cell Biol.* 131:709-20.

Hardwick, K.G., E. Weiss, F.C. Luca, M. Winey, and A.W. Murray. 1996. Activation of the budding yeast spindle assembly checkpoint without mitotic spindle disruption. *Science.* 273:953-6.

Harel, A., A.V. Orjalo, T. Vincent, A. Lachish-Zalait, S. Vasu, S. Shah, E. Zimmerman, M. Elbaum, and D.J. Forbes. 2003. Removal of a single pore subcomplex results in vertebrate nuclei devoid of nuclear pores. *Mol Cell.* 11:853-64.

Hatanaka, M. 1990. Discovery of the nucleolar targeting signal. *Bioessays.* 12:143-8.

Hawryluk-Gara, L.A., M. Platani, R. Santarella, R.W. Wozniak, and I.W. Mattaj. 2008. Nup53 is Required for Nuclear Envelope and Nuclear Pore Complex Assembly. *Mol Biol Cell.*

Hawryluk-Gara, L.A., E.K. Shibuya, and R.W. Wozniak. 2005. Vertebrate Nup53 interacts with the nuclear lamina and is required for the assembly of a Nup93-containing complex. *Mol Biol Cell.* 16:2382-94.

He, X., D.R. Rines, C.W. Espelin, and P.K. Sorger. 2001. Molecular analysis of kinetochore-microtubule attachment in budding yeast. *Cell.* 106:195-206.

Hediger, F., K. Dubrana, and S.M. Gasser. 2002. Myosin-like proteins 1 and 2 are not required for silencing or telomere anchoring, but act in the Tel1 pathway of telomere length control. *J Struct Biol.* 140:79-91.

Hediger, F., F.R. Neumann, G. Van Houwe, K. Dubrana, and S.M. Gasser. 2002. Live imaging of telomeres: yKu and Sir proteins define redundant telomere-anchoring pathways in yeast. *Curr Biol.* 12:2076-89.

Hetzer, M., D. Bilbao-Cortes, T.C. Walther, O.J. Gruss, and I.W. Mattaj. 2000. GTP hydrolysis by Ran is required for nuclear envelope assembly. *Mol Cell.* 5:1013-24.

Hodge, C.A., H.V. Colot, P. Stafford, and C.N. Cole. 1999. Rat8p/Dbp5p is a shuttling transport factor that interacts with Rat7p/Nup159p and Gle1p and suppresses the mRNA export defect of xpo1-1 cells. *Embo J.* 18:5778-88.

Howell, B.J., D.B. Hoffman, G. Fang, A.W. Murray, and E.D. Salmon. 2000. Visualization of Mad2 dynamics at kinetochores, along spindle fibers, and at spindle poles in living cells. *J Cell Biol.* 150:1233-50.

Howell, B.J., B. Moree, E.M. Farrar, S. Stewart, G. Fang, and E.D. Salmon. 2004. Spindle checkpoint protein dynamics at kinetochores in living cells. *Curr Biol.* 14:953-64.

Hoyt, M.A., L. Totis, and B.T. Roberts. 1991. S. cerevisiae genes required for cell cycle arrest in response to loss of microtubule function. *Cell.* 66:507-17.

Hsia, K.C., P. Stavropoulos, G. Blobel, and A. Hoelz. 2007. Architecture of a coat for the nuclear pore membrane. *Cell.* 131:1313-26.

Hwang, L.H., L.F. Lau, D.L. Smith, C.A. Mistrot, K.G. Hardwick, E.S. Hwang, A. Amon, and A.W. Murray. 1998. Budding yeast Cdc20: a target of the spindle checkpoint. *Science.* 279:1041-4.

Hwang, L.H., and A.W. Murray. 1997. A novel yeast screen for mitotic arrest mutants identifies DOC1, a new gene involved in cyclin proteolysis. *Mol Biol Cell.* 8:1877-87.

Ikui, A.E., K. Furuya, M. Yanagida, and T. Matsumoto. 2002. Control of localization of a spindle checkpoint protein, Mad2, in fission yeast. *J Cell Sci.* 115:1603-10.

Iouk, T., O. Kerscher, R.J. Scott, M.A. Basrai, and R.W. Wozniak. 2002. The yeast nuclear pore complex functionally interacts with components of the spindle

assembly checkpoint. *J Cell Biol.* 159:807-19.

Ishii, K., G. Arib, C. Lin, G. Van Houwe, and U.K. Laemmli. 2002. Chromatin boundaries in budding yeast: the nuclear pore connection. *Cell.* 109:551-62.

Janke, C., J. Ortiz, J. Lechner, A. Shevchenko, A. Shevchenko, M.M. Magiera, C. Schramm, and E. Schiebel. 2001. The budding yeast proteins Spc24p and Spc25p interact with Ndc80p and Nuf2p at the kinetochore and are important for kinetochore clustering and checkpoint control. *Embo J.* 20:777-91.

Janke, C., J. Ortiz, T.U. Tanaka, J. Lechner, and E. Schiebel. 2002. Four new subunits of the Dam1-Duo1 complex reveal novel functions in sister kinetochore biorientation. *Embo J.* 21:181-93.

Jones, M.H., X. He, T.H. Giddings, and M. Winey. 2001. Yeast Dam1p has a role at the kinetochore in assembly of the mitotic spindle. *Proc Natl Acad Sci U S A.* 98:13675-80.

Joseph, J., S.T. Liu, S.A. Jablonski, T.J. Yen, and M. Dasso. 2004. The RanGAP1-RanBP2 complex is essential for microtubule-kinetochore interactions in vivo. *Curr Biol.* 14:611-7.

Joseph, J., S.H. Tan, T.S. Karpova, J.G. McNally, and M. Dasso. 2002. SUMO-1 targets RanGAP1 to kinetochores and mitotic spindles. *J Cell Biol.* 156:595-602.

Kaffman, A., N.M. Rank, and E.K. O'Shea. 1998. Phosphorylation regulates association of the transcription factor Pho4 with its import receptor Pse1/Kap121. *Genes Dev.* 12:2673-83.

Kalab, P., K. Weis, and R. Heald. 2002. Visualization of a Ran-GTP gradient in interphase and mitotic Xenopus egg extracts. *Science.* 295:2452-6.

Karess, R.E., and D.M. Glover. 1989. rough deal: a gene required for proper mitotic segregation in Drosophila. *J Cell Biol.* 109:2951-61.

Kenna, M.A., J.G. Petranka, J.L. Reilly, and L.I. Davis. 1996. Yeast Nle3p/Nup170p is required for normal stoichiometry of FG nucleoporins within the nuclear pore complex. *Mol Cell Biol.* 16:2025-36.

Kerscher, O., L.B. Crotti, and M.A. Basrai. 2003. Recognizing chromosomes in trouble: association of the spindle checkpoint protein Bub3p with altered kinetochores and a unique defective centromere. *Mol Cell Biol.* 23:6406-18.

Kerscher, O., P. Hieter, M. Winey, and M.A. Basrai. 2001. Novel role for a *Saccharomyces cerevisiae* nucleoporin, Nup170p, in chromosome segregation. *Genetics.* 157:1543-53.

Kim, S.H., D.P. Lin, S. Matsumoto, A. Kitazono, and T. Matsumoto. 1998. Fission yeast Slp1: an effector of the Mad2-dependent spindle checkpoint. *Science.* 279:1045-7.

King, E.M., S.J. van der Sar, and K.G. Hardwick. 2007. Mad3 KEN boxes mediate both Cdc20 and Mad3 turnover, and are critical for the spindle checkpoint. *PLoS ONE.* 2:e342.

King, M.C., C.P. Lusk, and G. Blobel. 2006. Karyopherin-mediated import of integral inner nuclear membrane proteins. *Nature*. 442:1003-7.

King, R.W., J.M. Peters, S. Tugendreich, M. Rolfe, P. Hieter, and M.W. Kirschner. 1995. A 20S complex containing CDC27 and CDC16 catalyzes the mitosis-specific conjugation of ubiquitin to cyclin B. *Cell*. 81:279-88.

Kiseleva, E., T.D. Allen, S. Rutherford, M. Bucci, S.R. Wente, and M.W. Goldberg. 2004. Yeast nuclear pore complexes have a cytoplasmic ring and internal filaments. *J Struct Biol*. 145:272-88.

Knauer, S.K., C. Bier, N. Habtemichael, and R.H. Stauber. 2006. The Survivin-Crm1 interaction is essential for chromosomal passenger complex localization and function. *EMBO Rep*. 7:1259-65.

Kolling, R., T. Nguyen, E.Y. Chen, and D. Botstein. 1993. A new yeast gene with a myosin-like heptad repeat structure. *Mol Gen Genet*. 237:359-69.

Kops, G.J., Y. Kim, B.A. Weaver, Y. Mao, I. McLeod, J.R. Yates, 3rd, M. Tagaya, and D.W. Cleveland. 2005. ZW10 links mitotic checkpoint signaling to the structural kinetochore. *J Cell Biol*. 169:49-60.

Kose, S., N. Imamoto, T. Tachibana, T. Shimamoto, and Y. Yoneda. 1997. Ran-unassisted nuclear migration of a 97-kD component of nuclear pore-targeting complex. *J Cell Biol*. 139:841-9.

Krude, T. 2002. Chromatin assembly: the kinetochore connection. *Curr Biol*. 12:R256-8.

Kuersten, S., G.J. Arts, T.C. Walther, L. Englmeier, and I.W. Mattaj. 2002. Steady-state nuclear localization of exportin-t involves RanGTP binding and two distinct nuclear pore complex interaction domains. *Mol Cell Biol*. 22:5708-20.

Kusano, A., T. Yoshioka, H. Nishijima, H. Nishitani, and T. Nishimoto. 2004. Schizosaccharomyces pombe RanGAP homolog, SpRna1, is required for centromeric silencing and chromosome segregation. *Mol Biol Cell*. 15:4960-70.

Kutay, U., and S. Guttinger. 2005. Leucine-rich nuclear-export signals: born to be weak. *Trends Cell Biol*. 15:121-4.

Kutay, U., E. Izaurralde, F.R. Bischoff, I.W. Mattaj, and D. Görlich. 1997. Dominant-negative mutants of importin-beta block multiple pathways of import and export through the nuclear pore complex. *Embo J*. 16:1153-63.

Kvam, E., and D.S. Goldfarb. 2004. Nvj1p is the outer-nuclear-membrane receptor for oxysterol-binding protein homolog Osh1p in *Saccharomyces cerevisiae*. *J Cell Sci*. 117:4959-68.

la Cour, T., L. Kiemer, A. Molgaard, R. Gupta, K. Skriver, and S. Brunak. 2004. Analysis and prediction of leucine-rich nuclear export signals. *Protein Eng Des Sel*. 17:527-36.

Lee, D.C., and J.D. Aitchison. 1999. Kap104p-mediated nuclear import. Nuclear localization signals in mRNA-binding proteins and the role of Ran and Rna. *J Biol*

Chem. 274:29031-7.

Lee, S.J., Y. Matsuura, S.M. Liu, and M. Stewart. 2005. Structural basis for nuclear import complex dissociation by RanGTP. *Nature.* 435:693-6.

Lee, S.J., T. Sekimoto, E. Yamashita, E. Nagoshi, A. Nakagawa, N. Imamoto, M. Yoshimura, H. Sakai, K.T. Chong, T. Tsukihara, and Y. Yoneda. 2003. The structure of importin-beta bound to SREBP-2: nuclear import of a transcription factor. *Science.* 302:1571-5.

Leslie, D.M., B. Grill, M.P. Rout, R.W. Wozniak, and J.D. Aitchison. 2002. Kap121p-mediated nuclear import is required for mating and cellular differentiation in yeast. *Mol Cell Biol.* 22:2544-55.

Lew, D.J., and D.J. Burke. 2003. The spindle assembly and spindle position checkpoints. *Annu Rev Genet.* 37:251-82.

Li, R., and A.W. Murray. 1991. Feedback control of mitosis in budding yeast. *Cell.* 66:519-31.

Li, X., and R.B. Nicklas. 1995. Mitotic forces control a cell-cycle checkpoint. *Nature.* 373:630-2.

Li, Y., and R. Benezra. 1996. Identification of a human mitotic checkpoint gene: hsMAD2. *Science.* 274:246-8.

Liao, H., R.J. Winkfein, G. Mack, J.B. Rattner, and T.J. Yen. 1995. CENP-F is a protein of the nuclear matrix that assembles onto kinetochores at late G2 and is rapidly degraded after mitosis. *J Cell Biol.* 130:507-18.

Lim, R.Y., B. Fahrenkrog, J. Koser, K. Schwarz-Herion, J. Deng, and U. Aebi. 2007. Nanomechanical basis of selective gating by the nuclear pore complex. *Science.* 318:640-3.

Lim, R.Y., N.P. Huang, J. Koser, J. Deng, K.H. Lau, K. Schwarz-Herion, B. Fahrenkrog, and U. Aebi. 2006. Flexible phenylalanine-glycine nucleoporins as entropic barriers to nucleocytoplasmic transport. *Proc Natl Acad Sci U S A.* 103:9512-7.

Liu, S.M., and M. Stewart. 2005. Structural basis for the high-affinity binding of nucleoporin Nup1p to the *Saccharomyces cerevisiae* importin-beta homologue, Kap95p. *J Mol Biol.* 349:515-25.

Loiodice, I., A. Alves, G. Rabut, M. Van Overbeek, J. Ellenberg, J.B. Sibarita, and V. Doye. 2004. The entire Nup107-160 complex, including three new members, is targeted as one entity to kinetochores in mitosis. *Mol Biol Cell.* 15:3333-44.

Luo, X., Z. Tang, J. Rizo, and H. Yu. 2002. The Mad2 spindle checkpoint protein undergoes similar major conformational changes upon binding to either Mad1 or Cdc20. *Mol Cell.* 9:59-71.

Lusk, C.P., G. Blobel, and M.C. King. 2007. Highway to the inner nuclear membrane: rules for the road. *Nat Rev Mol Cell Biol.* 8:414-20.

Lusk, C.P., T. Makhnevych, M. Marelli, J.D. Aitchison, and R.W. Wozniak. 2002. Karyopherins in nuclear pore biogenesis: a role for Kap121p in the assembly of Nup53p into nuclear pore complexes. *J Cell Biol.* 159:267-78.

Luthra, R., S.C. Kerr, M.T. Harreman, L.H. Apponi, M.B. Fasken, S. Ramineni, S. Chaurasia, S.R. Valentini, and A.H. Corbett. 2007. Actively transcribed GAL genes can be physically linked to the nuclear pore by the SAGA chromatin modifying complex. *J Biol Chem.* 282:3042-9.

Lutzmann, M., R. Kunze, A. Buerer, U. Aebi, and E. Hurt. 2002. Modular self-assembly of a Y-shaped multiprotein complex from seven nucleoporins. *Embo J.* 21:387-97.

Lutzmann, M., R. Kunze, K. Stangl, P. Stelter, K.F. Toth, B. Bottcher, and E. Hurt. 2005. Reconstitution of Nup157 and Nup145N into the Nup84 complex. *J Biol Chem.* 280:18442-51.

Madrid, A.S., J. Mancuso, W.Z. Cande, and K. Weis. 2006. The role of the integral membrane nucleoporins Ndc1p and Pom152p in nuclear pore complex assembly and function. *J Cell Biol.* 173:361-71.

Makhnevych, T., C.P. Lusk, A.M. Anderson, J.D. Aitchison, and R.W. Wozniak. 2003. Cell cycle regulated transport controlled by alterations in the nuclear pore complex. *Cell.* 115:813-23.

Makhnevych, T., C. Ptak, C.P. Lusk, J.D. Aitchison, and R.W. Wozniak. 2007. The role of karyopherins in the regulated sumoylation of septins. *J Cell Biol.* 177:39-49.

Makkerh, J.P., C. Dingwall, and R.A. Laskey. 1996. Comparative mutagenesis of nuclear localization signals reveals the importance of neutral and acidic amino acids. *Curr Biol.* 6:1025-7.

Malim, M.H., D.F. McCarn, L.S. Tiley, and B.R. Cullen. 1991. Mutational definition of the human immunodeficiency virus type 1 Rev activation domain. *J Virol.* 65:4248-54.

Mans, B.J., V. Anantharaman, L. Aravind, and E.V. Koonin. 2004. Comparative genomics, evolution and origins of the nuclear envelope and nuclear pore complex. *Cell Cycle.* 3:1612-37.

Mansfeld, J., S. Guttinger, L.A. Hawryluk-Gara, N. Pante, M. Mall, V. Galy, U. Haselmann, P. Muhlhausser, R.W. Wozniak, I.W. Mattaj, U. Kutay, and W. Antonin. 2006. The conserved transmembrane nucleoporin NDC1 is required for nuclear pore complex assembly in vertebrate cells. *Mol Cell.* 22:93-103.

Mapelli, M., F.V. Filipp, G. Rancati, L. Massimiliano, L. Nezi, G. Stier, R.S. Hagan, S. Confalonieri, S. Piatti, M. Sattler, and A. Musacchio. 2006. Determinants of conformational dimerization of Mad2 and its inhibition by p31comet. *Embo J.* 25:1273-84.

Marelli, M., J.D. Aitchison, and R.W. Wozniak. 1998. Specific binding of the karyopherin Kap121p to a subunit of the nuclear pore complex containing Nup53p, Nup59p, and Nup170p. *J Cell Biol.* 143:1813-30.

Marelli, M., D.J. Dilworth, R.W. Wozniak, and J.D. Aitchison. 2001. The dynamics of karyopherin-mediated nuclear transport. *Biochem Cell Biol.* 79:603-12.

Martin-Lluesma, S., V.M. Stucke, and E.A. Nigg. 2002. Role of Hec1 in spindle checkpoint signaling and kinetochore recruitment of Mad1/Mad2. *Science.* 297:2267-70.

Matsuura, Y., and M. Stewart. 2004. Structural basis for the assembly of a nuclear export complex. *Nature.* 432:872-7.

Mattaj, I.W. 2004. Sorting out the nuclear envelope from the endoplasmic reticulum. *Nat Rev Mol Cell Biol.* 5:65-9.

Matunis, M.J., E. Coutavas, and G. Blobel. 1996. A novel ubiquitin-like modification modulates the partitioning of the Ran-GTPase-activating protein RanGAP1 between the cytosol and the nuclear pore complex. *J Cell Biol.* 135:1457-70.

McAinsh, A.D., J.D. Tytell, and P.K. Sorger. 2003. Structure, function, and regulation of budding yeast kinetochores. *Annu Rev Cell Dev Biol.* 19:519-39.

McDonald, K.L., E.T. O'Toole, D.N. Mastronarde, and J.R. McIntosh. 1992. Kinetochore microtubules in PTK cells. *J Cell Biol.* 118:369-83.

McIntosh, J.R. 1991. Structural and mechanical control of mitotic progression. *Cold Spring Harb Symp Quant Biol.* 56:613-9.

Miao, M., K.J. Ryan, and S.R. Wente. 2006. The integral membrane protein Pom34p functionally links nucleoporin subcomplexes. *Genetics.* 172:1441-57.

Moore, M.S., and G. Blobel. 1994. A G protein involved in nucleocytoplasmic transport: the role of Ran. *Trends Biochem Sci.* 19:211-6.

Murthi, A., and A.K. Hopper. 2005. Genome-wide screen for inner nuclear membrane protein targeting in *Saccharomyces cerevisiae*: roles for N-acetylation and an integral membrane protein. *Genetics.* 170:1553-60.

Musacchio, A., and K.G. Hardwick. 2002. The spindle checkpoint: structural insights into dynamic signalling. *Nat Rev Mol Cell Biol.* 3:731-41.

Musacchio, A., and E.D. Salmon. 2007. The spindle-assembly checkpoint in space and time. *Nat Rev Mol Cell Biol.* 8:379-93.

Nachury, M.V., T.J. Maresca, W.C. Salmon, C.M. Waterman-Storer, R. Heald, and K. Weis. 2001. Importin beta is a mitotic target of the small GTPase Ran in spindle assembly. *Cell.* 104:95-106.

Nakielny, S., and G. Dreyfuss. 1998. Import and export of the nuclear protein import receptor transportin by a mechanism independent of GTP hydrolysis. *Curr Biol.* 8:89-95.

Neville, M., and M. Rosbash. 1999. The NES-Crm1p export pathway is not a major mRNA export route in *Saccharomyces cerevisiae*. *Embo J.* 18:3746-56.

Nezi, L., G. Rancati, A. De Antoni, S. Pasqualato, S. Piatti, and A. Musacchio. 2006.

Accumulation of Mad2-Cdc20 complex during spindle checkpoint activation requires binding of open and closed conformers of Mad2 in *Saccharomyces cerevisiae*. *J Cell Biol.* 174:39-51.

Niepel, M., C. Strambio-de-Castillia, J. Fasolo, B.T. Chait, and M.P. Rout. 2005. The nuclear pore complex-associated protein, Mlp2p, binds to the yeast spindle pole body and promotes its efficient assembly. *J Cell Biol.* 170:225-35.

Nishijima, H., J. Nakayama, T. Yoshioka, A. Kusano, H. Nishitani, K. Shibahara, and T. Nishimoto. 2006. Nuclear RanGAP is required for the heterochromatin assembly and is reciprocally regulated by histone H3 and Clr4 histone methyltransferase in Schizosaccharomyces pombe. *Mol Biol Cell.* 17:2524-36.

Oeffinger, M., K.E. Wei, R. Rogers, J.A. DeGrasse, B.T. Chait, J.D. Aitchison, and M.P. Rout. 2007. Comprehensive analysis of diverse ribonucleoprotein complexes. *Nat Methods.* 4:951-6.

Palazzo, A.F., M. Springer, Y. Shibata, C.S. Lee, A.P. Dias, and T.A. Rapoport. 2007. The signal sequence coding region promotes nuclear export of mRNA. *PLoS Biol.* 5:e322.

Pangilinan, F., and F. Spencer. 1996. Abnormal kinetochore structure activates the spindle assembly checkpoint in budding yeast. *Mol Biol Cell.* 7:1195-208.

Panse, V.G., B. Kuster, T. Gerstberger, and E. Hurt. 2003. Unconventional tethering of Ulp1 to the transport channel of the nuclear pore complex by karyopherins. *Nat Cell Biol.* 5:21-7.

Pemberton, L.F., J.S. Rosenblum, and G. Blobel. 1999. Nuclear import of the TATA-binding protein: mediation by the karyopherin Kap114p and a possible mechanism for intranuclear targeting. *J Cell Biol.* 145:1407-17.

Peters, J.M. 2006. The anaphase promoting complex/cyclosome: a machine designed to destroy. *Nat Rev Mol Cell Biol.* 7:644-56.

Petosa, C., G. Schoehn, P. Askjaer, U. Bauer, M. Moulin, U. Steuerwald, M. Soler-Lopez, F. Baudin, I.W. Mattaj, and C.W. Muller. 2004. Architecture of CRM1/Exportin1 suggests how cooperativity is achieved during formation of a nuclear export complex. *Mol Cell.* 16:761-75.

Pinsky, B.A., S.Y. Tatsutani, K.A. Collins, and S. Biggins. 2003. An Mtw1 complex promotes kinetochore biorientation that is monitored by the Ipl1/Aurora protein kinase. *Dev Cell.* 5:735-45.

Pyhtila, B., and M. Rexach. 2003. A gradient of affinity for the karyopherin Kap95p along the yeast nuclear pore complex. *J Biol Chem.* 278:42699-709.

Quimby, B.B., A. Arnaoutov, and M. Dasso. 2005. Ran GTPase regulates Mad2 localization to the nuclear pore complex. *Eukaryot Cell.* 4:274-80.

Radu, A., G. Blobel, and M.S. Moore. 1995. Identification of a protein complex that is required for nuclear protein import and mediates docking of import substrate to

distinct nucleoporins. *Proc Natl Acad Sci U S A.* 92:1769-73.

Reichelt, R., A. Holzenburg, E.L. Buhle, Jr., M. Jarnik, A. Engel, and U. Aebi. 1990. Correlation between structure and mass distribution of the nuclear pore complex and of distinct pore complex components. *J Cell Biol.* 110:883-94.

Rexach, M., and G. Blobel. 1995. Protein import into nuclei: association and dissociation reactions involving transport substrate, transport factors, and nucleoporins. *Cell.* 83:683-92.

Ribbeck, K., and D. Görlich. 2001. Kinetic analysis of translocation through nuclear pore complexes. *Embo J.* 20:1320-30.

Ribbeck, K., and D. Görlich. 2002. The permeability barrier of nuclear pore complexes appears to operate via hydrophobic exclusion. *Embo J.* 21:2664-71.

Ribbeck, K., U. Kutay, E. Paraskeva, and D. Görlich. 1999. The translocation of transportin-cargo complexes through nuclear pores is independent of both Ran and energy. *Curr Biol.* 9:47-50.

Ribbeck, K., G. Lipowsky, H.M. Kent, M. Stewart, and D. Görlich. 1998. NTF2 mediates nuclear import of Ran. *Embo J.* 17:6587-98.

Rieder, C.L., R.W. Cole, A. Khodjakov, and G. Sluder. 1995. The checkpoint delaying anaphase in response to chromosome monoorientation is mediated by an inhibitory signal produced by unattached kinetochores. *J Cell Biol.* 130:941-8.

Rieder, C.L., A. Schultz, R. Cole, and G. Sluder. 1994. Anaphase onset in vertebrate somatic cells is controlled by a checkpoint that monitors sister kinetochore attachment to the spindle. *J Cell Biol.* 127:1301-10.

Robbins, J., S.M. Dilworth, R.A. Laskey, and C. Dingwall. 1991. Two interdependent basic domains in nucleoplasmin nuclear targeting sequence: identification of a class of bipartite nuclear targeting sequence. *Cell.* 64:615-23.

Roos, U.P. 1973. Light and electron microscopy of rat kangaroo cells in mitosis. II. Kinetochore structure and function. *Chromosoma.* 41:195-220.

Rout, M.P., J.D. Aitchison, M.O. Magnasco, and B.T. Chait. 2003. Virtual gating and nuclear transport: the hole picture. *Trends Cell Biol.* 13:622-8.

Rout, M.P., J.D. Aitchison, A. Suprapto, K. Hjertaas, Y. Zhao, and B.T. Chait. 2000. The yeast nuclear pore complex: composition, architecture, and transport mechanism. *J Cell Biol.* 148:635-51.

Rudner, A.D., K.G. Hardwick, and A.W. Murray. 2000. Cdc28 activates exit from mitosis in budding yeast. *J Cell Biol.* 149:1361-76.

Ryan, K.J., J.M. McCaffery, and S.R. Wente. 2003. The Ran GTPase cycle is required for yeast nuclear pore complex assembly. *J Cell Biol.* 160:1041-53.

Saitoh, H., R. Pu, M. Cavenagh, and M. Dasso. 1997. RanBP2 associates with Ubc9p and a modified form of RanGAP1. *Proc Natl Acad Sci U S A.* 94:3736-41.

Salina, D., P. Enarson, J.B. Rattner, and B. Burke. 2003. Nup358 integrates nuclear envelope breakdown with kinetochore assembly. *J Cell Biol.* 162:991-1001.

Scannell, D.R., G. Butler, and K.H. Wolfe. 2007. Yeast genome evolution-the origin of the species. *Yeast.* 24:929-42.

Scherthan, H., M. Jerratsch, B. Li, S. Smith, M. Hulten, T. Lock, and T. de Lange. 2000. Mammalian meiotic telomeres: protein composition and redistribution in relation to nuclear pores. *Mol Biol Cell.* 11:4189-203.

Schlenstedt, G., C. Saavedra, J.D. Loeb, C.N. Cole, and P.A. Silver. 1995. The GTP-bound form of the yeast Ran/TC4 homologue blocks nuclear protein import and appearance of poly(A)+ RNA in the cytoplasm. *Proc Natl Acad Sci U S A.* 92:225-9.

Schlenstedt, G., E. Smirnova, R. Deane, J. Solsbacher, U. Kutay, D. Görlich, H. Ponstingl, and F.R. Bischoff. 1997. Yrb4p, a yeast ran-GTP-binding protein involved in import of ribosomal protein L25 into the nucleus. *Embo J.* 16:6237-49.

Schmitt, C., C. von Kobbe, A. Bachi, N. Pante, J.P. Rodrigues, C. Boscheron, G. Rigaut, M. Wilm, B. Seraphin, M. Carmo-Fonseca, and E. Izaurralde. 1999. Dbp5, a DEAD-box protein required for mRNA export, is recruited to the cytoplasmic fibrils of nuclear pore complex via a conserved interaction with CAN/Nup159p. *Embo J.* 18:4332-47.

Schrader, N., P. Stelter, D. Flemming, R. Kunze, E. Hurt, and I.R. Vetter. 2008. Structural basis of the Nic96 subcomplex organization in the nuclear pore channel. *Mol Cell.* 29:46-55.

Schultz, J., F. Milpetz, P. Bork, and C.P. Ponting. 1998. SMART, a simple modular architecture research tool: identification of signaling domains. *Proc Natl Acad Sci U S A.* 95:5857-64.

Schultz, M.C., D.J. Hockman, T.A. Harkness, W.I. Garinther, and B.A. Altheim. 1997. Chromatin assembly in a yeast whole-cell extract. *Proc Natl Acad Sci U S A.* 94:9034-9.

Schwartz, T.U. 2005. Modularity within the architecture of the nuclear pore complex. *Curr Opin Struct Biol.* 15:221-6.

Schwoebel, E.D., T.H. Ho, and M.S. Moore. 2002. The mechanism of inhibition of Ran-dependent nuclear transport by cellular ATP depletion. *J Cell Biol.* 157:963-74.

Schwoebel, E.D., B. Talcott, I. Cushman, and M.S. Moore. 1998. Ran-dependent signal-mediated nuclear import does not require GTP hydrolysis by Ran. *J Biol Chem.* 273:35170-5.

Scott, R.J., C.P. Lusk, D.J. Dilworth, J.D. Aitchison, and R.W. Wozniak. 2005. Interactions between Mad1p and the nuclear transport machinery in the yeast *Saccharomyces cerevisiae*. *Mol Biol Cell.* 16:4362-74.

Shah, J.V., E. Botvinick, Z. Bonday, F. Furnari, M. Berns, and D.W. Cleveland. 2004.

Dynamics of centromere and kinetochore proteins; implications for checkpoint signaling and silencing. *Curr Biol.* 14:942-52.

Sherman, F., G.R. Fink, J.B. Hicks. 1983. Methods in yeast genetics : laboratory manual. . *Cold Spring Harbor.*:120 pp.

Shulga, N., and D.S. Goldfarb. 2003. Binding dynamics of structural nucleoporins govern nuclear pore complex permeability and may mediate channel gating. *Mol Cell Biol.* 23:534-42.

Shulga, N., N. Mosammaparast, R. Wozniak, and D.S. Goldfarb. 2000. Yeast nucleoporins involved in passive nuclear envelope permeability. *J Cell Biol.* 149:1027-38.

Shulga, N., P. Roberts, Z. Gu, L. Spitz, M.M. Tabb, M. Nomura, and D.S. Goldfarb. 1996. In vivo nuclear transport kinetics in *Saccharomyces cerevisiae*: a role for heat shock protein 70 during targeting and translocation. *J Cell Biol.* 135:329-39.

Sigler, A., P. Schubert, W. Hillen, and M. Niederweis. 2000. Permeation of tetracyclines through membranes of liposomes and Escherichia coli. *Eur J Biochem.* 267:527-34.

Siniossoglou, S., C. Wimmer, M. Rieger, V. Doye, H. Tekotte, C. Weise, S. Emig, A. Segref, and E.C. Hurt. 1996. A novel complex of nucleoporins, which includes Sec13p and a Sec13p homolog, is essential for normal nuclear pores. *Cell.* 84:265-75.

Sironi, L., M. Mapelli, S. Knapp, A. De Antoni, K.T. Jeang, and A. Musacchio. 2002. Crystal structure of the tetrameric Mad1-Mad2 core complex: implications of a 'safety belt' binding mechanism for the spindle checkpoint. *Embo J.* 21:2496-506.

Smith, A., A. Brownawell, and I.G. Macara. 1998. Nuclear import of Ran is mediated by the transport factor NTF2. *Curr Biol.* 8:1403-6.

Stade, K., C.S. Ford, C. Guthrie, and K. Weis. 1997. Exportin 1 (Crm1p) is an essential nuclear export factor. *Cell.* 90:1041-50.

Starr, D.A., B.C. Williams, Z. Li, B. Etemad-Moghadam, R.K. Dawe, and M.L. Goldberg. 1997. Conservation of the centromere/kinetochore protein ZW10. *J Cell Biol.* 138:1289-301.

Stewart, M. 2007. Ratcheting mRNA out of the nucleus. *Mol Cell.* 25:327-30.

Strahm, Y., B. Fahrenkrog, D. Zenklusen, E. Rychner, J. Kantor, M. Rosbach, and F. Stutz. 1999. The RNA export factor Gle1p is located on the cytoplasmic fibrils of the NPC and physically interacts with the FG-nucleoporin Rip1p, the DEAD-box protein Rat8p/Dbp5p and a new protein Ymr 255p. *Embo J.* 18:5761-77.

Straight, A.F., and A.W. Murray. 1997. The spindle assembly checkpoint in budding yeast. *Methods Enzymol.* 283:425-40.

Strambio-de-Castillia, C., G. Blobel, and M.P. Rout. 1999. Proteins connecting the nuclear pore complex with the nuclear interior. *J Cell Biol.* 144:839-55.

Strawn, L.A., T. Shen, N. Shulga, D.S. Goldfarb, and S.R. Wente. 2004. Minimal nuclear pore complexes define FG repeat domains essential for transport. *Nat Cell Biol.* 6:197-206.

Strom, A.C., and K. Weis. 2001. Importin-beta-like nuclear transport receptors. *Genome Biol.* 2:REVIEWS3008.

Sudakin, V., G.K. Chan, and T.J. Yen. 2001. Checkpoint inhibition of the APC/C in HeLa cells is mediated by a complex of BUBR1, BUB3, CDC20, and MAD2. *J Cell Biol.* 154:925-36.

Suntharalingam, M., and S.R. Wente. 2003. Peering through the pore: nuclear pore complex structure, assembly, and function. *Dev Cell.* 4:775-89.

Tanaka, T.U., N. Rachidi, C. Janke, G. Pereira, M. Galova, E. Schiebel, M.J. Stark, and K. Nasmyth. 2002. Evidence that the Ipl1-Sli15 (Aurora kinase-INCENP) complex promotes chromosome bi-orientation by altering kinetochore-spindle pole connections. *Cell.* 108:317-29.

Tanaka, T.U., M.J. Stark, and K. Tanaka. 2005. Kinetochore capture and bi-orientation on the mitotic spindle. *Nat Rev Mol Cell Biol.* 6:929-42.

Tang, Z., R. Bharadwaj, B. Li, and H. Yu. 2001. Mad2-Independent inhibition of APCCdc20 by the mitotic checkpoint protein BubR1. *Dev Cell.* 1:227-37.

Taylor, S.S., E. Ha, and F. McKeon. 1998. The human homologue of Bub3 is required for kinetochore localization of Bub1 and a Mad3/Bub1-related protein kinase. *J Cell Biol.* 142:1-11.

Taylor, S.S., and F. McKeon. 1997. Kinetochore localization of murine Bub1 is required for normal mitotic timing and checkpoint response to spindle damage. *Cell.* 89:727-35.

Taylor, S.S., M.I. Scott, and A.J. Holland. 2004. The spindle checkpoint: a quality control mechanism which ensures accurate chromosome segregation. *Chromosome Res.* 12:599-616.

Terry, L.J., E.B. Shows, and S.R. Wente. 2007. Crossing the nuclear envelope: hierarchical regulation of nucleocytoplasmic transport. *Science.* 318:1412-6.

Thompson, J.R., E. Register, J. Curotto, M. Kurtz, and R. Kelly. 1998. An improved protocol for the preparation of yeast cells for transformation by electroporation. *Yeast.* 14:565-71.

Tran, E.J., Y. Zhou, A.H. Corbett, and S.R. Wente. 2007. The DEAD-box protein Dbp5 controls mRNA export by triggering specific RNA:protein remodeling events. *Mol Cell.* 28:850-9.

Vasu, S., S. Shah, A. Orjalo, M. Park, W.H. Fischer, and D.J. Forbes. 2001. Novel vertebrate nucleoporins Nup133 and Nup160 play a role in mRNA export. *J Cell Biol.* 155:339-54.

Vink, M., M. Simonetta, P. Transidico, K. Ferrari, M. Mapelli, A. De Antoni, L.

Massimiliano, A. Ciliberto, M. Faretta, E.D. Salmon, and A. Musacchio. 2006. In vitro FRAP identifies the minimal requirements for Mad2 kinetochore dynamics. *Curr Biol.* 16:755-66.

Walther, T.C., A. Alves, H. Pickersgill, I. Loiodice, M. Hetzer, V. Galy, B.B. Hulsmann, T. Kocher, M. Wilm, T. Allen, I.W. Mattaj, and V. Doye. 2003. The conserved Nup107-160 complex is critical for nuclear pore complex assembly. *Cell.* 113:195-206.

Wang, W., A. Budhu, M. Forgues, and X.W. Wang. 2005. Temporal and spatial control of nucleophosmin by the Ran-Crm1 complex in centrosome duplication. *Nat Cell Biol.* 7:823-30.

Watson, M.L. 1959. Further observations on the nuclear envelope of the animal cell. *J Biophys Biochem Cytol.* 6:147-56.

Wei, R.R., P.K. Sorger, and S.C. Harrison. 2005. Molecular organization of the Ndc80 complex, an essential kinetochore component. *Proc Natl Acad Sci U S A.* 102:5363-7.

Weirich, C.S., J.P. Erzberger, J.M. Berger, and K. Weis. 2004. The N-terminal domain of Nup159 forms a beta-propeller that functions in mRNA export by tethering the helicase Dbp5 to the nuclear pore. *Mol Cell.* 16:749-60.

Weirich, C.S., J.P. Erzberger, J.S. Flick, J.M. Berger, J. Thorner, and K. Weis. 2006. Activation of the DExD/H-box protein Dbp5 by the nuclear-pore protein Gle1 and its coactivator InsP6 is required for mRNA export. *Nat Cell Biol.* 8:668-76.

Weis, K. 2003. Regulating access to the genome: nucleocytoplasmic transport throughout the cell cycle. *Cell.* 112:441-51.

Wen, W., J.L. Meinkoth, R.Y. Tsien, and S.S. Taylor. 1995. Identification of a signal for rapid export of proteins from the nucleus. *Cell.* 82:463-73.

Wiese, C., A. Wilde, M.S. Moore, S.A. Adam, A. Merdes, and Y. Zheng. 2001. Role of importin-beta in coupling Ran to downstream targets in microtubule assembly. *Science.* 291:653-6.

Wilde, A., S.B. Lizarraga, L. Zhang, C. Wiese, N.R. Gliksman, C.E. Walczak, and Y. Zheng. 2001. Ran stimulates spindle assembly by altering microtubule dynamics and the balance of motor activities. *Nat Cell Biol.* 3:221-7.

Williams, B.C., Z. Li, S. Liu, E.V. Williams, G. Leung, T.J. Yen, and M.L. Goldberg. 2003. Zwilch, a new component of the ZW10/ROD complex required for kinetochore functions. *Mol Biol Cell.* 14:1379-91.

Winey, M., C.L. Mamay, E.T. O'Toole, D.N. Mastronarde, T.H. Giddings, Jr., K.L. McDonald, and J.R. McIntosh. 1995. Three-dimensional ultrastructural analysis of the *Saccharomyces cerevisiae* mitotic spindle. *J Cell Biol.* 129:1601-15.

Winey, M., and E.T. O'Toole. 2001. The spindle cycle in budding yeast. *Nat Cell Biol.* 3:E23-7.

Wozniak, R.W., E. Bartnik, and G. Blobel. 1989. Primary structure analysis of an integral membrane glycoprotein of the nuclear pore. *J Cell Biol.* 108:2083-92.

Wozniak, R.W., G. Blobel, and M.P. Rout. 1994. POM152 is an integral protein of the pore membrane domain of the yeast nuclear envelope. *J Cell Biol.* 125:31-42.

Wozniak, R.W., M.P. Rout, and J.D. Aitchison. 1998. Karyopherins and kissing cousins. *Trends Cell Biol.* 8:184-8.

Xia, G., X. Luo, T. Habu, J. Rizo, T. Matsumoto, and H. Yu. 2004. Conformation-specific binding of p31(comet) antagonizes the function of Mad2 in the spindle checkpoint. *Embo J.* 23:3133-43.

Yang, L., T. Guan, and L. Gerace. 1997. Integral membrane proteins of the nuclear envelope are dispersed throughout the endoplasmic reticulum during mitosis. *J Cell Biol.* 137:1199-210.

Yang, Q., M.P. Rout, and C.W. Akey. 1998. Three-dimensional architecture of the isolated yeast nuclear pore complex: functional and evolutionary implications. *Mol Cell.* 1:223-34.

York, J.D., A.R. Odom, R. Murphy, E.B. Ives, and S.R. Wente. 1999. A phospholipase C-dependent inositol polyphosphate kinase pathway required for efficient messenger RNA export. *Science.* 285:96-100.

Zachariae, W., T.H. Shin, M. Galova, B. Obermaier, and K. Nasmyth. 1996. Identification of subunits of the anaphase-promoting complex of *Saccharomyces cerevisiae*. *Science.* 274:1201-4.

Zeitler, B., and K. Weis. 2004. The FG-repeat asymmetry of the nuclear pore complex is dispensable for bulk nucleocytoplasmic transport in vivo. *J Cell Biol.* 167:583-90.

Zhang, C., M. Hughes, and P.R. Clarke. 1999. Ran-GTP stabilises microtubule asters and inhibits nuclear assembly in Xenopus egg extracts. *J Cell Sci.* 112 (Pt 14):2453-61.

Zhang, H., H. Saitoh, and M.J. Matunis. 2002. Enzymes of the SUMO modification pathway localize to filaments of the nuclear pore complex. *Mol Cell Biol.* 22:6498-508.

Zhao, X., C.Y. Wu, and G. Blobel. 2004. Mlp-dependent anchorage and stabilization of a desumoylating enzyme is required to prevent clonal lethality. *J Cell Biol.* 167:605-11.

Zuccolo, M., A. Alves, V. Galy, S. Bolhy, E. Formstecher, V. Racine, J.B. Sibarita, T. Fukagawa, R. Shiekhattar, T. Yen, and V. Doye. 2007. The human Nup107-160 nuclear pore subcomplex contributes to proper kinetochore functions. *Embo J.* 26:1853-64.

Chapter VII: *Appendix*

Contained within this appendix are the results of several unpublished experiments that are not a part of the previously presented results chapters. The first is the steady-state localization of Mad1-GFP in wild type yeast cells, which demonstrates that Mad1-GFP is not uniformly distributed along the NE (Fig. 7-1). Fig. 7-2 shows that Mad1 interacts directly with Nup60p, consistent with an interaction between these two proteins at the NPC. In Fig. 7-3 the localization of Mad1-GFP in the *xpo1-1* temperature sensitive mutant is analyzed, showing that its normal localization to the NE requires function al Xpo1p. Lastly, Fig. 7-4 shows that Rna1-GFP (RanGAP) is not readily detected in the nucleus of M-phase cells and that other kinetochore proteins, both yeast and human, contain predicted NESs.

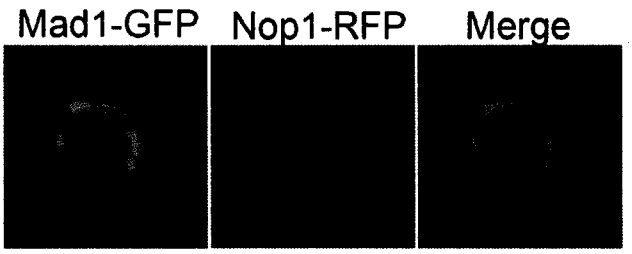

Figure 7-1. Mad1-GFP is excluded from the region of the NE overlaying the nucleolus.

A strain expressing Mad1-GFP (Y3028) was transformed with the plasmid pNop1-mRFP. Asynchronous populations of cells were visualized using an epifluorescence microscope.

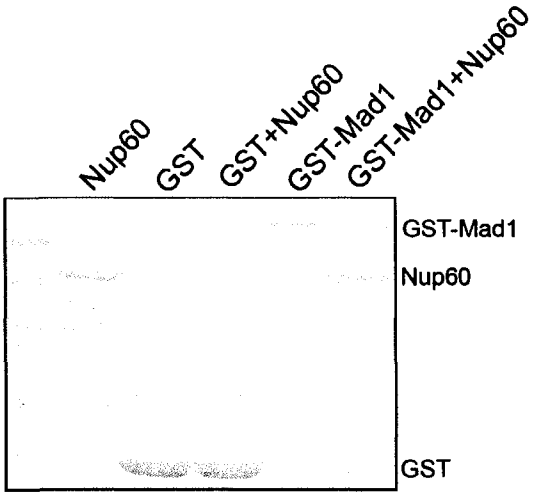

Figure 7-2. Mad1p interacts directly with Nup60p

Recombinant GST and GST-Mad1 were synthesized in *E. coli*, purified and immobilized on a glutathione column and were incubated in the presence or absence of Nup60. After washing, bound fractions were eluted with SDS-PAGE sample buffer and resolved by SDS-PAGE and visualized by Coomassie Blue staining.

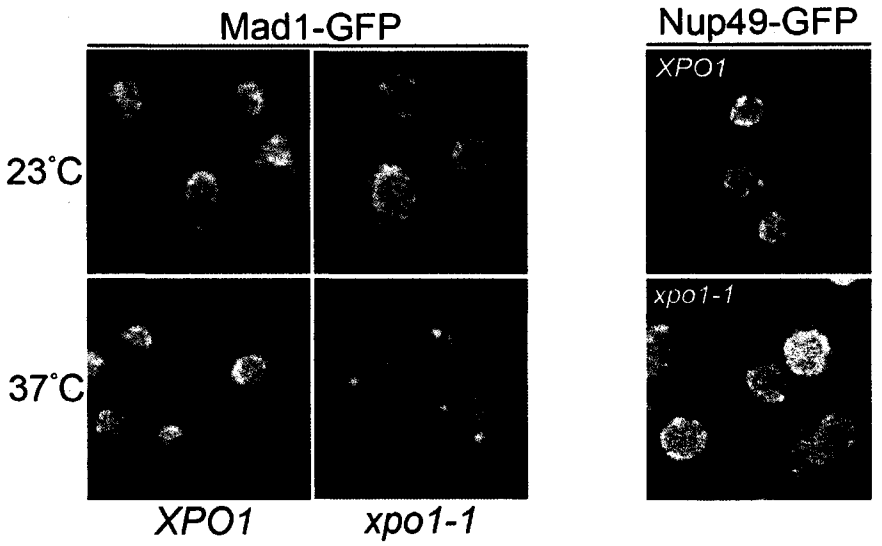

Figure 7-3. Mad1-GFP is mislocalized in the *xpo1-1* strain.

Wild type (WT) and *xpo1-1* mutant strains producing Mad1-GFP were grown to mid-log phase at 23°C and visualized directly or were shifted to 37°C for 30 min and imaged. As controls, wild type and the *xpo1-1* strain were transformed with a plasmid encoding *NUP49-GFP*. These cells were treated like the Mad1-GFP cells, and no mislocalization of this construct was observed at 37°C.

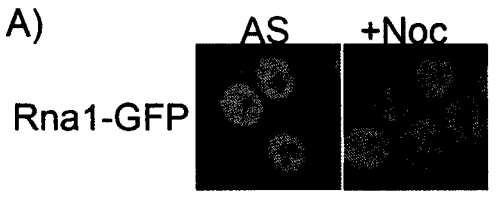

B)
Yeast
Bub1p: LEDMDDPLDLFLDYMI
Nec80p: LKLEELKVDLNRKRYKL

Human
ZW10: VLQKQLLDLPLDTDL
ROD: ELLLLYIEDLLNRCSS

Figure 7-4. Rna1-GFP (RanGAP-GFP) localization and predicted NESs in kinetochore proteins.

(A) A strain expressing Rna1-GFP was grown to mid logarithmic phase and directly visualized (AS) or treated with 12.5 μg/ml nocodazole for 1.5 h and visualized (+Noc). (B) NetNES was used to predict NESs within the primary sequences of kinetochore proteins. Presented here are two proteins in yeast and vertebrate that showed predicted NESs.

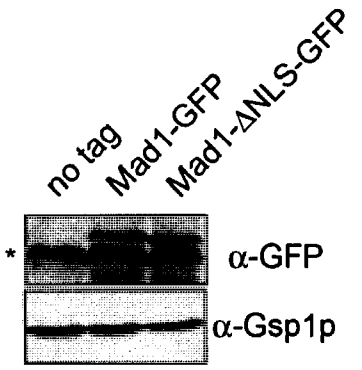

Figure 7-5. Mad1-GFP and Mad1-ΔNLS-GFP are produced at similar levels.

The yeast strain Y3020 (*mad1Δ*) transformed with p*MAD1-GFP* or p*mad1-ΔNLS-GFP* were blotted with antibodies against GFP (3B4, 1:5000) to detect expression of each construct. The asterisk indicates a cross-reacting band recognized by the 3B4 serum.